

# Chemistry–A European Journal

Supporting Information

## **Designing Ionic Ir(III) Cyclometalated Complexes as Photocatalysts for Light Assisted ATRP of MMA. A Combined Experimental and Mechanistic Study**

Giulia Vigarani, Edoardo Marchini,\* Eleonora Previati, Loris Giorgini, Stefano Zacchini, Roberto Argazzi, Massimiliano Massi, Valentina Fiorini,\* Stefano Caramori, and Stefano Stagni\*

# Designing Ionic Ir(III) cyclometalated complexes as photocatalysts for light assisted ATRP of MMA. A combined experimental and mechanistic study

Giulia Vigarani,<sup>a</sup> Edoardo Marchini,<sup>b\*</sup> Eleonora Previati,<sup>a</sup> Loris Giorgini,<sup>a</sup> Stefano Zacchini,<sup>a</sup> Roberto Argazzi,<sup>c</sup> Massimiliano Massi,<sup>d</sup> Valentina Fiorini,<sup>a\*</sup> Stefano Caramori,<sup>b</sup> and Stefano Stagni<sup>a\*</sup>

<sup>a</sup>: Department of Industrial Chemistry "Toso Montanari", University of Bologna, Via P. Gobetti 85, 40129 - Viale del Risorgimento 4, 40126 Bologna, Italy

<sup>b</sup>: Department of Chemical, Pharmaceutical and Agricultural Sciences, University of Ferrara, via Luigi Borsari 46, 44121 Ferrara, Italy

<sup>c</sup>: CNR-ISOF c/o Department of Chemical, Pharmaceutical and Agricultural Sciences, University of Ferrara, Via L. Borsari 46, 44121, Ferrara, Italy

<sup>d</sup>: Department of Chemistry, Curtin University, Bentley, Western Australia 6102, Australia

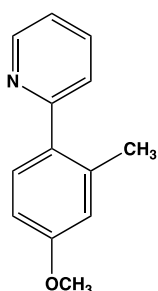
## ELECTRONIC SUPPLEMENTARY INFORMATION

### Index

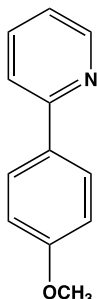
Ligand Synthesis .....	1
Synthesis of [Ir(C <sup>^</sup> N) <sub>2</sub> (N <sup>^</sup> N)] <sup>+</sup> -type complexes .....	3
Synthesis of [Ir(C <sup>^</sup> N) <sub>2</sub> (bpy)][Br] -type complexes .....	7
NMR Spectroscopy .....	8
ESI-MS .....	27
Cyclic Voltammetry .....	32
Photophysics and Stern Volmer quenching studies .....	37
X-Ray Crystallography .....	50
General Procedure for the photopolymerization of MMA .....	51
First-order kinetic plots, <i>M<sub>n</sub></i> and PDI versus conversion .....	52
Synthesis of poly(methyl methacrylate- <i>b</i> -hexyl methacrylate) using PMMA as macroinitiator ..	64
Transient Absorption Spectroscopy .....	65
TDDFT calculations .....	68

## Ligand Synthesis

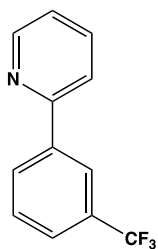
**(2Me-4OMe-ppy)**, **(4OMe-ppy)**, **(3CF<sub>3</sub>-ppy)** and **4-chloro-2-phenylpyridine** were obtained by standard Suzuki-Miyaura coupling conditions of 2-methyl 4-methoxy boronic acid or 3-trifluoromethyl boronic acid or 4-methoxy boronic acid or phenyl boronic acid (0.8 eq) with 2-bromopyridine or 2,4-dichloropyridine (1 eq.), [Pd(pph<sub>3</sub>)<sub>4</sub>] (0.1 eq) and K<sub>2</sub>CO<sub>3</sub> (2N, aq) in freshly distilled THF. Subsequent purification by SiO<sub>2</sub> column chromatography (Hexane/EtoAc 7:3, EP/DCM 8:2) yielded the desired products as pale-yellow oils (second fraction).



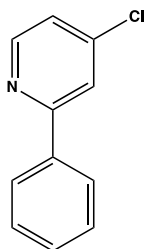
**(2Me-4OMe-ppy)** Y = 0.804 g, 6.10 mmol, 98%; <sup>1</sup>H-NMR, (CDCl<sub>3</sub>, 400 MHz) (δ) ppm = 8.66 – 8.64 (m, 1H), 7.69 – 7.64 (m, 1H), 7.35 – 7.32 (m, 2H), 7.18 – 7.14 (m, 1H), 6.81 – 6.79 (m, 2H), 3.79 (s, 3H), 2.36 (s, 3H). <sup>13</sup>C-NMR (CDCl<sub>3</sub>, 100 MHz) (δ) ppm = 159.72, 159.50, 149.08, 137.36, 136.03, 133.21, 130.97, 124.08, 121.23, 116.12, 111.24, 55.18, 20.64..



**(4OMe-ppy)** Y = 0.707 g, 3.78 mmol, 51%; <sup>1</sup>H-NMR, (CDCl<sub>3</sub>, 400 MHz) (δ) ppm = 8.66 – 8.64 (m, 2H), 7.96 – 7.94 (m, 2H), 7.71 – 7.66 (m, 2H), 7.18 – 7.16 (m, 1H), 7.04 – 6.98 (m, 2H), 3.86 (s, 3H). <sup>13</sup>C-NMR (CDCl<sub>3</sub>, 100 MHz) (δ) ppm = 159.21, 154.63, 149.26, 137.21, 131.38, 128.63, 123.61, 120.54, 114.89, 55.83.

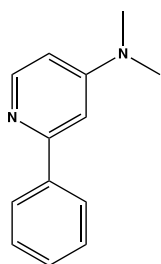


**(3CF<sub>3</sub>-ppy)** Y = 0.611 g, 2.69 mmol, 73%; <sup>1</sup>H-NMR, (CDCl<sub>3</sub>, 400 MHz) (δ) ppm = 8.74 – 8.72 (m, 1H), 8.29 (s, 1H), 8.19 – 8.17 (d, J<sub>H-H</sub> = 7.6 Hz, 1H), 7.82 – 7.57 (m, 2H), 7.68 – 7.66 (d, J<sub>H-H</sub> = 7.6 Hz, 1H), 7.62 – 7.57 (m, 1H), 7.33 – 7.27 (m, 2H). <sup>13</sup>C-NMR (CDCl<sub>3</sub>, 100 MHz) (δ) ppm = 149.85, 140.06, 137.03, 130.05, 129.21, 125.56, 125.53, 125.49, 123.81, 123.78, 122.82, 120.62. <sup>19</sup>F-NMR (CDCl<sub>3</sub>, 376 MHz) (δ) ppm = -62.



**4-chloro-2-phenylpyridine** Y = 0.380 g, 2.01 mmol, 47%; <sup>1</sup>H-NMR, (CDCl<sub>3</sub>, 400 MHz) (δ) ppm = 8.51 – 8.49 (m, 1H), 7.94 – 7.92 (m, 2H), 7.63 – 7.38 (m, 3H), 7.13 – 7.11 (m, 1H). <sup>13</sup>C-NMR (CDCl<sub>3</sub>, 100 MHz) (δ) ppm = 159.15, 150.63, 144.88, 138.28, 129.74, 129.00, 127.12, 122.42, 121.00.

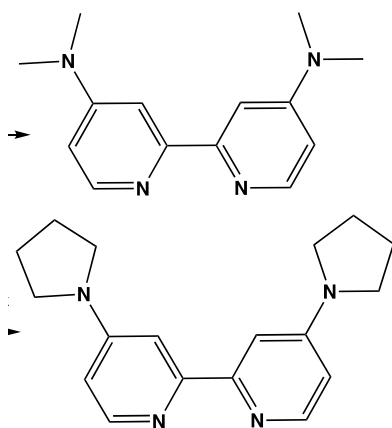
***N,N*-dimethyl-2-phenylpyridin-4-amine - (ppy-NMe<sub>2</sub>)**. In a 50 mL heavy-walled Schlenk flask equipped with a pressure plug valve, 4-chloro-2-phenylpyridine (0.380 g, 2.01 mmol) and HN(CH<sub>3</sub>)<sub>2</sub> 33 wt.% (5 mL) were heated at 140 °C for 24 h under argon atmosphere. After complete cooling to room temperature, the reaction mixture was extracted with EtOAc (3x10 mL). The resulting organic phase was dried over MgSO<sub>4</sub> and the solvent removed under reduced pressure. The crude was then purified by chromatography on SiO<sub>2</sub> (EP/EtOAc 8:2) to give the desired product as pale-yellow oil (second fraction).



Y = 0.351 g, 1.77 mmol, 88%; <sup>1</sup>H-NMR, (CDCl<sub>3</sub>, 400 MHz) (δ) ppm = 8.31 – 8.29 (m, 1H), 7.92 – 7.89 (m, 2H), 7.47 – 7.39 (m, 2H), 7.36 – 7.34 (m, 1H), 6.86 – 6.85 (m, 1H), 6.44 – 6.42 (m, 1H), 3.05 (s, 6H). <sup>13</sup>C-NMR (CDCl<sub>3</sub>, 100 MHz) (δ) ppm = 157.89, 155.08, 149.44, 140.54, 128.52, 127.09, 105.41, 105.00, 103.76, 39.26.

Dichlorobridged Ir(III) dimers [Ir(C<sup>^</sup>N)<sub>2</sub>-μ-Cl]<sub>2</sub> were obtained according to the Nonoyama protocol.

**(bpy-(NMe<sub>2</sub>)<sub>2</sub>)** and **(bpy-(pyr)<sub>2</sub>)** were obtained by slight modifications on a previously reported procedure [i].



**(bpy-(NMe<sub>2</sub>)<sub>2</sub>)**, off-white solid, Y = 0.150 g, 0.62 mmol, 58%; <sup>1</sup>H-NMR (400 MHz, CDCl<sub>3</sub>) (δ) ppm = 8.29 (d, *J*<sub>H-H</sub> = 5.9 Hz, 2H), 7.67 (d, *J*<sub>H-H</sub> = 2.7 Hz, 2H), 6.51 (dd, *J*<sub>H-H</sub> = 5.9, 2.7 Hz, 2H), 3.09 (s, 12H, CH<sub>3</sub>). <sup>13</sup>C-NMR (100 MHz, CDCl<sub>3</sub>) (δ) ppm = 157.01, 155.39, 149.13, 106.54, 104.26, 39.48.

**(bpy-(pyr)<sub>2</sub>)**, off-white solid, Y = 0.162 g, 0.55 mmol, 89%; <sup>1</sup>H-NMR (400 MHz, CDCl<sub>3</sub>) (δ) ppm = 8.26 (d, *J*<sub>H-H</sub> = 5.9 Hz, 2H), 7.52 (d, *J*<sub>H-H</sub> = 2.79 Hz, 2H), 6.38 – 6.36 (m, 2H), 3.44– 3.40 (m, 8H, pyrrolidine), 2.04 – 2.01 (m, 8H, pyrrolidine). <sup>13</sup>C-NMR (100 MHz, CDCl<sub>3</sub>) (δ) ppm = 152.67, 148.80, 136.01, 106.66, 104.44, 47.15, 25.36.

## Synthesis of $[\text{Ir}(\text{C}^{\wedge}\text{N})_2(\text{N}^{\wedge}\text{N})]^+$ -type complexes

In a 100 mL flask,  $[\text{Ir}(\text{C}^{\wedge}\text{N})_2\text{Cl}]_2$  (1 eq., 0.100 g) and  $(\text{bpy}-(\text{NMe}_2)_2)$  or  $(\text{bpy}-(\text{pyr})_2)$  (2.5 eq.) were dissolved in 15 mL  $\text{CH}_2\text{Cl}_2/\text{CH}_3\text{OH}$  3:1 mixture and stirred at room temperature for 8h. Anion metathesis was carried out by adding an excess of  $\text{NH}_4\text{PF}_6$  or  $\text{TBABr}$  to the solution and stirring for 2 h. The product was then extracted against  $\text{H}_2\text{O}$  ( $3 \times 10$  mL) and the organic components were combined and dried over anhydrous  $\text{MgSO}_4$ . Subsequent purification by column chromatography on  $\text{Al}_2\text{O}_3$  (gradient:  $\text{CH}_2\text{Cl}_2$  then  $\text{CH}_2\text{Cl}_2/\text{Methanol}$  40:1) yielded the desired product as second fraction. The synthesis of **1** $[\text{BF}_4]$  was accomplished by following the same procedure as before except of anion metathesis, that was carried out by adding a slight excess of  $\text{AgBF}_4$  (1.1 eq.) to the solution protected from light. After 4 hours, the crude was filtered through a celite pad to remove the precipitated  $\text{AgCl}$ .

**1**  $[\text{PF}_6]$  bright yellow solid, Y = 0.145 g, 0.163 mmol, 55%. **ESI-MS** ( $m/z$ ),  $\text{CH}_3\text{CN}$ :  $[\text{M}]^+ = 743$ ,  $[\text{M}]^- = 145$ .  **$^1\text{H-NMR}$** , 400 MHz,  $\text{Acetone-}d^6$  ( $\delta$ ) ppm = 8.19 – 8.18 (d,  $J_{\text{H-H}} = 6.4$  Hz, 2H), 7.93 – 7.88 (m, 4H), 7.85 – 7.83 (d,  $J_{\text{H-H}} = 8.79$  Hz, 2H), 7.76 – 7.75 (d,  $J_{\text{H-H}} = 2.79$  Hz, 2H), 7.45 – 7.43 (d,  $J_{\text{H-H}} = 6.39$  Hz, 2H), 7.22 – 7.17 (m, 2H), 6.97 – 6.95 (m, 2H), 6.87 – 6.81 (m, 2H), 6.73 – 6.70 (m, 2H), 6.36 – 6.34 (d,  $J_{\text{H-H}} = 7.99$  Hz, 2H), 3.18 (s, 12H).  **$^{13}\text{C-NMR}$**  100 MHz,  $\text{Acetone-}d^6$  ( $\delta$ ) ppm = 169.27, 157.08, 156.08, 153.84, 149.80, 149.64, 145.25, 138.96, 132.78, 131.03, 125.71, 124.11, 122.65, 120.48, 110.41, 106.71, 39.75. Anal. Calcd. For  $\text{C}_{36}\text{H}_{34}\text{N}_6\text{Ir}_1\text{P}_1\text{F}_6$  (887.88): C 48.70, H 3.86, N 9.47. Found: C 49.12, H 4.07, N 9.17%

**1**  $[\text{BF}_4]$  bright yellow solid, Y = 0.067 g, 0.081 mmol, 58%. **ESI-MS** ( $m/z$ ),  $\text{CH}_3\text{CN}$ :  $[\text{M}]^+ = 743$ ,  $[\text{M}]^- = 87$ .  **$^1\text{H-NMR}$** , 400 MHz,  $\text{DMSO-}d^6$  ( $\delta$ ) ppm = 8.22 – 8.21 (m, 2H), 7.92 – 7.86 (m, 4H), 7.69 (s, 4H), 7.26 – 7.20 (m, 4H), 6.97 – 6.95 (m, 2H), 6.85 – 6.84 (m, 2H), 6.78 – 6.77 (m, 2H), 6.21 – 6.20 (m, 2H), 3.13 (s, 12H).  **$^{13}\text{C-NMR}$** , 100 MHz,  $\text{DMSO-}d^6$  ( $\delta$ ) ppm = 167.75, 155.79, 155.03, 153.29, 148.71, 148.34, 138.55, 131.68, 130.36, 125.31, 123.93, 121.90, 120.11, 110.11, 106.30. N-( $\text{CH}_3$ )<sub>2</sub> signal falls within the non-deuterated residual of  $\text{DMSO-}d^6$ . Anal. Calcd. For  $\text{C}_{36}\text{H}_{34}\text{Ir}_1\text{N}_6\text{B}_1\text{F}_4$  (829.67) C 52.11, H 4.13, N 10.13. Found: C 48.59, H 3.97, N 9.19%

**1**  $[\text{Br}]$  bright yellow solid, Y = 0.061 g, 0.074 mmol, 64%. **ESI-MS** ( $m/z$ ),  $\text{CH}_3\text{CN}$ :  $[\text{M}]^+ = 743$ ,  $[\text{M}]^- = 79$ , 81.  **$^1\text{H-NMR}$** , 400 MHz,  $\text{DMSO-}d^6$  ( $\delta$ ) ppm = 8.21 (d,  $J_{\text{H-H}} = 7.99$  Hz, 2H), 7.90 – 7.83 (m, 4H), 7.68 – 7.66 (m, 4H), 7.24 – 7.17 (m, 4H), 6.95 – 6.91 (m, 2H), 6.83 – 6.79 (m, 2H), 6.76 – 6.74 (m, 2H), 6.19

– 6.17 (m, 2H), 3.12 (s, 12H). **<sup>13</sup>C-NMR** 150 MHz, DMSO-*d*<sup>6</sup> (δ) ppm = 167.77, 155.82, 155.06, 153.32, 148.73, 148.36, 144.46, 138.58, 131.71, 130.39, 125.34, 123.97, 121.95, 120.14, 110.13, 106.35. N-(CH<sub>3</sub>)<sub>2</sub> signal falls within the non-deuterated residual of DMSO-*d*<sup>6</sup>. Anal. Calcd. For C<sub>36</sub>H<sub>34</sub>N<sub>6</sub>Ir<sub>1</sub>Br<sub>1</sub>(822.8): C 52.55, H 4.17, N 10.21. Found: C 50.66, H 4.08, N 9.71%

**2 [PF<sub>6</sub>]** bright yellow solid, Y = 0.097 g, 0.099 mmol, 80.5%. **ESI-MS** (m/z), CH<sub>3</sub>CN: [M]<sup>+</sup> = 831, [M]<sup>–</sup> = 145. **<sup>1</sup>H-NMR**, 400 MHz, Acetone-*d*<sup>6</sup> (δ) ppm = 8.21 – 8.19 (d, *J*<sub>H-H</sub> = 8.4 Hz, 2H), 7.91 – 7.85 (m, 4H), 7.76 – 7.75 (d, *J*<sub>H-H</sub> = 2.8 Hz, 2H), 7.43 – 7.41 (d, *J*<sub>H-H</sub> = 6.8 Hz, 2H), 7.09 – 7.06 (m, 2H), 6.74 – 6.72 (m, 2H), 6.42 – 6.41 (m, 2H), 5.65 – 5.62 (m, 2H), 3.51 (s, 6H), 3.19 (s, 12H), 2.73 (s, 6H). **<sup>13</sup>C-NMR** 100 MHz, Acetone-*d*<sup>6</sup> (δ) ppm = 169.21, 160.89, 158.69, 156.91, 156.06, 150.09, 149.59, 139.39, 138.36, 136.44, 123.25, 122.13, 115.57, 112.55, 110.39, 106.65, 54.78, 39.74, 24.34. Anal. Calcd. For C<sub>40</sub>H<sub>42</sub>N<sub>6</sub>O<sub>2</sub>Ir<sub>1</sub>P<sub>1</sub>F<sub>6</sub> (975.98): C 49.23, H 4.34, N 8.61. Found: C 46.42, H 4.18, N 7.92%

**2 [Br]** bright yellow solid, Y = 0.070 g, 0.077 mmol, 96%. **ESI-MS** (m/z), CH<sub>3</sub>CN: [M]<sup>+</sup> = 831, [M]<sup>–</sup> = 79, 81. **<sup>1</sup>H-NMR**, 400 MHz, DMSO-*d*<sup>6</sup> (δ) ppm = 8.06 – 8.05 (m, 2H), 7.80 – 7.79 (m, 2H), 7.65 – 7.63 (m, 4H), 7.17 – 7.15 (m, 2H), 7.06 – 7.04 (m, 2H), 6.75 – 6.74 (m, 2H), 6.37 – 6.36 (m, 2H), 5.39 – 5.38 (m, 2H), 3.43 (s, 6H), 3.08 (s, 12H), 2.63 (s, 6H). **<sup>13</sup>C-NMR** 150 MHz, DMSO-*d*<sup>6</sup> (δ) ppm = 167.56, 159.49, 157.91, 155.61, 155.02, 149.99, 148.23, 138.65, 138.03, 135.60, 122.61, 121.00, 114.85, 111.39, 110.15, 106.28, 54.57, 24.31. N-(CH<sub>3</sub>)<sub>2</sub> signal falls within the non-deuterated residual of DMSO-*d*<sup>6</sup>. Anal. Calcd. For C<sub>40</sub>H<sub>42</sub>N<sub>6</sub>O<sub>2</sub>Ir<sub>1</sub>Br<sub>1</sub> (910.87): C 52.74, H 4.65, N 9.23. Found: C 52.61, H 4.71, N 9.15%

**3 [PF<sub>6</sub>]** bright yellow solid, Y = 0.072 g, 0.079 mmol, 93%. **ESI-MS** (m/z), CH<sub>3</sub>CN: [M]<sup>+</sup> = 879, [M]<sup>–</sup> = 145. **<sup>1</sup>H-NMR**, 400 MHz, Acetone-*d*<sup>6</sup> (δ) ppm = 8.49 – 8.46 (m, 2H), 8.18 (s, 2H), 8.08 – 8.04 (m, 2H), 8.00 – 7.98 (m, 2H), 7.79 – 7.78 (d, *J*<sub>H-H</sub> = 2.4 Hz, 2H), 7.42 – 7.41 (m, 2H), 7.38 – 7.34 (m, 2H), 7.15 – 7.13 (m, 2H), 6.76 – 6.74 (m, 2H), 6.56 – 6.54 (m, 2H), 3.20 (s, 12H). **<sup>13</sup>C-NMR** 100 MHz, Acetone-*d*<sup>6</sup> (δ) ppm = 167.58, 159.66, 156.85, 156.20, 150.16, 149.52, 146.21, 139.77, 134.74 (CF<sub>3</sub>), 134.65 (CF<sub>3</sub>), 133.36, 131.40 (CF<sub>3</sub>), 131.37 (CF<sub>3</sub>), 130.23 (CF<sub>3</sub>), 129.08 (CF<sub>3</sub>), 128.98 (CF<sub>3</sub>), 127.53 (CF<sub>3</sub>), 126.97, 126.94, 126.90, 126.86, 125.43, 124.94 (CF<sub>3</sub>), 124.84 (CF<sub>3</sub>), 124.63 (CF<sub>3</sub>), 121.90, 121.47, 110.59, 106.86, 39.74 (N-CH<sub>3</sub>). Anal. Calcd. For C<sub>38</sub>H<sub>32</sub>N<sub>6</sub>Ir<sub>1</sub>P<sub>1</sub>F<sub>12</sub> (1023.87): C 44.58, H 3.15, N 8.21. Found: C 43.13, H 3.11, N 7.82%

**4 [PF<sub>6</sub>]** bright yellow solid, Y = 0.074 g, 0.078 mmol, 93%. **ESI-MS** (m/z), CH<sub>3</sub>CN: [M]<sup>+</sup> = 803, [M]<sup>-</sup> = 145. **<sup>1</sup>H-NMR**, 400 MHz, Acetone-*d*<sup>6</sup> (δ) ppm = 8.06 – 8.03 (m, 2H), 7.87 – 7.75 (m, 8H), 7.51– 7.49 (d, *J*<sub>H-H</sub> = 7.9 Hz, 2H), 7.11 – 7.07 (m, 2H), 6.75 – 6.73 (m, 2H), 6.60 – 6.57 (m, 2H), 5.84 (m, 2H), 3.56 (s, 6H), 3.19 (s, 12H). **<sup>13</sup>C-NMR** 100 MHz, Acetone-*d*<sup>6</sup> (δ) ppm = 169.89, 162.98, 157.86, 156.91, 150.54, 150.30, 139.51, 138.86, 128.15, 123.52, 120.47, 118.68, 111.22, 108.69, 107.46, 55.78, 40.55. Anal. Calcd. For C<sub>38</sub>H<sub>38</sub>N<sub>6</sub>O<sub>2</sub>Ir<sub>1</sub>P<sub>1</sub>F<sub>6</sub> (947.88): C 48.15, H 4.04, N 8.87. Found: C 46.01, H 3.94, N 8.31%

**4 [Br]** bright yellow solid, Y = 0.063 g, 0.071 mmol, 84%. **ESI-MS** (m/z), CH<sub>3</sub>CN: [M]<sup>+</sup> = 803, [M]<sup>-</sup> = 79, 81. **<sup>1</sup>H-NMR**, 400 MHz, DMSO-*d*<sup>6</sup> (δ) ppm = 8.04 – 8.03 (m, 2H), 7.79 – 7.78 (m, 4H), 7.65 – 7.64 (m, 2H), 7.55 – 7.54 (m, 2H), 7.25 – 7.24 (m, 2H), 7.07 – 7.04 (m, 2H), 6.75 – 6.74 (m, 2H), 6.54 – 6.52 (m, 2H), 5.59 – 5.58 (m, 2H), 3.47 (s, 6H), 3.08 (s, 12H). **<sup>13</sup>C-NMR** 150 MHz, DMSO-*d*<sup>6</sup> (δ) ppm = 167.53, 160.80, 155.76, 155.46, 155.02, 148.28, 137.32, 126.99, 122.56, 119.29, 117.04, 110.13, 106.87, 106.28, 54.77. N-(CH<sub>3</sub>)<sub>2</sub> signal falls within the non-deuterated residual of DMSO-*d*<sup>6</sup>. Anal. Calcd. For C<sub>38</sub>H<sub>38</sub>N<sub>6</sub>O<sub>2</sub>Ir<sub>1</sub>Br<sub>1</sub> (882.82): C 51.69, H 4.34, N 9.52. Found: C 51.99, H 4.43, N 9.43%

**7 [Br]** bright yellow solid, Y = 0.075 g, 0.086 mmol, 92%. **ESI-MS** (m/z), CH<sub>3</sub>CN: [M]<sup>+</sup> = 795, [M]<sup>-</sup> = 79, 81. **<sup>1</sup>H-NMR**, 600 MHz, DMSO-*d*<sup>6</sup> (δ) ppm = 8.23 – 8.21 (m, 2H), 7.92 – 7.86 (m, 4H), 7.72 – 7.70 (m, 2H), 7.56 – 7.55 (m, 2H), 7.23 – 7.19 (m, 4H), 6.97–6.94 (m, 2H), 6.85 – 6.82 (m, 2H), 6.64 – 6.61 (m, 2H), 6.22 – 6.20 (m, 2H), 3.51 – 3.27 (s, br, H<sub>2</sub>O-DMSO-*d*<sup>6</sup>+ 8H pyrrolidine), 1.98 (m, br, 8H pyrrolidine). **<sup>13</sup>C-NMR** 150 MHz, DMSO-*d*<sup>6</sup> (δ) ppm = 167.76, 155.71, 153.42, 152.25 (pyrrolidine), 148.69 (pyrrolidine), 148.20, 144.46, 138.52, 131.73, 130.36, 125.33, 123.93, 121.87, 120.11, 110.52, 106.79 (pyrrolidine), 48.08 (pyrrolidine), 25.19 (pyrrolidine). Anal. Calcd. For C<sub>40</sub>H<sub>38</sub>N<sub>6</sub>Ir<sub>1</sub>Br<sub>1</sub> (874.84): C 54.91, H 4.38, N 9.61. Found: C 54.48, H 4.58, N 9.37%

**8 [Br]** bright yellow solid, Y = 0.085 g, 0.088 mmol, 89 %. **ESI-MS** (m/z), CH<sub>3</sub>CN: [M+H]<sup>+</sup> = 884, [M]<sup>-</sup> = 79, 81. **<sup>1</sup>H-NMR**, 400 MHz, Acetone-*d*<sup>6</sup> (δ) ppm = 8.21 – 8.19 (m, 2H), 7.94 – 7.92 (m, 2H), 7.87 – 7.85 (m, 2H), 7.80 – 7.79 (m, 2H), 7.11 – 7.07 (m, 2H), 6.56 – 6.54 (m, 2H), 6.42 – 6.41 (m, 2H), 3.51 (s, br, 8H, pyrrolidine), 2.79 (s, 6H, -OCH<sub>3</sub>), 2.73 (s, 6H, -CH<sub>3</sub>), 2.06 – 2.03 (Acetone-*d*<sup>6</sup> + 8H pyrrolidine). **<sup>13</sup>C-NMR** 150 MHz, DMSO-*d*<sup>6</sup> (δ) ppm = 167.58, 159.51, 158.03, 155.54, 152.24, 148.99, 148.13, 138.66, 138.01, 135.63, 122.60, 121.99, 114.93, 111.36, 110.58, 106.69, 54.59 (-OCH<sub>3</sub>), 48.00 (pyrrolidine),

25.18 (pyrrolidine), 24.17 (-CH<sub>3</sub>). Anal. Calcd. For C<sub>44</sub>H<sub>46</sub>N<sub>6</sub>O<sub>2</sub>Ir<sub>1</sub>Br<sub>1</sub> (962.94): C 54.88, H 4.82, N 8.73. Found: C 54.92, H 4.85, N 9.05%

**9 [Br]** bright yellow solid, Y = 0.082 g, 0.088 mmol, 94%. **ESI-MS** (m/z), CH<sub>3</sub>CN: [M]<sup>+</sup> = 855, [M]<sup>-</sup> = 79, 81. **<sup>1</sup>H-NMR**, 600 MHz, DMSO-*d*<sup>6</sup> (δ) ppm = 8.09 – 8.07 (m, 2H), 7.84 – 7.82 (m, 2H), 7.62 – 7.61 (m, 2H), 7.56 – 7.55 (m, 2H), 7.27 – 7.26 (m, 2H), 7.11 – 7.09 (m, 2H), 6.65 – 6.64 (m, 2H), 6.59 – 6.57 (m, 2H), 5.65 – 5.64 (m, 2H), 3.52 (s, br, 6H -OCH<sub>3</sub>), 3.32 (s, br, H<sub>2</sub>O DMSO-*d*<sup>6</sup> + 8H pyrrolidine), 1.98 (s, br, 8H pyrrolidine). **<sup>13</sup>C-NMR** 150 MHz, DMSO-*d*<sup>6</sup> (δ) ppm = 167.55, 160.81, 155.68, 155.58, 152.24 (pyrrolidine), 148.39 (pyrrolidine), 148.28, 138.26, 137.35, 127.00, 122.55, 119.29, 117.10, 110.55, 106.84 (pyrrolidine), 106.70 (pyrrolidine), 54.79 (-OCH<sub>3</sub>), 48.02 (pyrrolidine), 40.53, 25.18 (pyrrolidine). Anal. Calcd. For C<sub>42</sub>H<sub>42</sub>N<sub>6</sub>O<sub>2</sub>Ir<sub>1</sub>Br<sub>1</sub> (934.89): C 53.95, H 4.53, N 8.99. Found: C 51.57, H 4.40, N 8.45%

**10 [Br]** bright yellow solid, Y = 0.045 g, 0.049 mmol, 77%. **ESI-MS** (m/z), CH<sub>3</sub>CN: [M+H]<sup>+</sup> = 830, [M+K]<sup>+</sup> = 865, [M]<sup>-</sup> = 79, 81. **<sup>1</sup>H-NMR**, 600 MHz, DMSO-*d*<sup>6</sup> (δ) ppm = 7.81 – 7.79 (m, 2H), 7.66 – 7.65 (m, 2H), 7.29 – 7.28 (m, 2H), 7.22 – 7.21 (m, 2H), 7.09 – 7.08 (m, 2H), 6.87 – 6.85 (m, 2H), 6.79 – 6.74 (m, 4H), 6.47 – 6.45 (m, 2H), 6.35 – 6.33 (m, 2H), 3.13 (s, 12H, CH<sub>3</sub> bpy), 3.08 (s, 12H, CH<sub>3</sub> ppy). **<sup>13</sup>C-NMR** 150 MHz, DMSO-*d*<sup>6</sup> (δ) ppm = 166.33, 156.02, 154.83, 154.73, 153.77, 148.32, 145.74, 132.31, 129.82, 124.40, 121.01, 109.82, 106.74, 106.08. N-(CH<sub>3</sub>)<sub>2</sub> signals from (ppy-(NMe<sub>2</sub>)) and (bpy-(NMe<sub>2</sub>)<sub>2</sub>) falls within the non-deuterated residual of DMSO-*d*<sup>6</sup>. Anal. Calcd. For C<sub>40</sub>H<sub>44</sub>N<sub>8</sub>Ir<sub>1</sub>Br<sub>1</sub> (908.89): C 52.85, H 4.88, N 12.33. Found: C 53.38, H 4.97, N 12.15%

**11 [Br]** bright yellow solid, Y = 0.057 g, 0.059 mmol, 93%. **ESI-MS** (m/z), CH<sub>3</sub>CN: [M+H]<sup>+</sup> = 882, [M+K]<sup>+</sup> = 917, [M]<sup>-</sup> = 79, 81. **<sup>1</sup>H-NMR**, 600 MHz, DMSO-*d*<sup>6</sup> (δ) ppm = 7.80 – 7.79 (m, 2H), 7.53 (m, 2H), 7.26 – 7.25 (m, 2H), 7.22 (m, 2H), 7.11 – 7.10 (m, 2H), 6.87 – 6.85 (m, 2H), 6.78 – 6.75 (m, 2H), 6.59 – 6.58 (m, 2H), 6.47 – 6.45 (m, 2H), 6.35 – 6.34 (m, 2H), 3.37 (s, br, H<sub>2</sub>O DMSO-*d*<sup>6</sup> + 8H pyrrolidine), 3.08 (s, 12H, ppy), 1.98 (s, br, 8H pyrrolidine). **<sup>13</sup>C-NMR** 150 MHz, DMSO-*d*<sup>6</sup> (δ) ppm = 166.33, 155.93, 154.72, 153.89, 152.03, 148.15, 147.26, 145.76, 132.35, 129.26, 124.40, 120.96, 110.17, 106.71, 106.49, 101.55, 47.95, 25.19. N-(CH<sub>3</sub>)<sub>2</sub> signal of (ppy-(NMe<sub>2</sub>)) falls within the non-deuterated residual of DMSO-*d*<sup>6</sup>. Anal. Calcd. For C<sub>44</sub>H<sub>48</sub>N<sub>8</sub>Ir<sub>1</sub>Br<sub>1</sub> (960.97): C 54.99, H 5.03, N 11.66. Found: C 51.67, H 4.82, N 10.71%



## Synthesis of [Ir(C<sup>N</sup>)<sub>2</sub>(bpy)][Br] -type complexes

In a 100 mL flask, [Ir(C<sup>N</sup>)<sub>2</sub>Cl]<sub>2</sub> (1 eq., 0.1 g) and (bpy) (2.5 eq.) were dissolved in 15 mL CH<sub>2</sub>Cl<sub>2</sub>/CH<sub>3</sub>OH 3:1 mixture and stirred at room temperature for 8h. Anion metathesis was carried out by adding an excess of TBABr to the solution and stirring for 2h. The product was then extracted using H<sub>2</sub>O (3 × 10 mL) and the organic components were combined and dried over anhydrous MgSO<sub>4</sub>. Subsequent purification by column chromatography on Al<sub>2</sub>O<sub>3</sub> (gradient: CH<sub>2</sub>Cl<sub>2</sub> then CH<sub>2</sub>Cl<sub>2</sub>/CH<sub>3</sub>OH 40:1) yielded the desired product as second fraction.

**5 [Br]** bright yellow solid, Y = 0.060 g, 0.081 mmol, 87%. **ESI-MS** (m/z), CH<sub>3</sub>CN: [M]<sup>+</sup> = 657, [M]<sup>-</sup> = 79, 81. **<sup>1</sup>H-NMR**, 400 MHz, DMSO-*d*<sup>6</sup> (δ) ppm = 8.85 – 8.84 (m, 2H), 8.23 – 8.21 (m, 4H), 7.90 – 7.86 (m, 4H), 7.82 – 7.81 (m, 2H), 7.66 – 7.63 (m, 2H), 7.57 – 7.56 (m, 2H), 7.12 – 7.09 (m, 2H), 6.98 – 6.95 (m, 2H), 6.87 – 6.84 (m, 2H), 6.14 – 6.13 (m, 2H). **<sup>13</sup>C-NMR** 150 MHz, DMSO-*d*<sup>6</sup> (δ) ppm = 167.23, 155.79, 150.87, 150.25, 149.29, 144.22, 140.10, 139.21, 131.49, 130.67, 129.12, 125.51, 125.46, 124.36, 122.70, 120.49. Anal. Calcd. For C<sub>32</sub>H<sub>24</sub>N<sub>4</sub>IrBr<sub>1</sub> (736.64): C 52.17, H 3.28, N 7.61. Found: C 51.56, H 3.67, N 7.28%

**6 [Br]** bright yellow solid, Y = 0.061 g, 0.074 mmol, 92%. **ESI-MS** (m/z), CH<sub>3</sub>CN: [M]<sup>+</sup> = 745, [M]<sup>-</sup> = 79, 81. **<sup>1</sup>H-NMR**, 400 MHz, DMSO-*d*<sup>6</sup> (δ) ppm = 8.84 – 8.82 (m, 2H), 8.22 – 8.19 (m, 2H), 8.09 – 8.08 (m, 2H), 7.84 – 7.81 (m, 2H), 7.79 – 7.78 (m, 2H), 7.66 – 7.64 (m, 2H), 7.56 – 7.55 (m, 2H), 7.01 – 6.98 (m, 2H), 6.49 – 6.43 (m, 2H), 5.37 – 5.36 (m, 2H), 3.46 (s, 6H), 2.65 (s, 6H). **<sup>13</sup>C-NMR** 150 MHz, DMSO-*d*<sup>6</sup> (δ) ppm = 167.11, 159.56, 155.59, 155.41, 150.14, 149.70, 139.98, 138.99, 138.69, 135.33, 129.11, 125.39, 124.62, 122.94, 122.42, 114.83, 112.05, 54.66, 24.13. Anal. Calcd. For C<sub>36</sub>H<sub>32</sub>N<sub>4</sub>O<sub>2</sub>IrBr<sub>1</sub> (824.74) C 52.42, H 3.91, N 6.79. Found: C 48.56, H 3.68, N 6.20%

## NMR Spectroscopy

**Figure S1:**  $^1\text{H}$ -NMR of **4-chloro-2-phenylpyridine**, 400 MHz,  $\text{CDCl}_3$ , 298K.

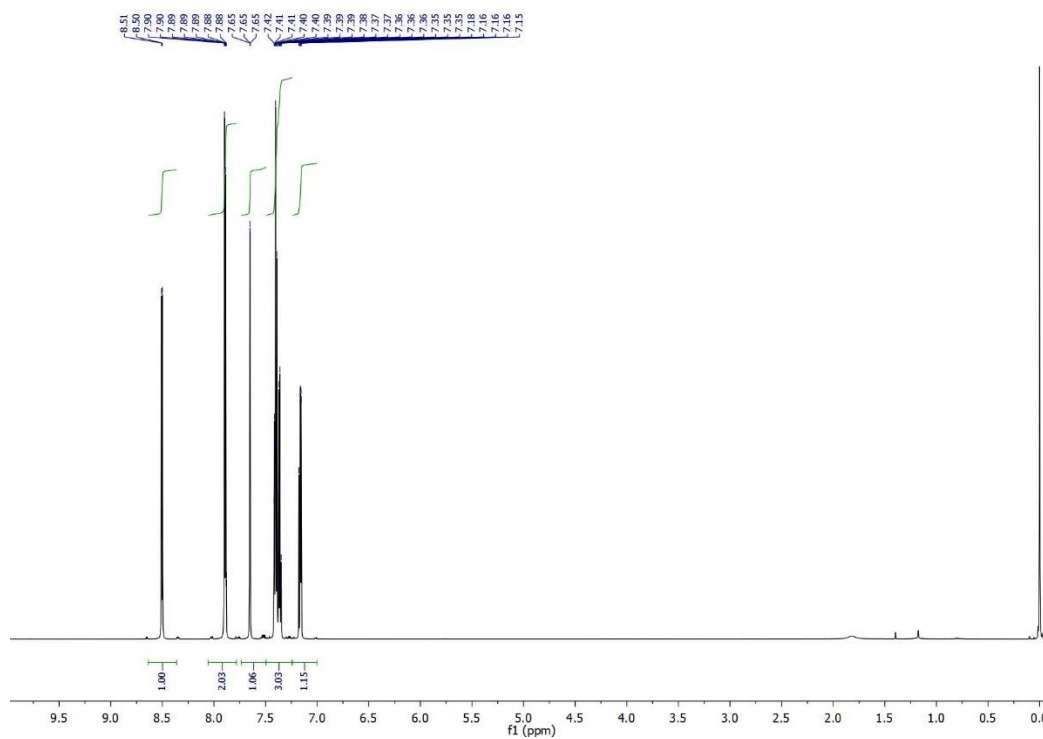


**Figure S2:**  $^{13}\text{C}$ -NMR of **4-chloro-2-phenylpyridine**, 100 MHz,  $\text{CDCl}_3$ , 298K.

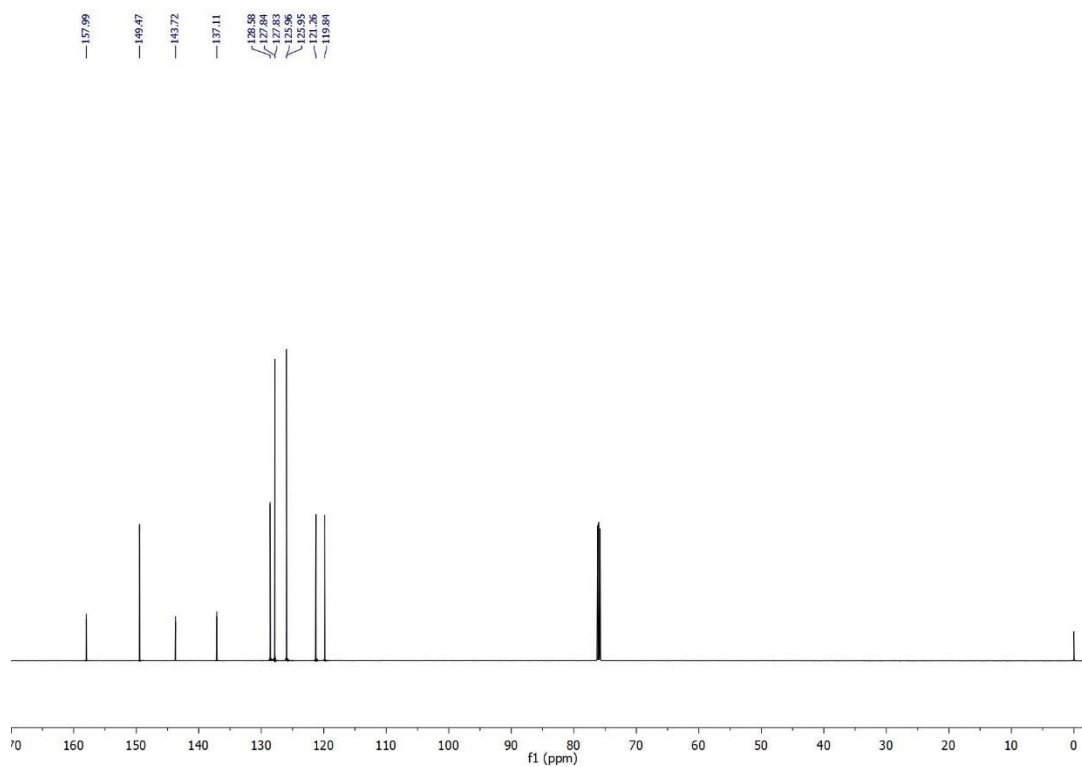


**Figure S3:**  $^1\text{H}$ -NMR of *N,N*-dimethyl-2-phenylpyridin-4-amine (ppy-NMe<sub>2</sub>), 400 MHz, CDCl<sub>3</sub>, 298K.

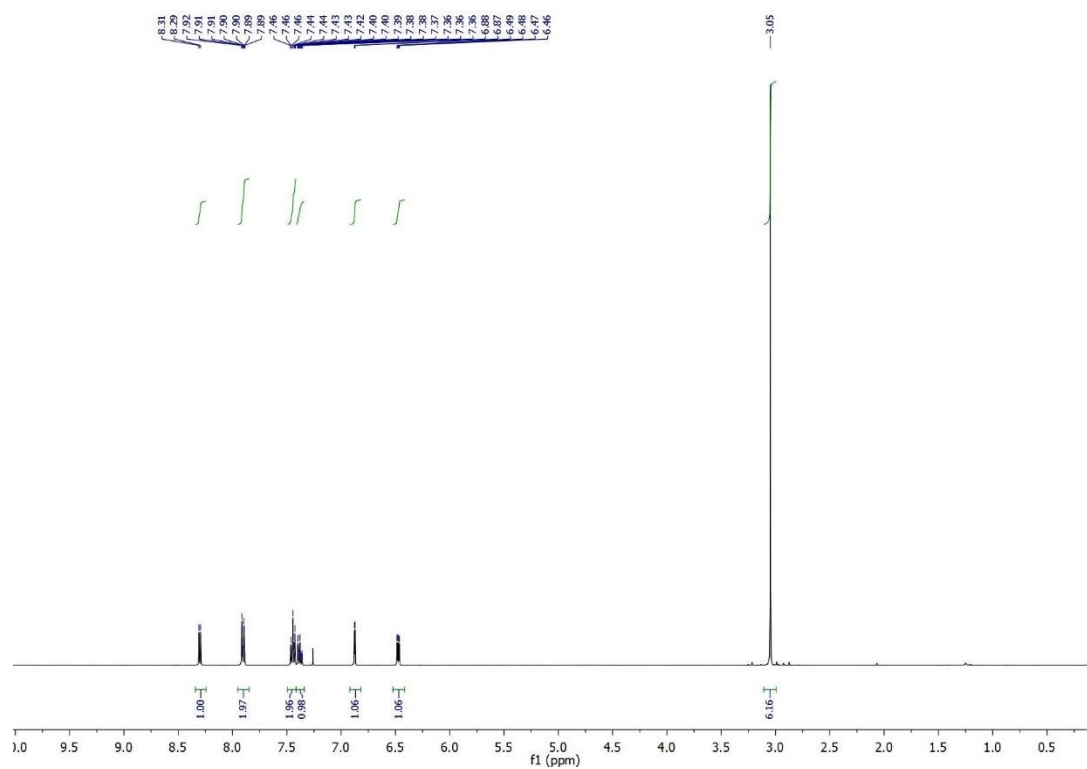


**Figure S4:**  $^{13}\text{C}$ -NMR of *N,N*-dimethyl-2-phenylpyridin-4-amine (ppy-NMe<sub>2</sub>), 100 MHz, CDCl<sub>3</sub>, 298K.

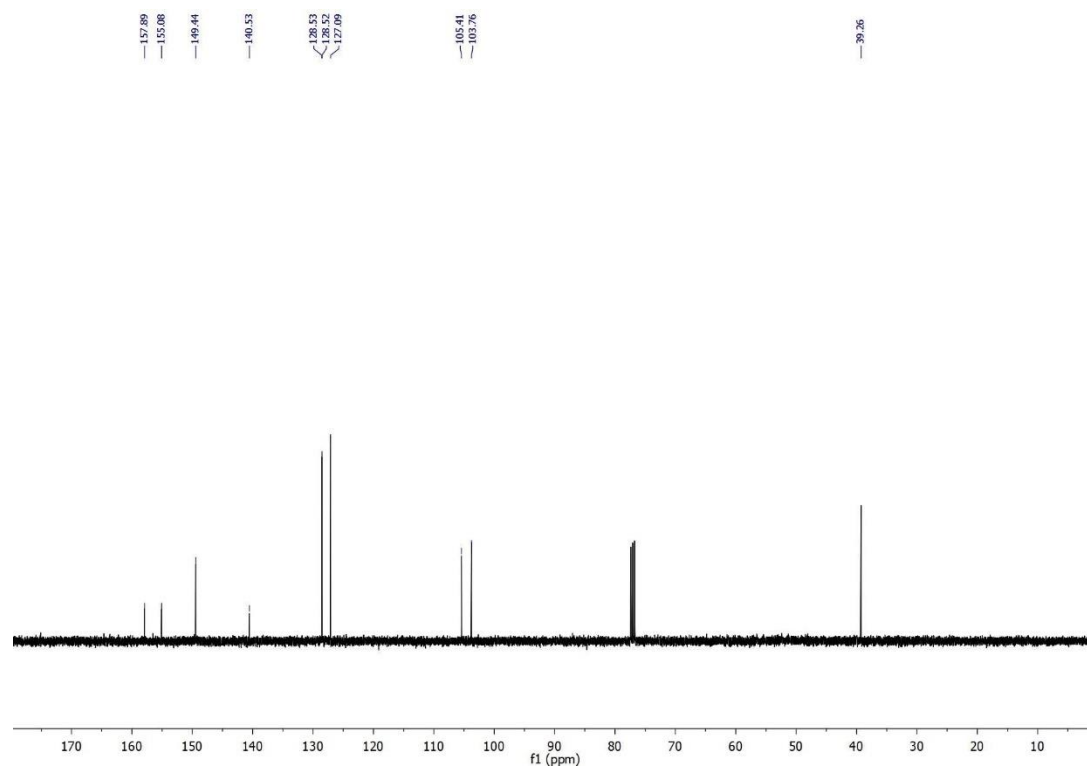


Figure S5:  $^1\text{H}$ -NMR of **4,4'-Bis(dimethylamino)-2,2'-bipyridine - (bpy-(NMe<sub>2</sub>)<sub>2</sub>)**, CDCl<sub>3</sub>, 400 MHz.

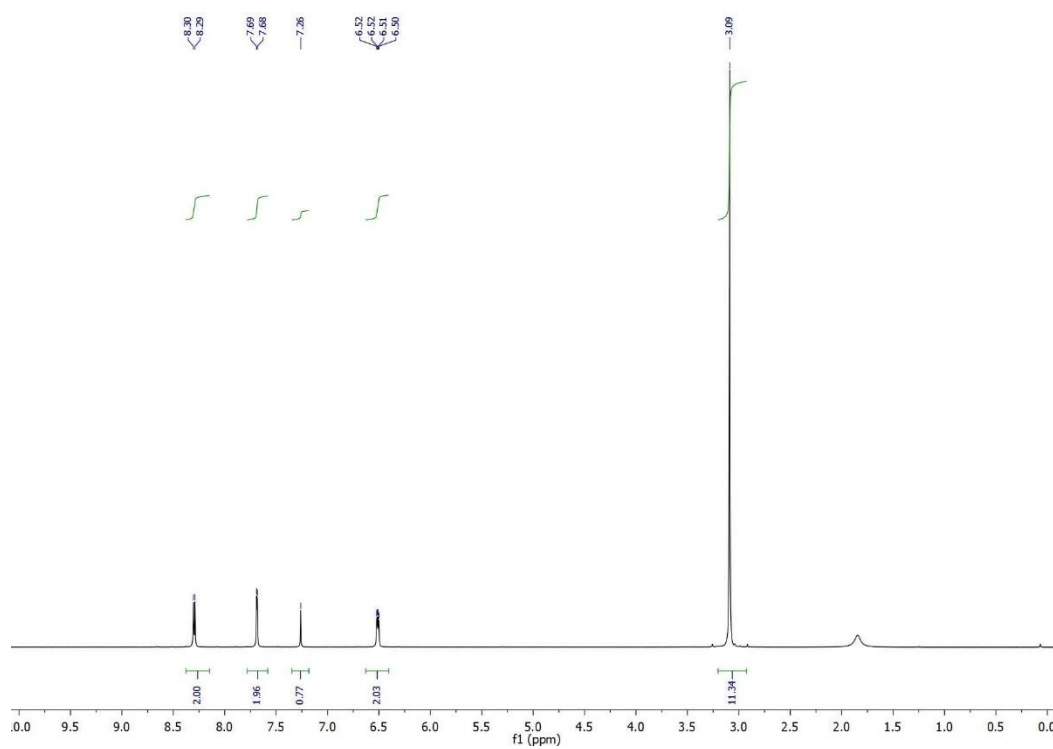


Figure S6:  $^{13}\text{C}$ -NMR of **4,4'-Bis(dimethylamino)-2,2'-bipyridine - (bpy-(NMe<sub>2</sub>)<sub>2</sub>)**, CDCl<sub>3</sub>, 100 MHz.

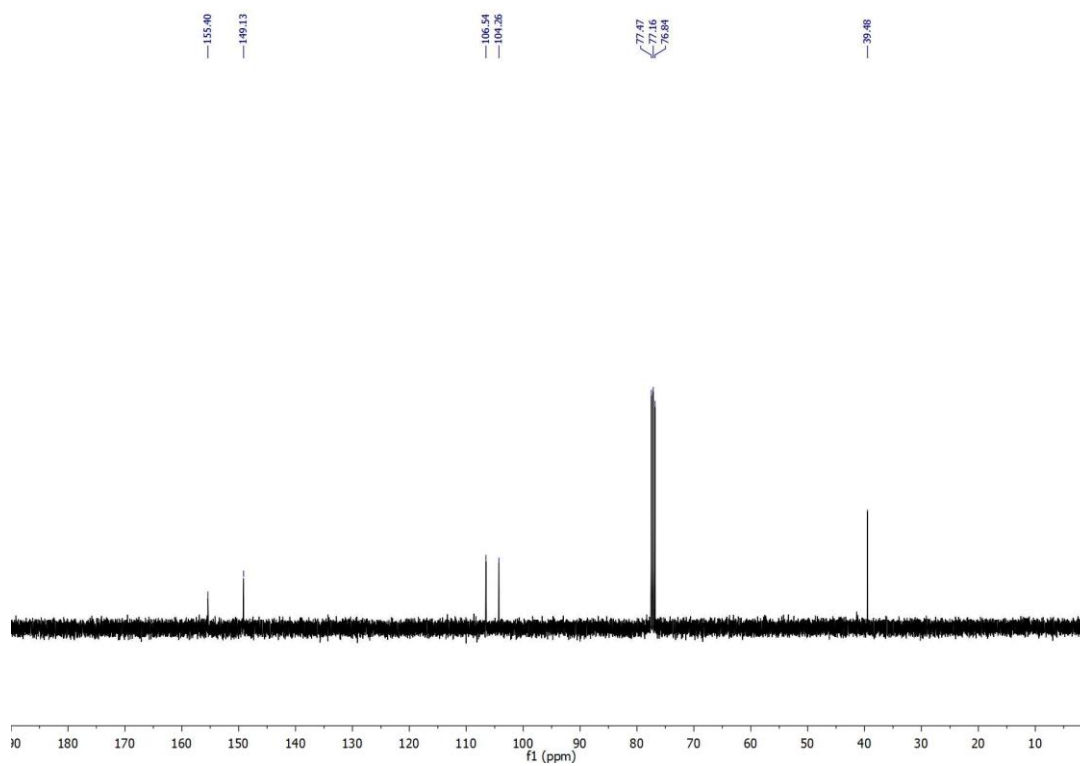


Figure S7:  $^1\text{H}$ -NMR of - (**bpy**-(**pyr**) $_2$ ),  $\text{CDCl}_3$ , 400 MHz.

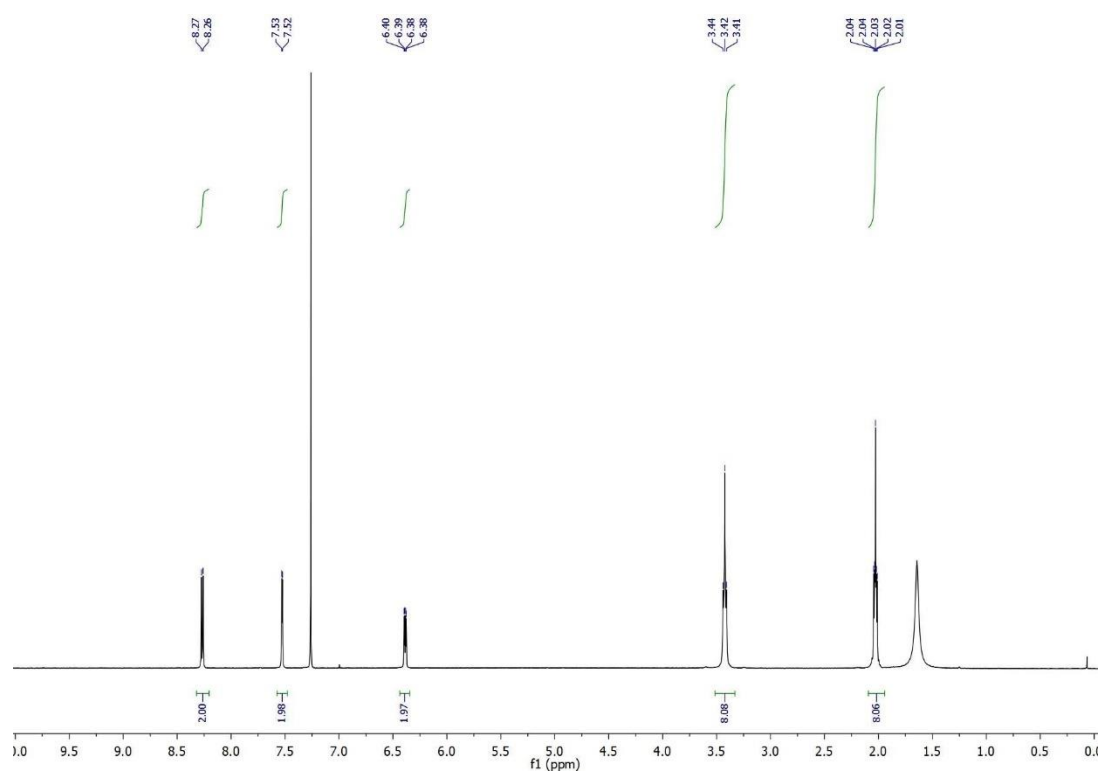


Figure S8:  $^{13}\text{C}$ -NMR of - (**bpy**-(**pyr**) $_2$ ),  $\text{CDCl}_3$ , 100 MHz.

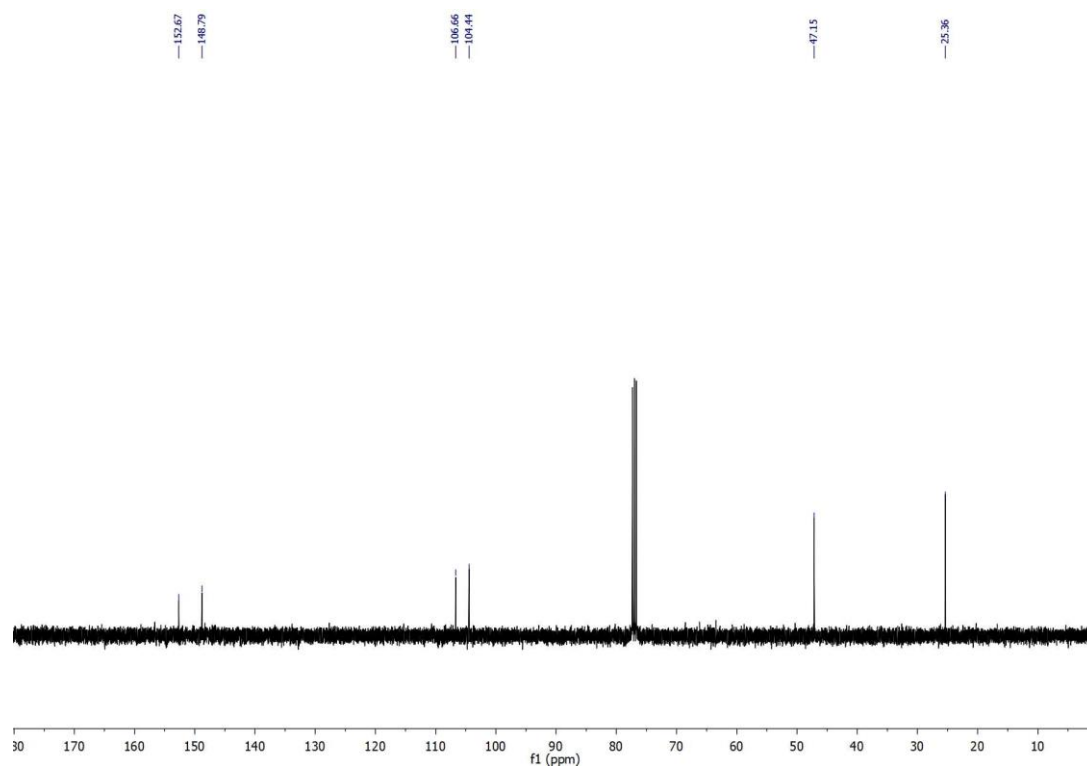


Figure S9:  $^1\text{H}$ -NMR of **1** [ $\text{PF}_6$ ], Acetone- $d^6$ , 400 MHz.

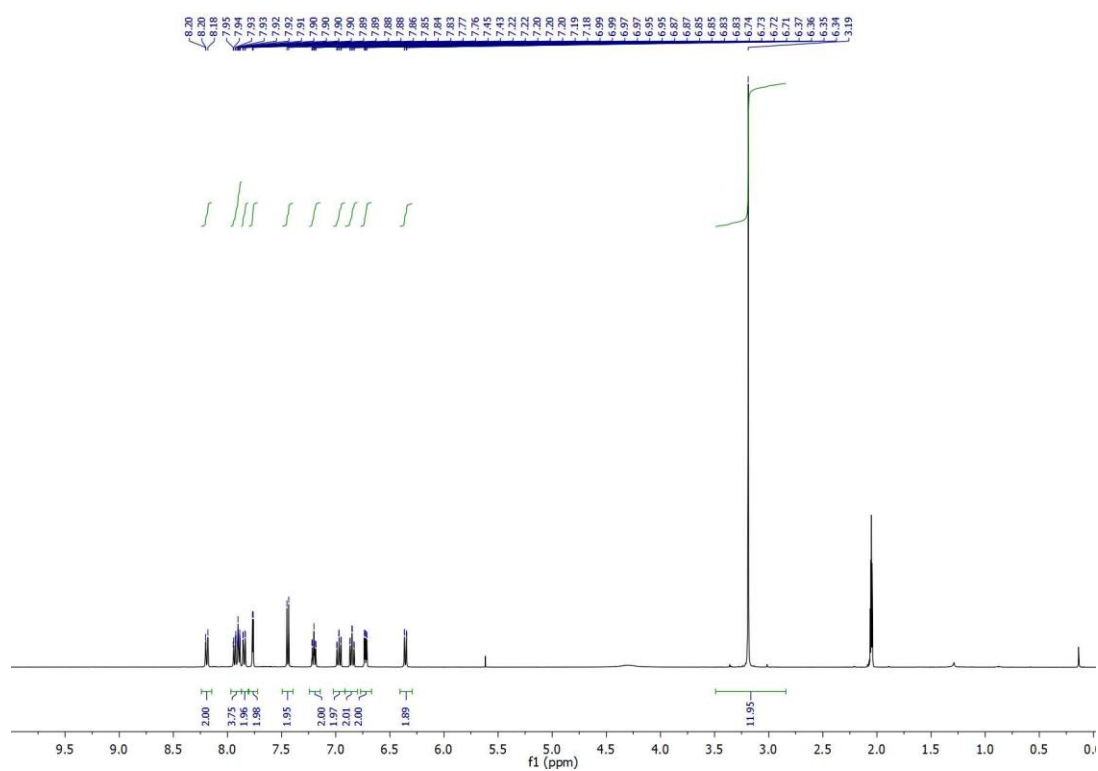


Figure S10:  $^{13}\text{C}$ -NMR of **1** [ $\text{PF}_6$ ], Acetone- $d^6$ , 100 MHz.

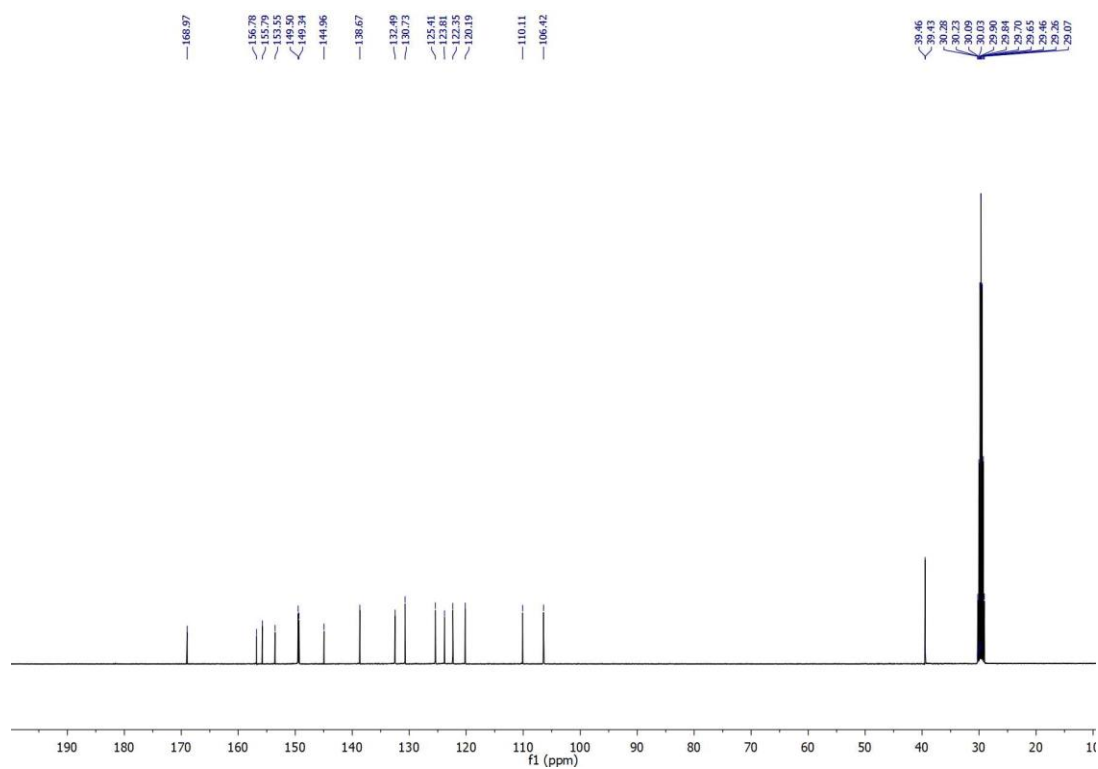


Figure S11:  $^1\text{H}$ -NMR of **1[Br]**,  $\text{DMSO-}d^6$ , 400 MHz.

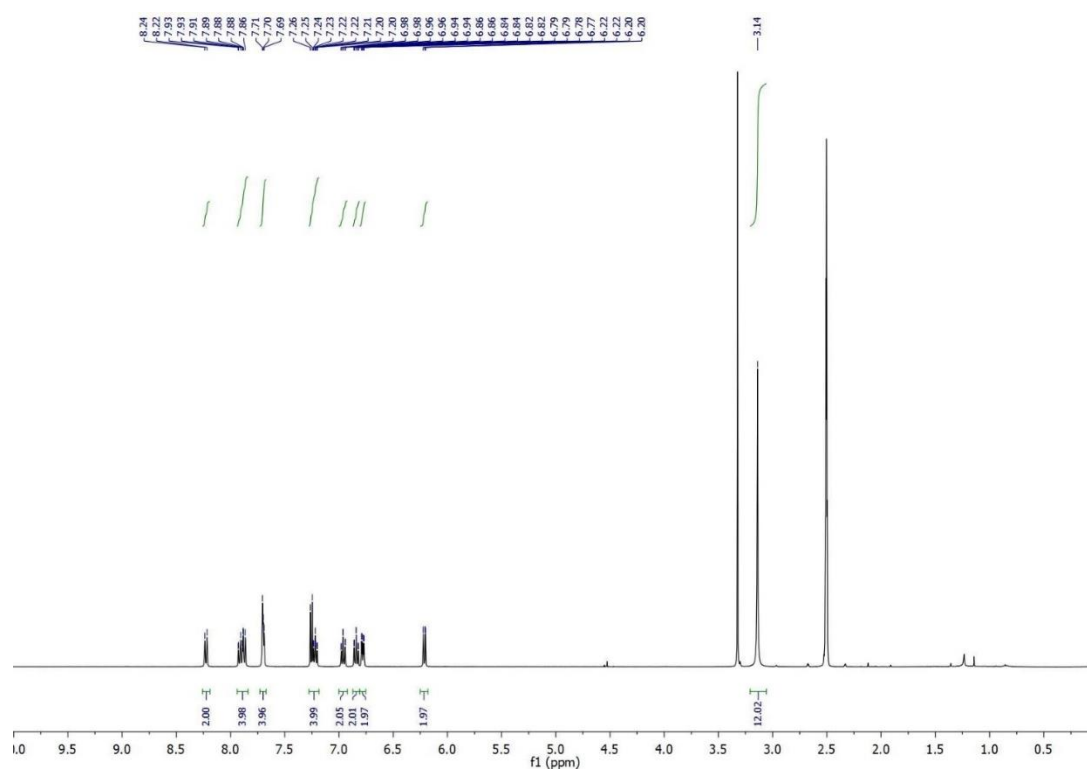


Figure S12:  $^{13}\text{C}$ -NMR of **1[Br]**,  $\text{DMSO-}d^6$ , 100 MHz.  $\text{N-(CH}_3)_2$  signal falls within the non-deuterated residual of  $\text{DMSO-}d^6$ .

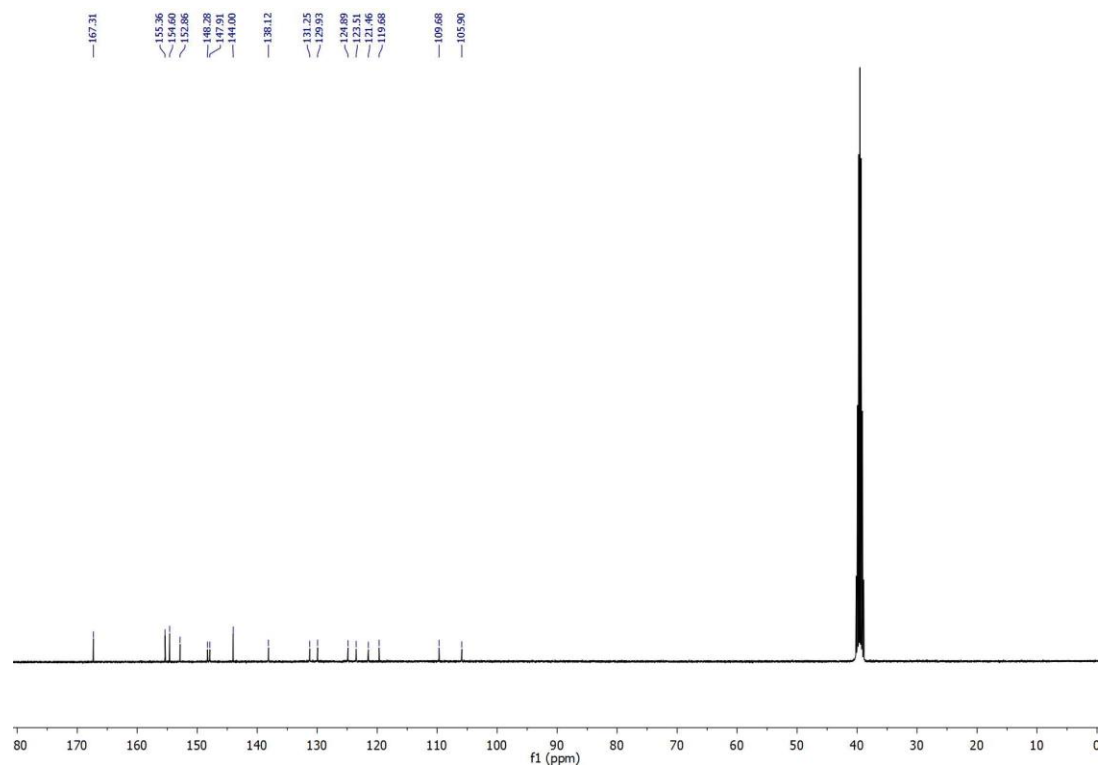


Figure S13:  $^1\text{H}$ -NMR of **1**[ $\text{BF}_4$ ], Acetone- $d_6$ , 400 MHz.

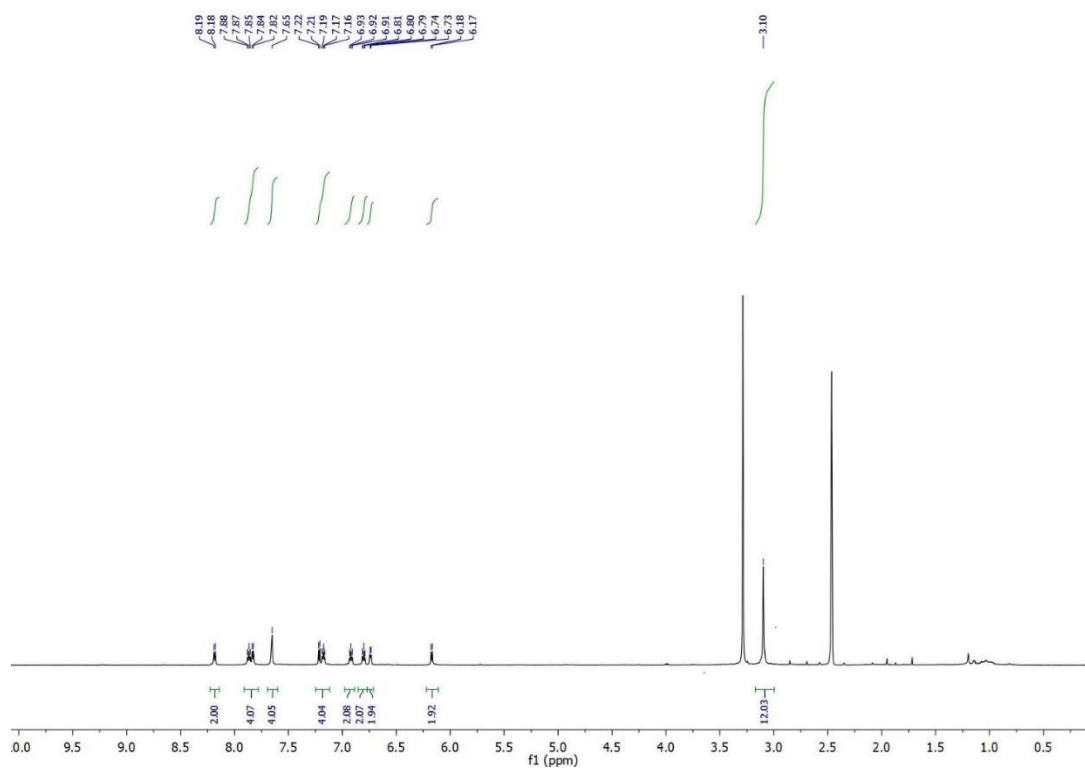


Figure S14:  $^{13}\text{C}$ -NMR of **1**[ $\text{BF}_4$ ], DMSO- $d_6$ , 100 MHz.

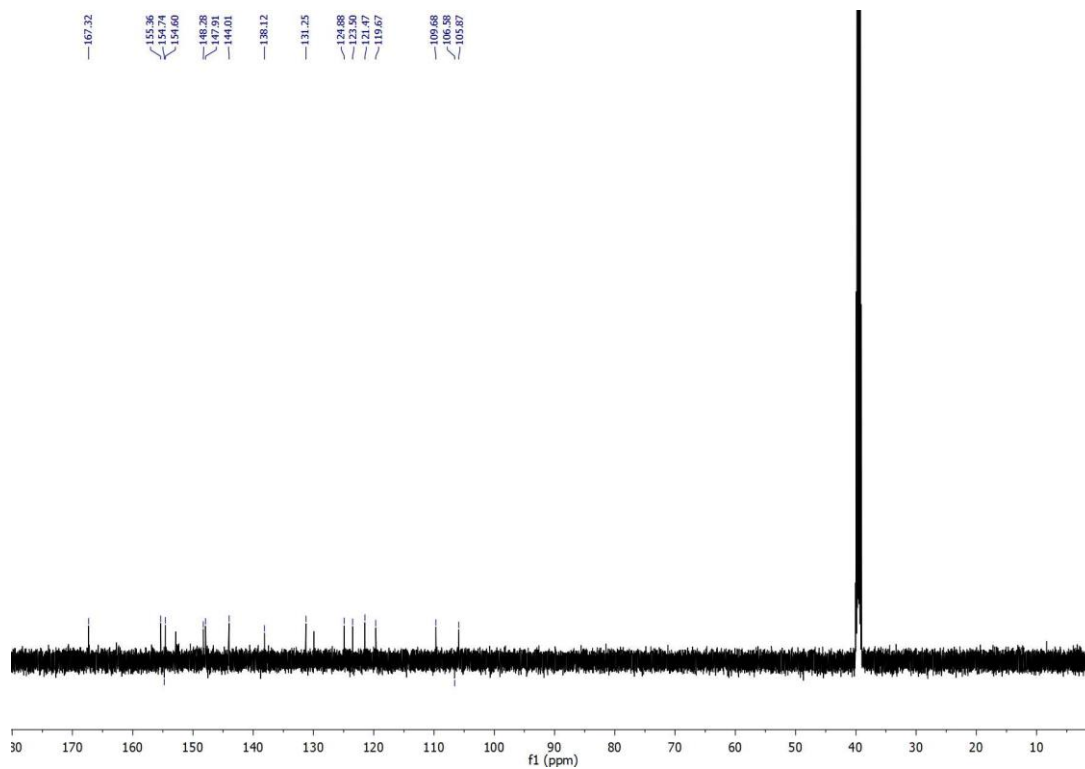




Figure S15:  $^1\text{H}$ -NMR of **2**[PF<sub>6</sub>], Acetone- $d_6$ , 400 MHz.

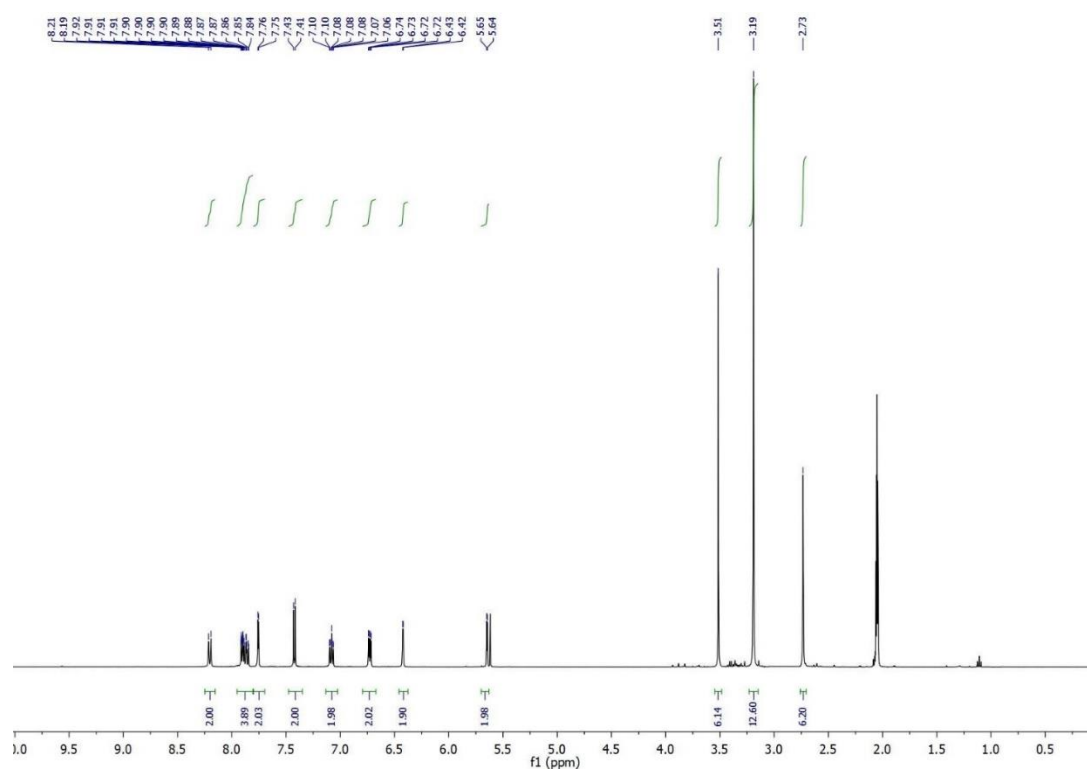


Figure S16:  $^{13}\text{C}$ -NMR of **2**[PF<sub>6</sub>], Acetone- $d_6$ , 100 MHz.

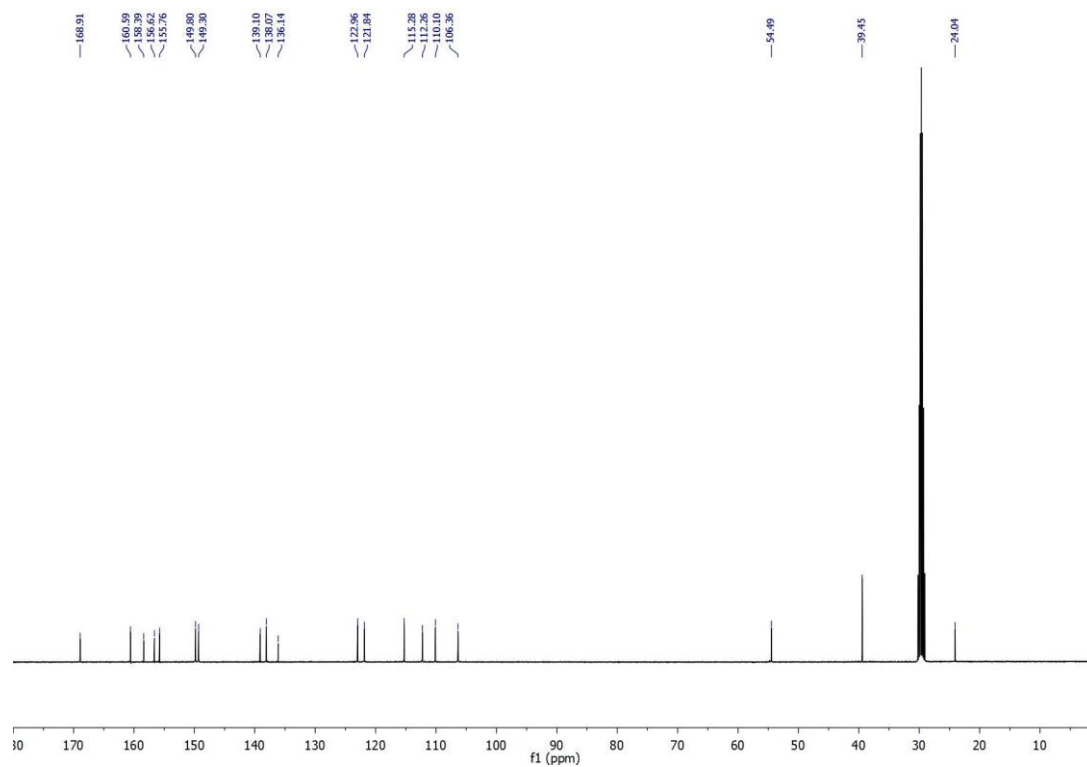


Figure S17:  $^1\text{H}$ -NMR of **2[Br]**,  $\text{DMSO-}d^6$ , 400 MHz.

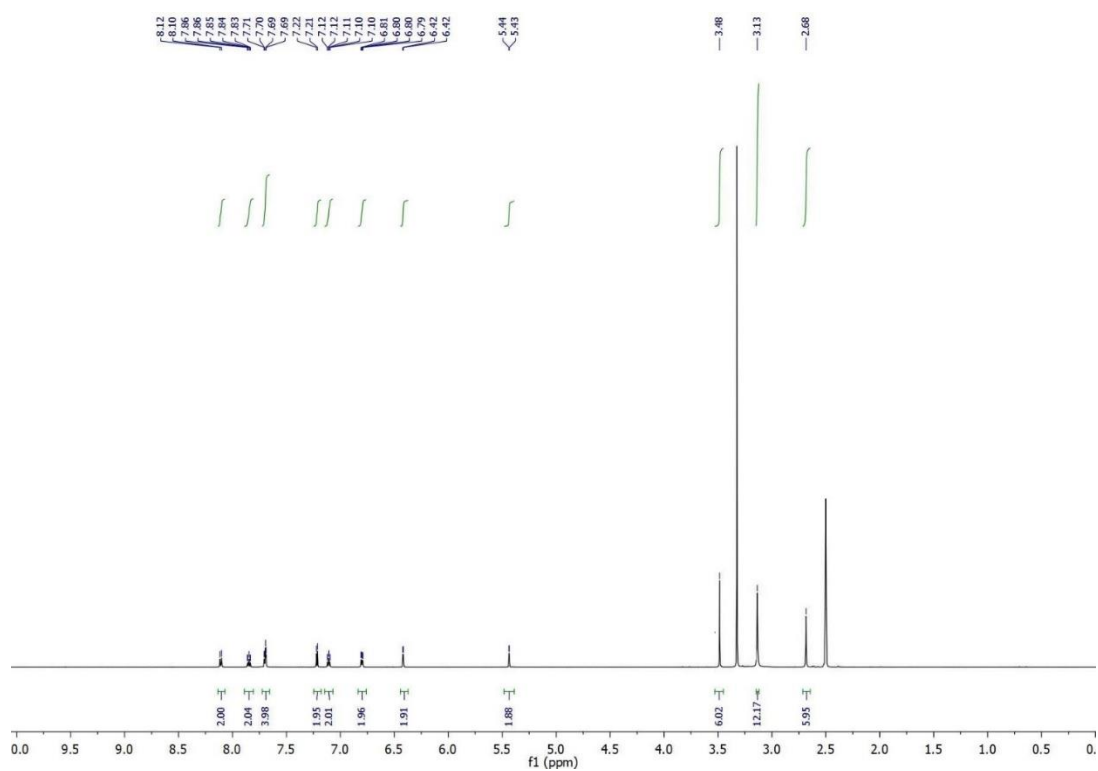


Figure S18:  $^{13}\text{C}$ -NMR of **2[Br]**,  $\text{DMSO-}d^6$ , 100 MHz.  $\text{N-(CH}_3)_2$  signal falls within the non-deuterated residual of  $\text{DMSO-}d^6$ .

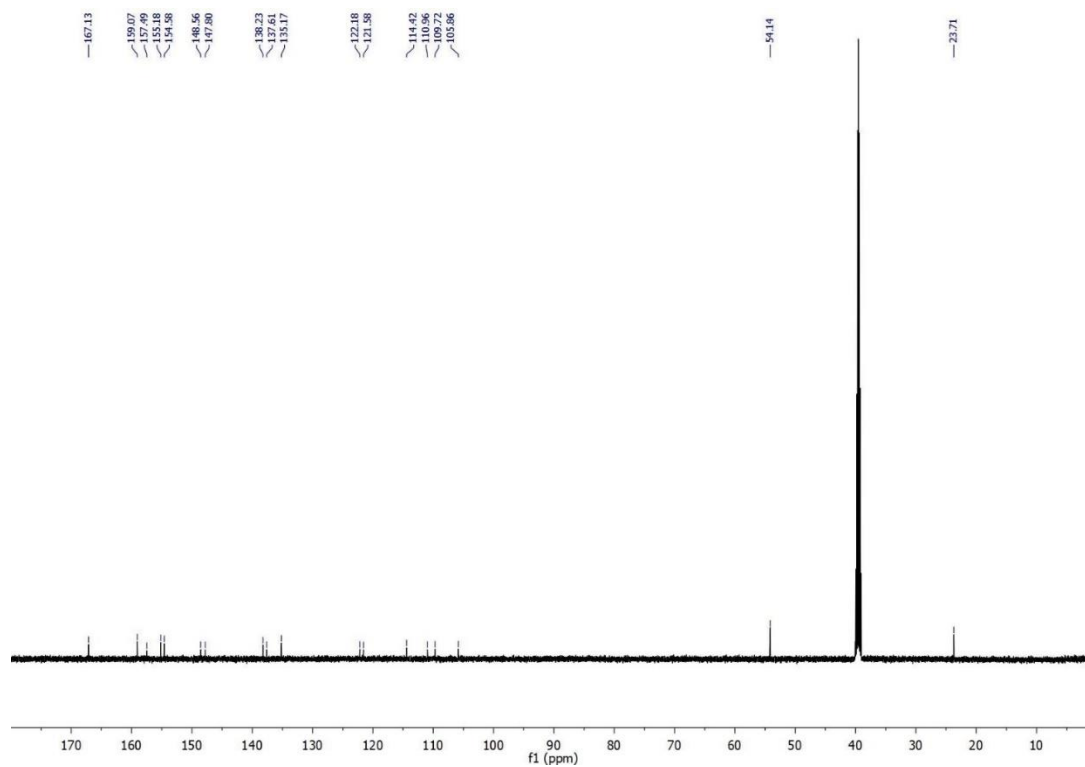


Figure S19:  $^1\text{H}$ -NMR of **3**[PF<sub>6</sub>], Acetone-*d*<sup>6</sup>, 400 MHz.

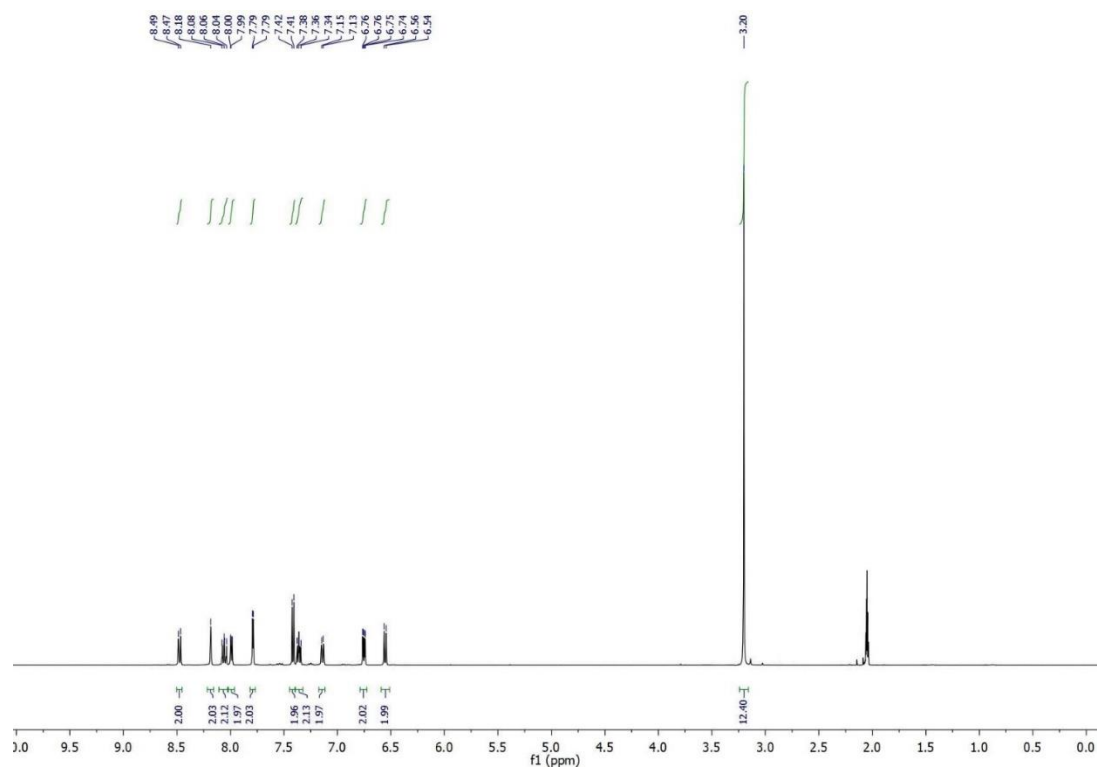


Figure S20:  $^{13}\text{C}$ -NMR of **3**[PF<sub>6</sub>], Acetone-*d*<sup>6</sup>, 100 MHz.

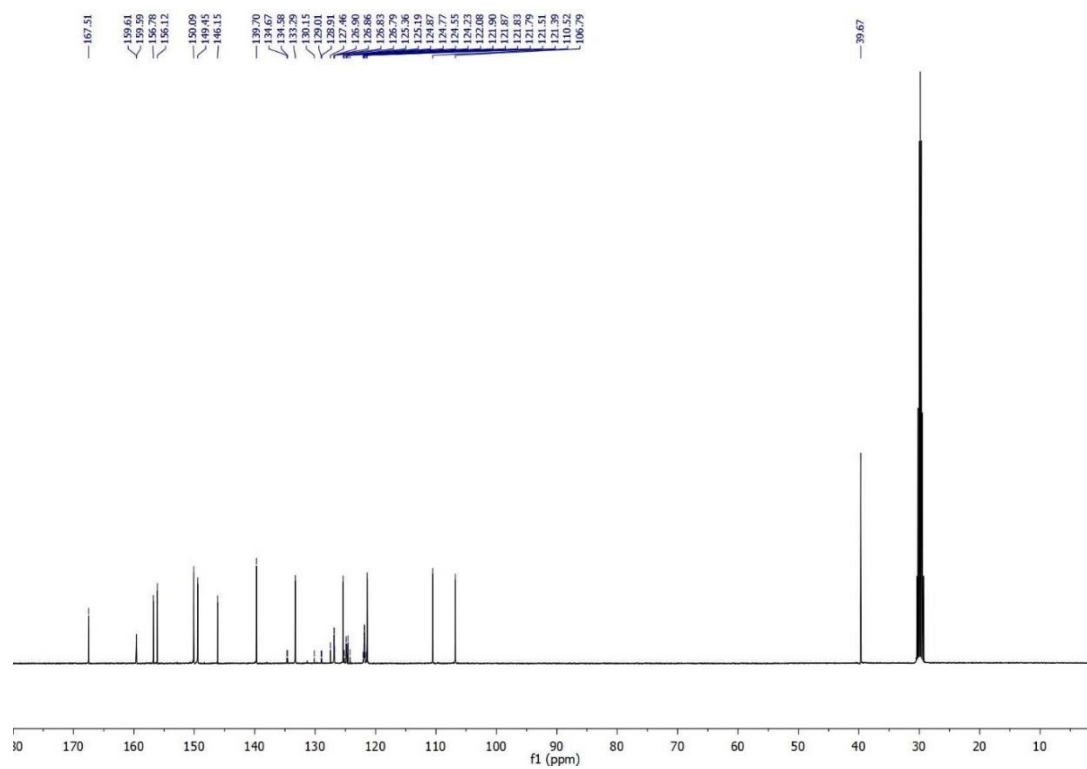


Figure S21:  $^1\text{H}$ -NMR of **4**[PF<sub>6</sub>], Acetone-*d*<sup>6</sup>, 400 MHz.

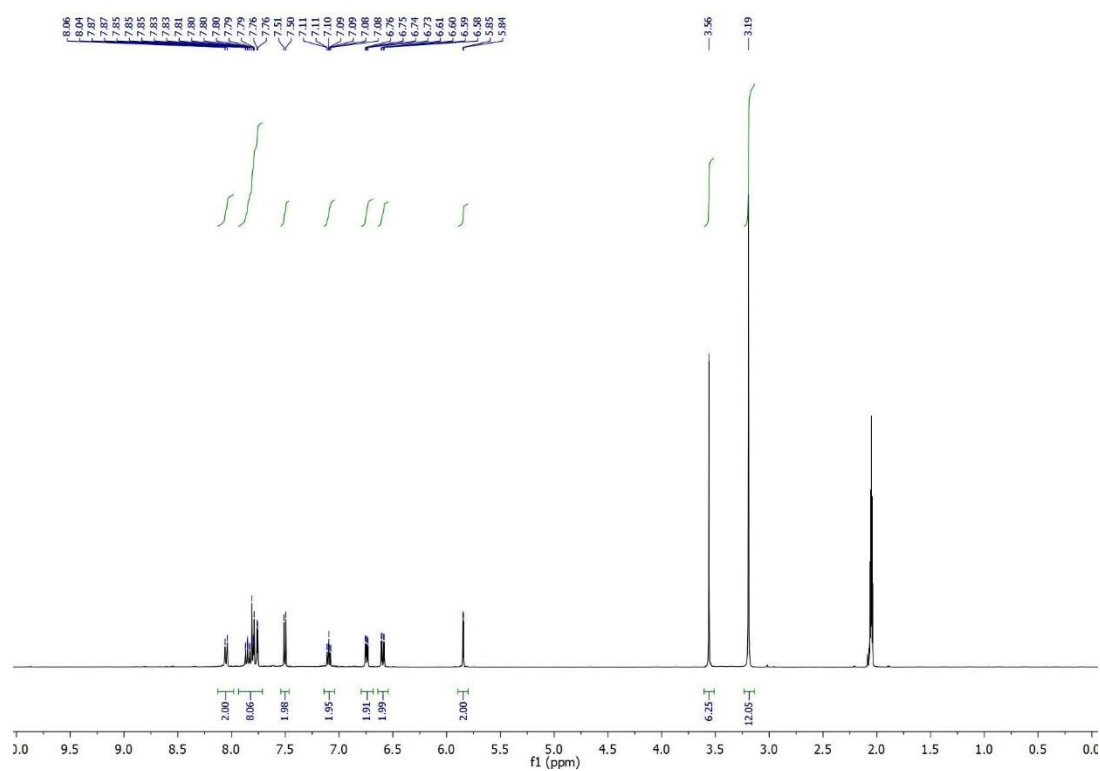


Figure S22:  $^{13}\text{C}$ -NMR of **4**[PF<sub>6</sub>], Acetone-*d*<sup>6</sup>, 100 MHz.

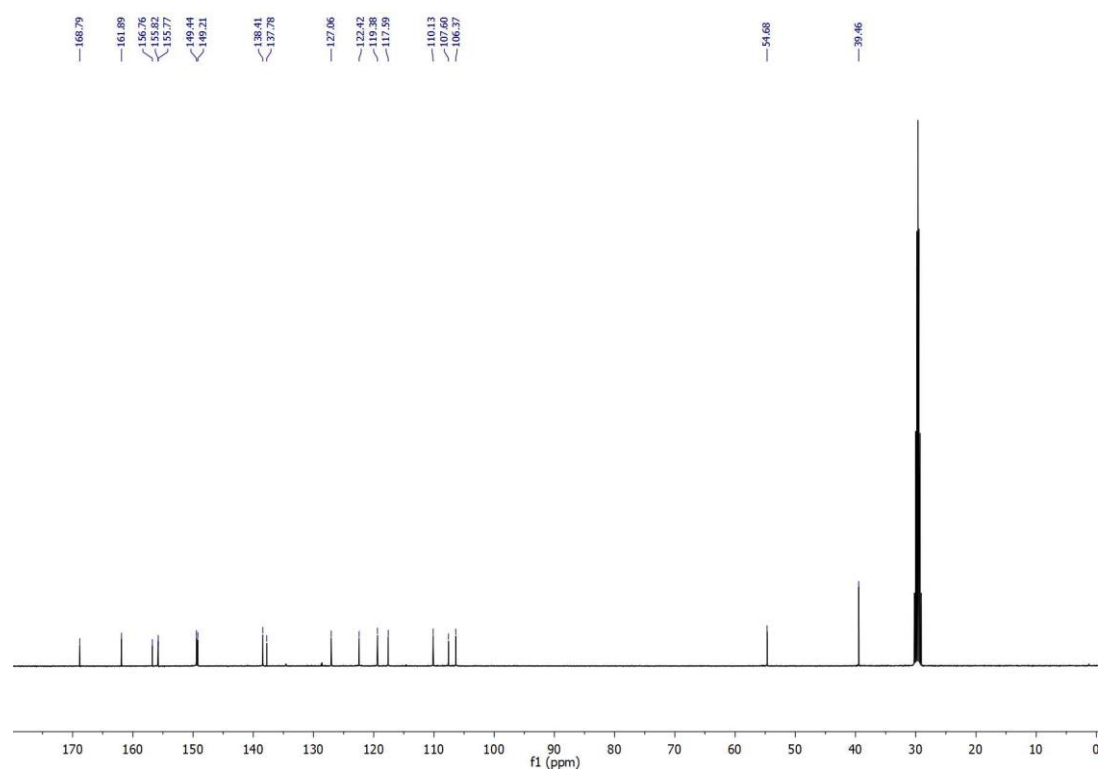


Figure S23:  $^1\text{H}$ -NMR of **4[Br]**,  $\text{DMSO-}d^6$ , 400 MHz.

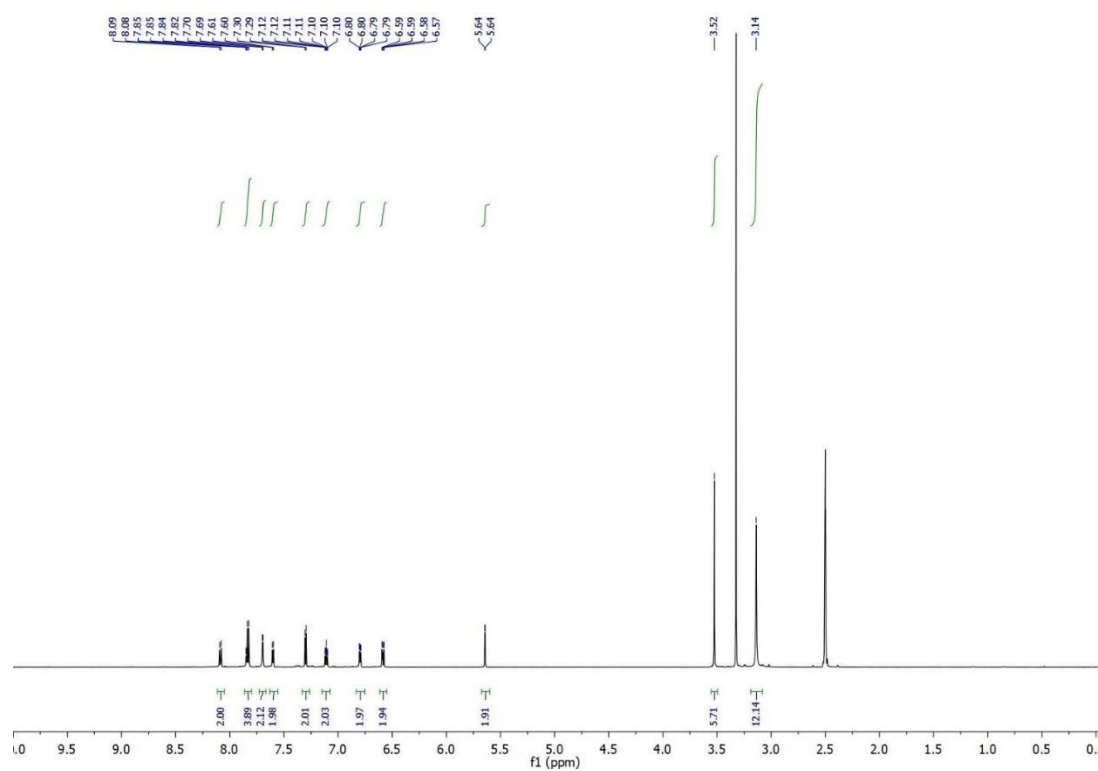


Figure S24:  $^{13}\text{C}$ -NMR of **4[Br]**,  $\text{DMSO-}d^6$ , 100 MHz.  $\text{N-(CH}_3)_2$  signal falls within the non-deuterated residual of  $\text{DMSO-}d^6$ .

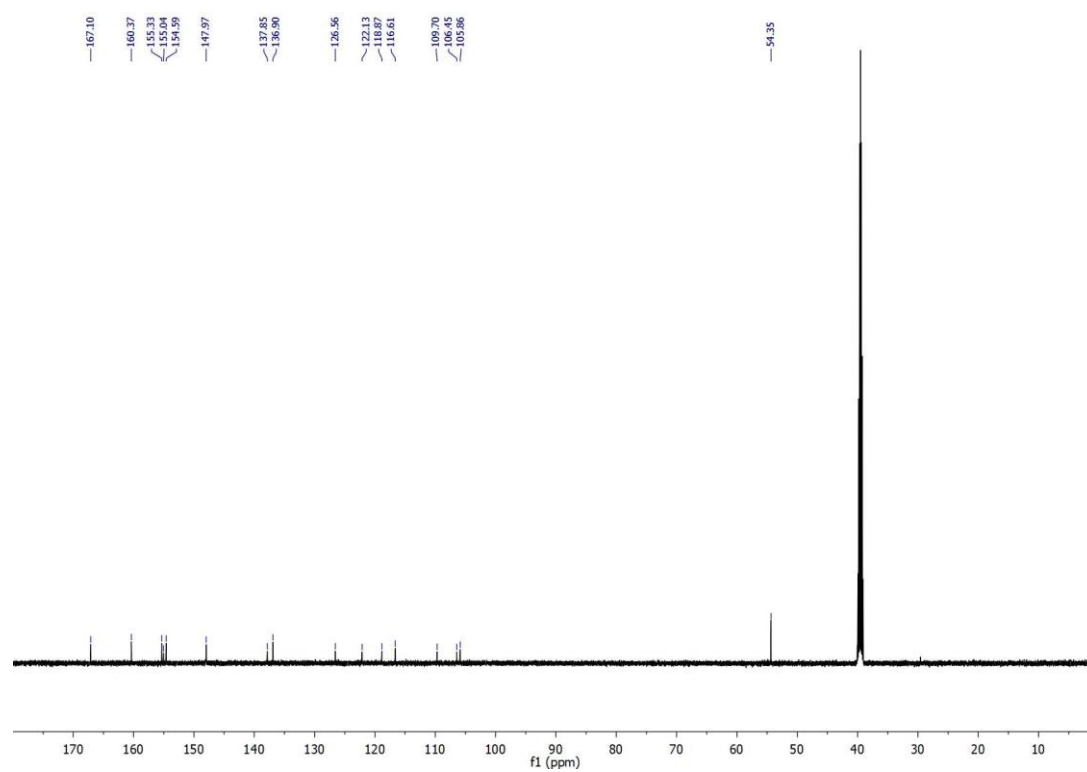


Figure S25:  $^1\text{H}$ -NMR of **7[Br]**, DMSO- $d^6$ , 400 MHz.

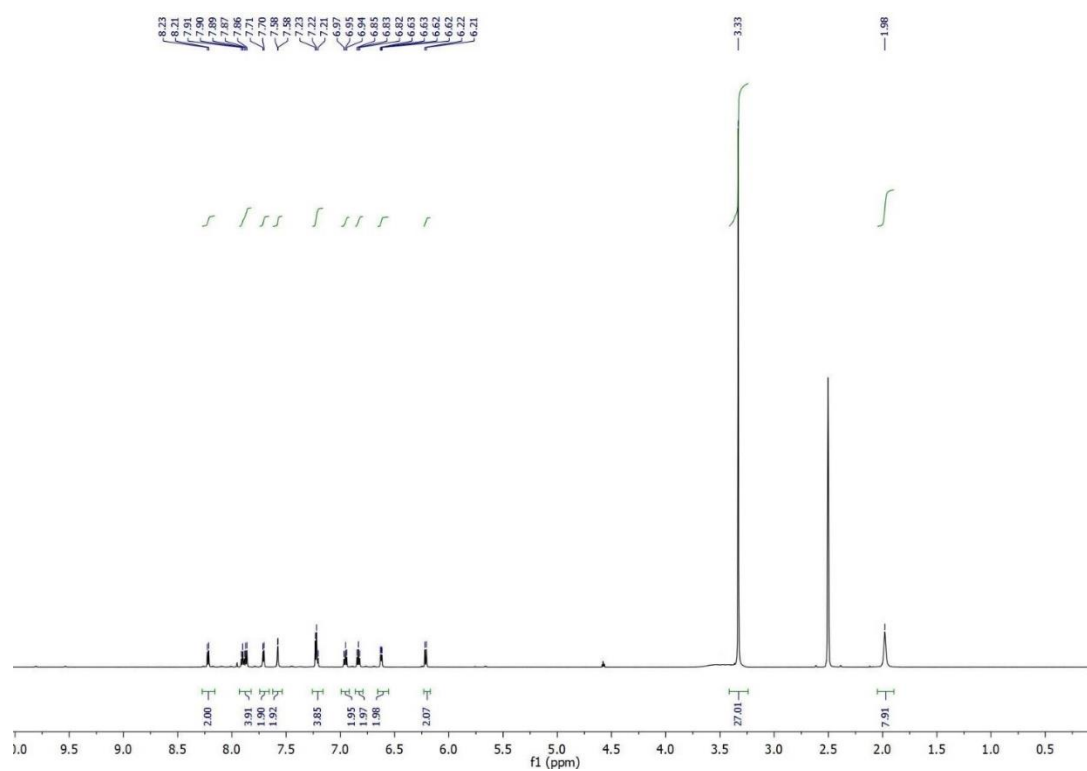


Figure S26:  $^{13}\text{C}$ -NMR of **7[Br]**, DMSO- $d^6$ , 100 MHz.

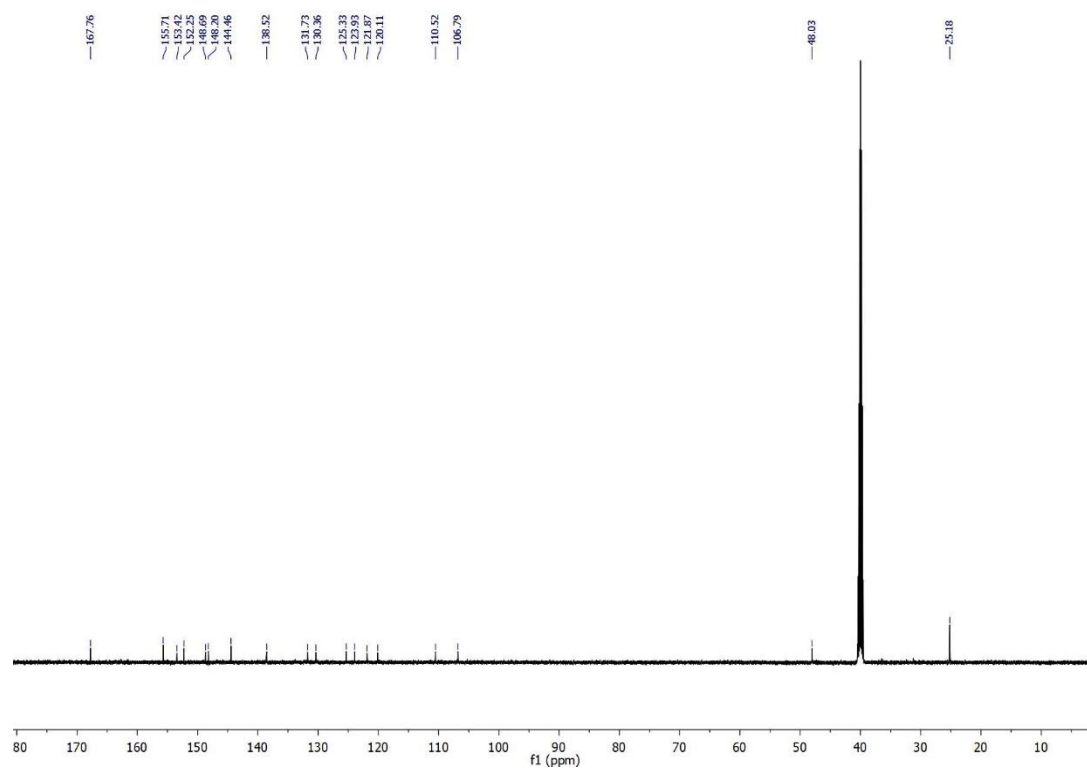


Figure S27:  $^1\text{H}$ -NMR of **8[Br]**, Acetone- $d_6$ , 400 MHz.

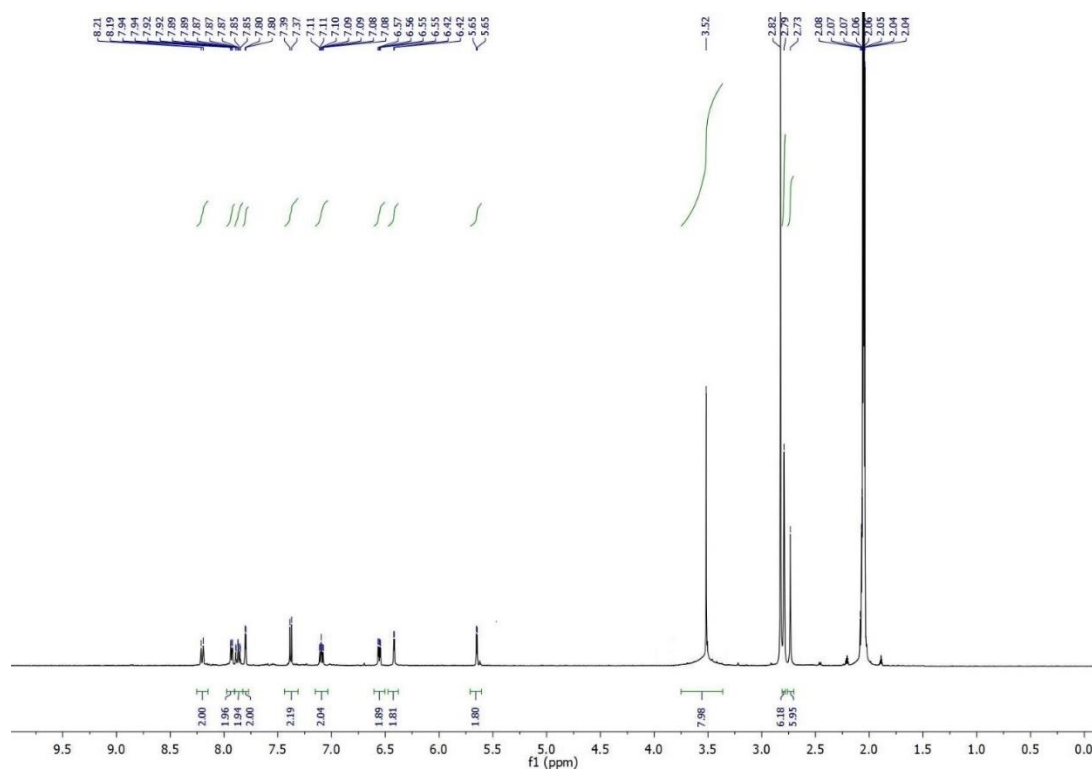


Figure S28:  $^{13}\text{C}$ -NMR of **8[Br]**, DMSO- $d_6$ , 150 MHz.

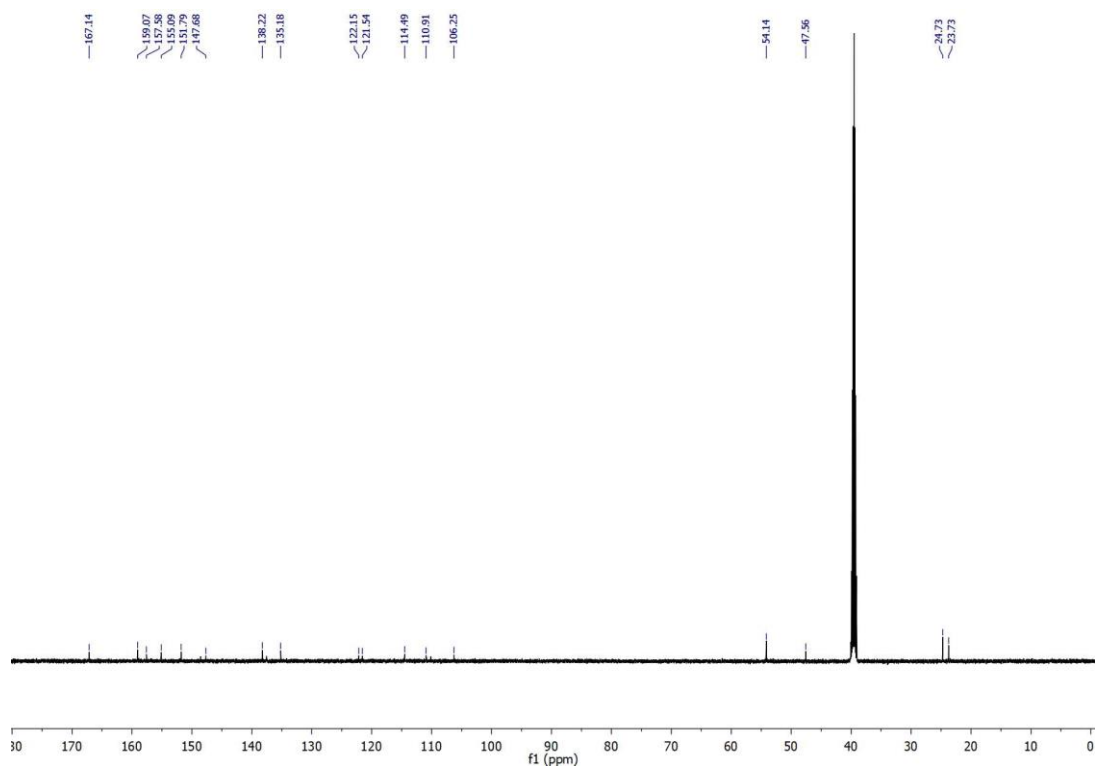


Figure S29:  $^1\text{H}$ -NMR of **9[Br]**,  $\text{DMSO-}d^6$ , 400 MHz.

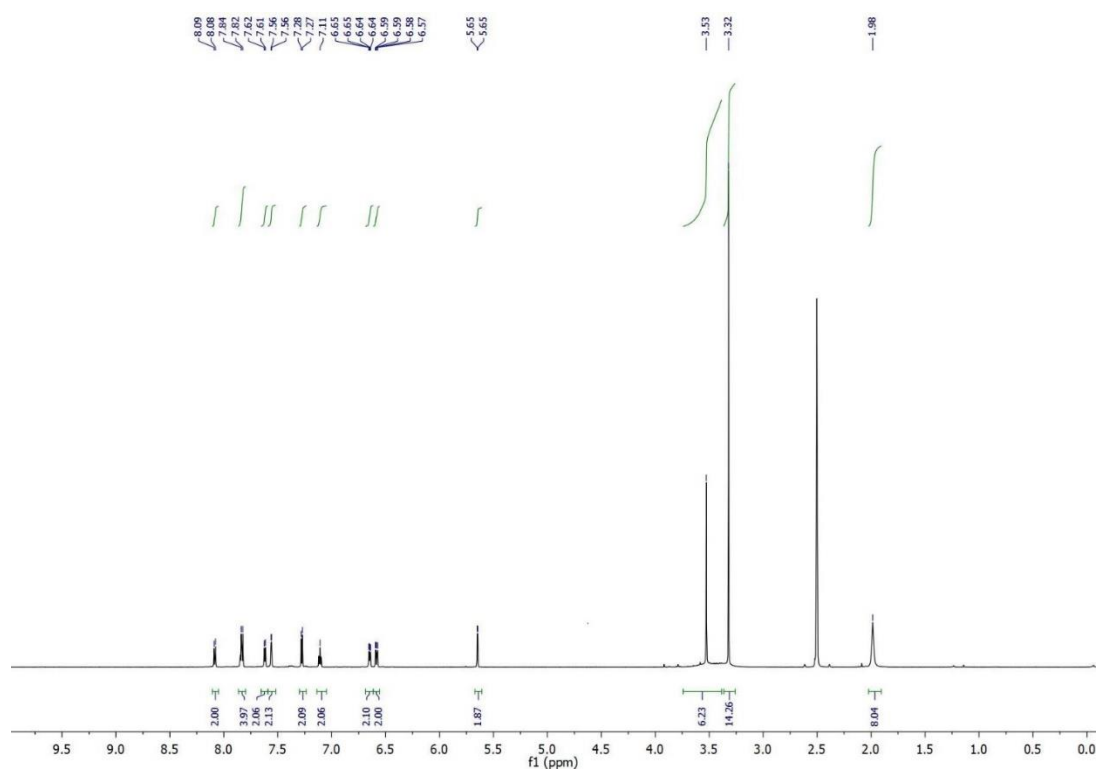


Figure S30:  $^{13}\text{C}$ -NMR of **9[Br]**,  $\text{DMSO-}d^6$ , 100 MHz.

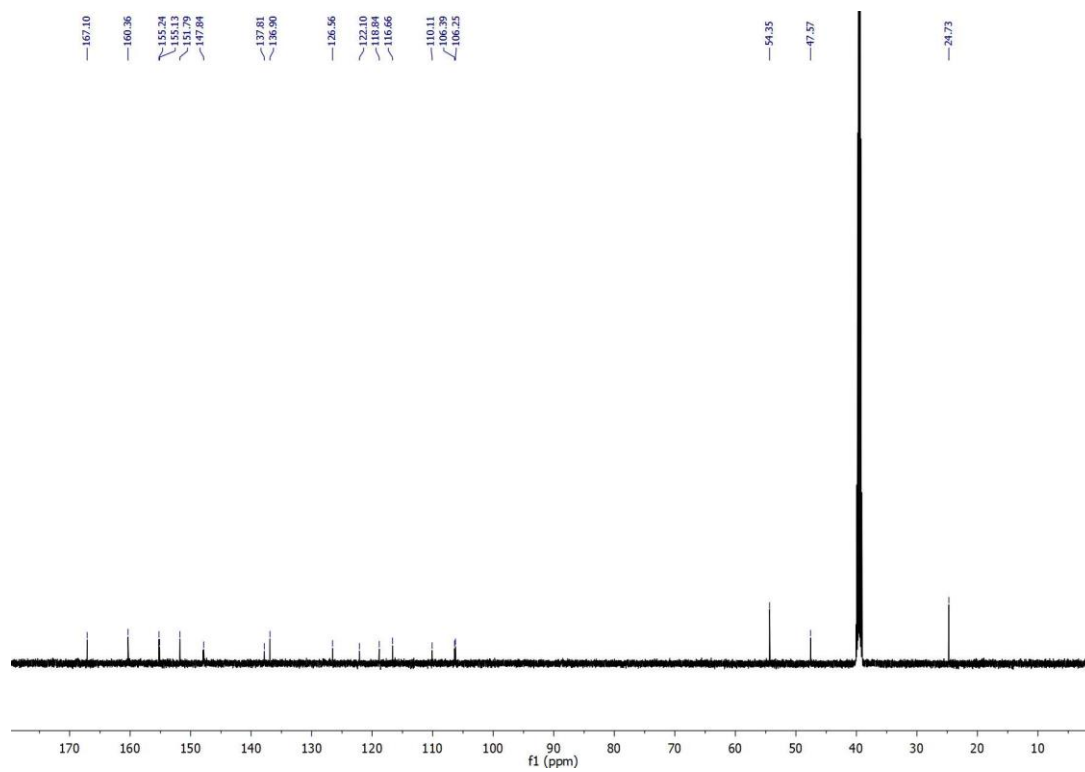




Figure S31:  $^1\text{H}$ -NMR of **10[Br]**,  $\text{DMSO-}d^6$ , 400 MHz.

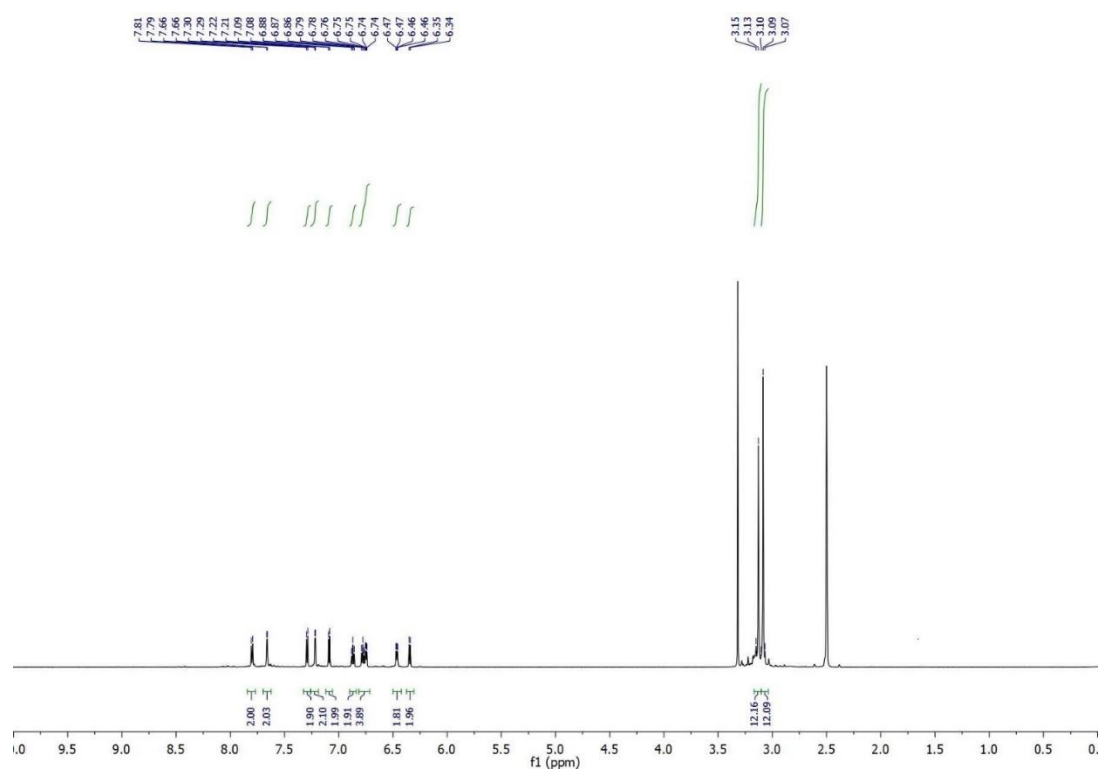


Figure S32:  $^{13}\text{C}$ -NMR of **10[Br]**,  $\text{DMSO-}d^6$ , 100 MHz.

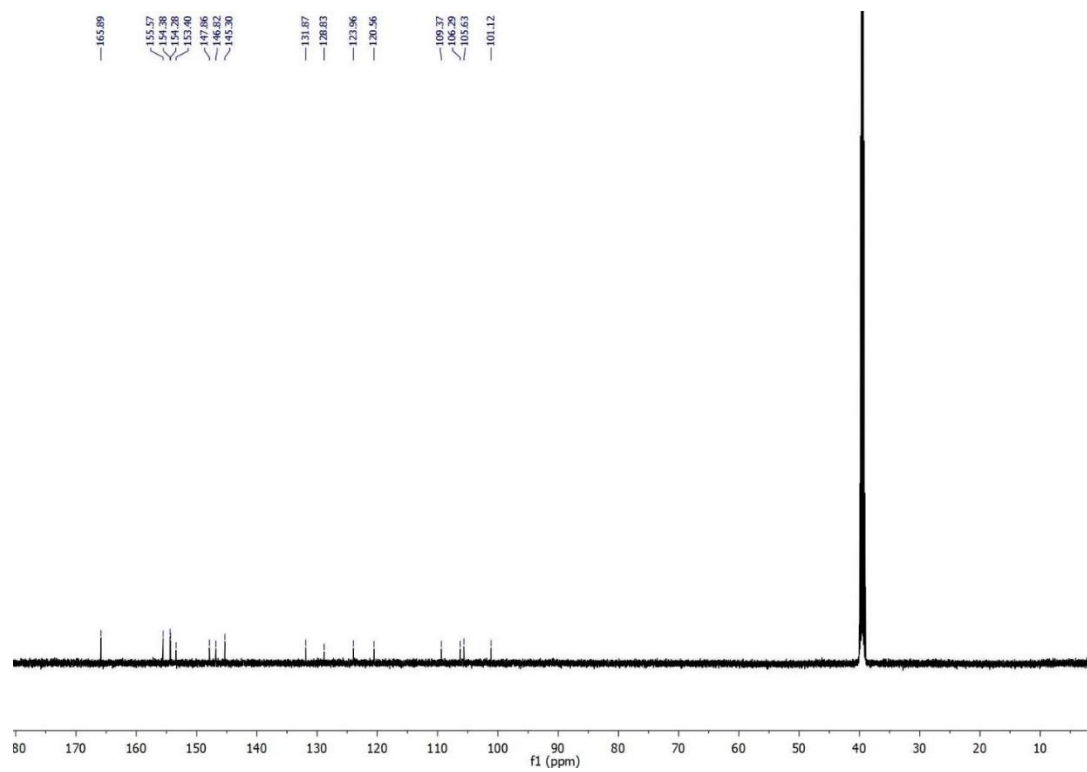


Figure S33:  $^1\text{H}$ -NMR of **11[Br]**,  $\text{DMSO-}d^6$ , 400 MHz.

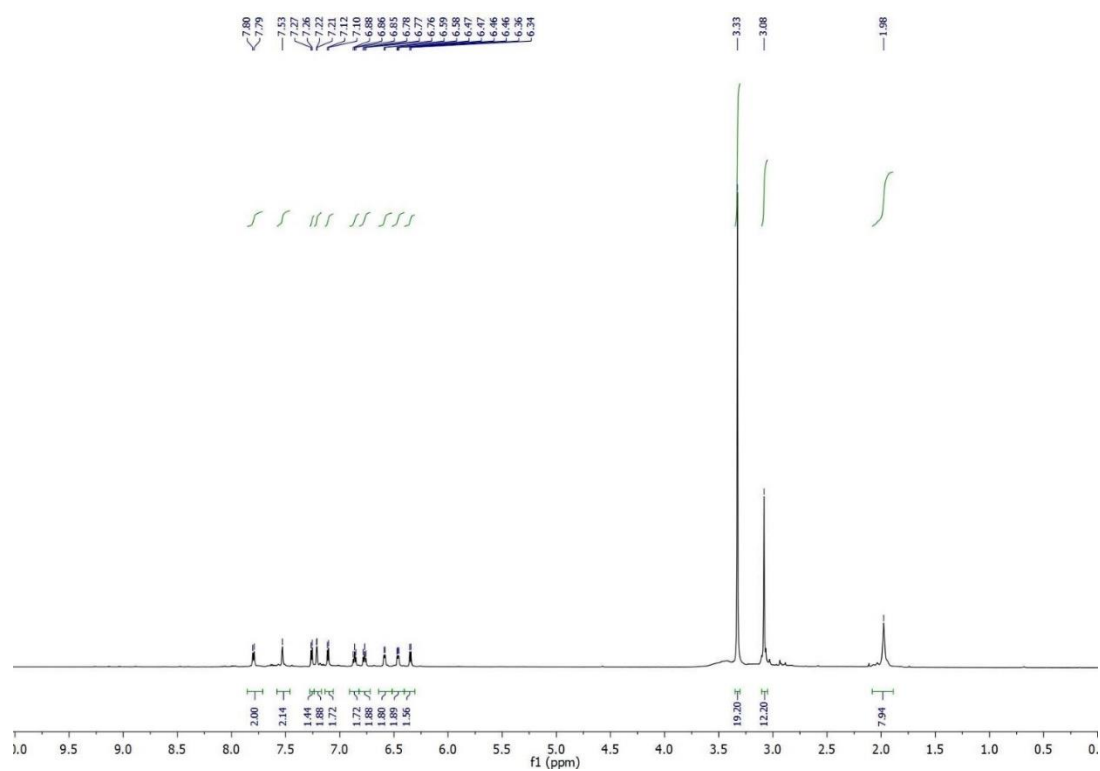


Figure S34:  $^{13}\text{C}$ -NMR of **11[Br]**,  $\text{DMSO-}d^6$ , 100 MHz.

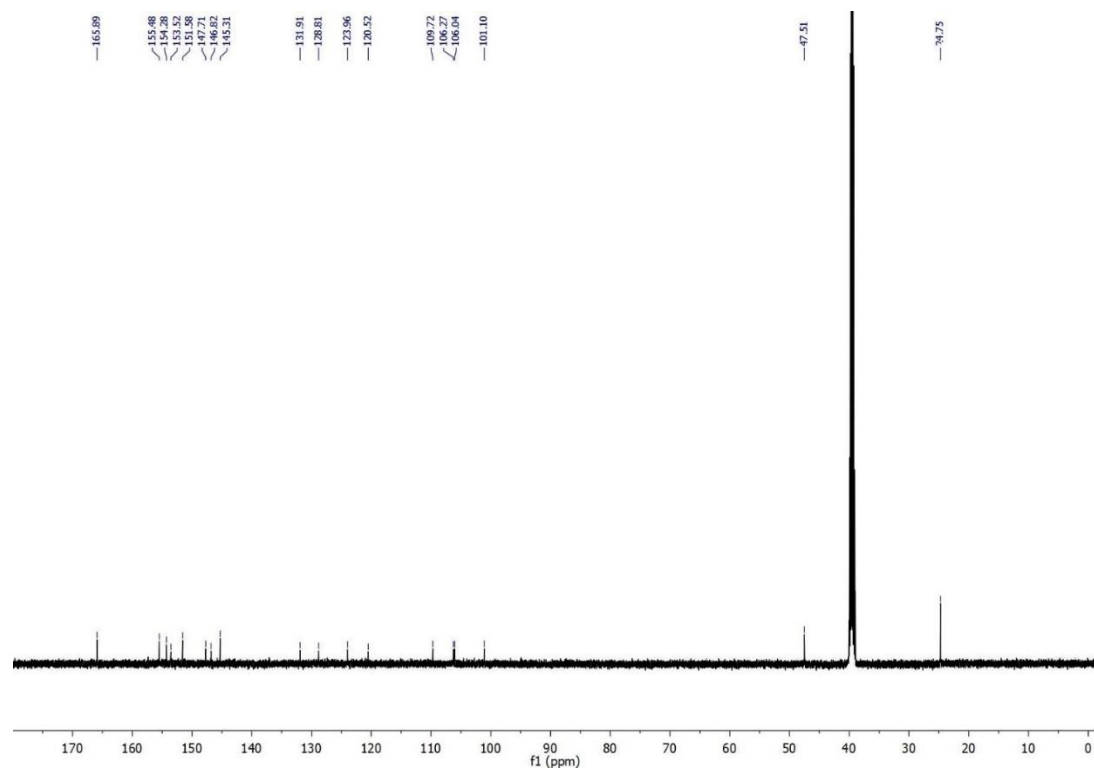


Figure S35:  $^1\text{H}$ -NMR of **5[Br]**,  $\text{DMSO-}d^6$ , 400 MHz.

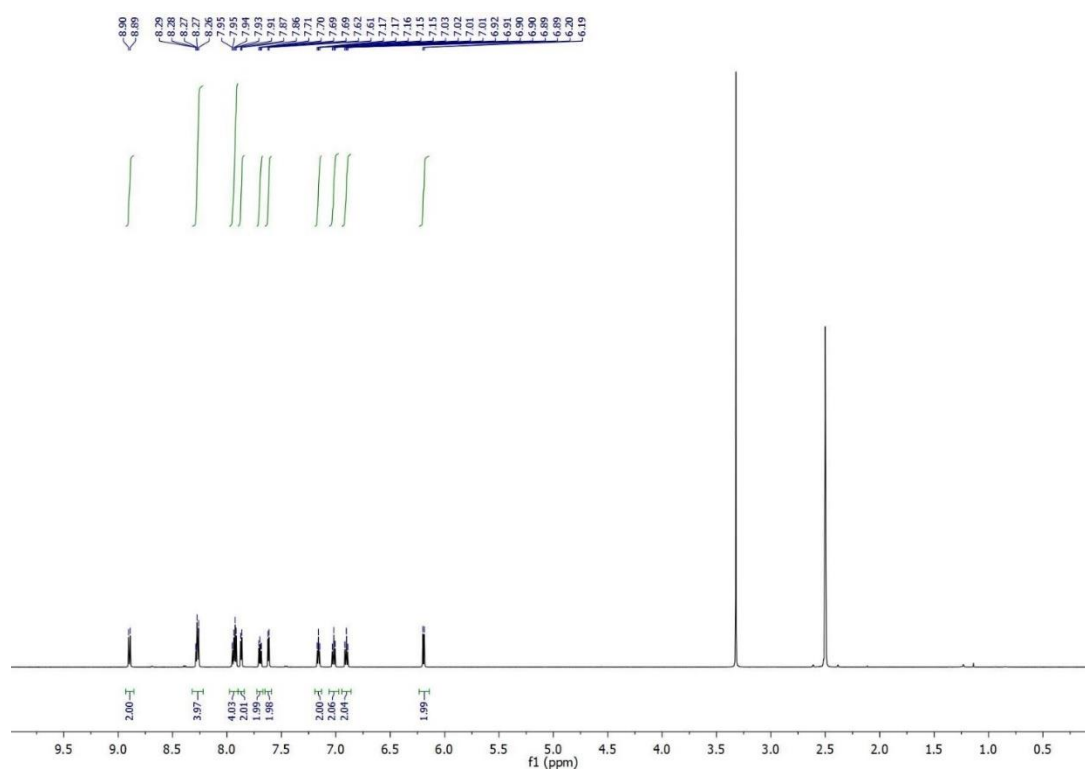


Figure S36:  $^{13}\text{C}$ -NMR of **5[Br]**,  $\text{DMSO-}d^6$ , 100 MHz.

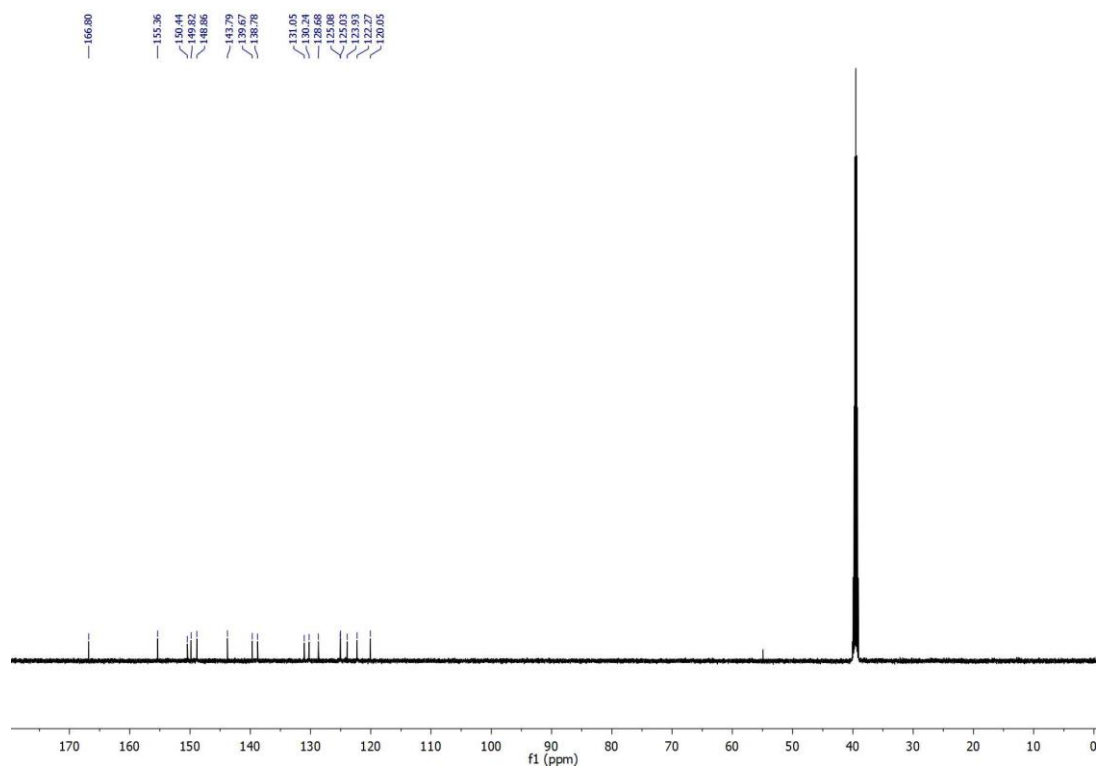


Figure S37:  $^1\text{H}$ -NMR of **6[Br]**,  $\text{DMSO-}d^6$ , 400 MHz.

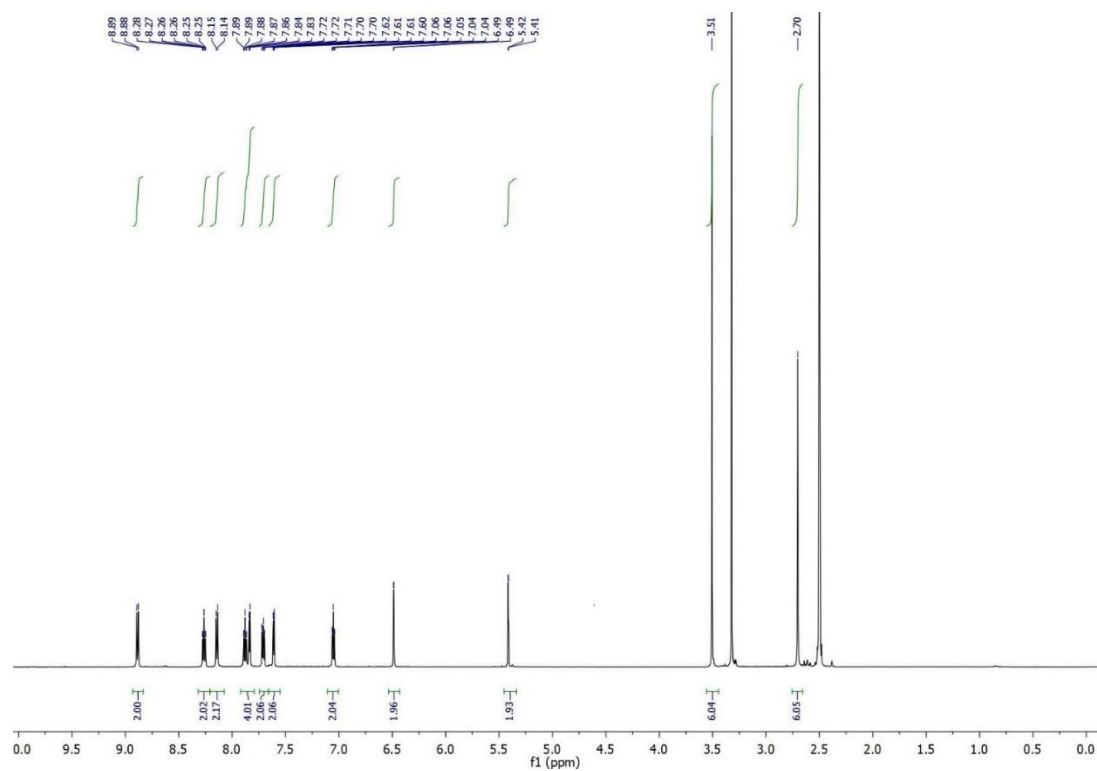
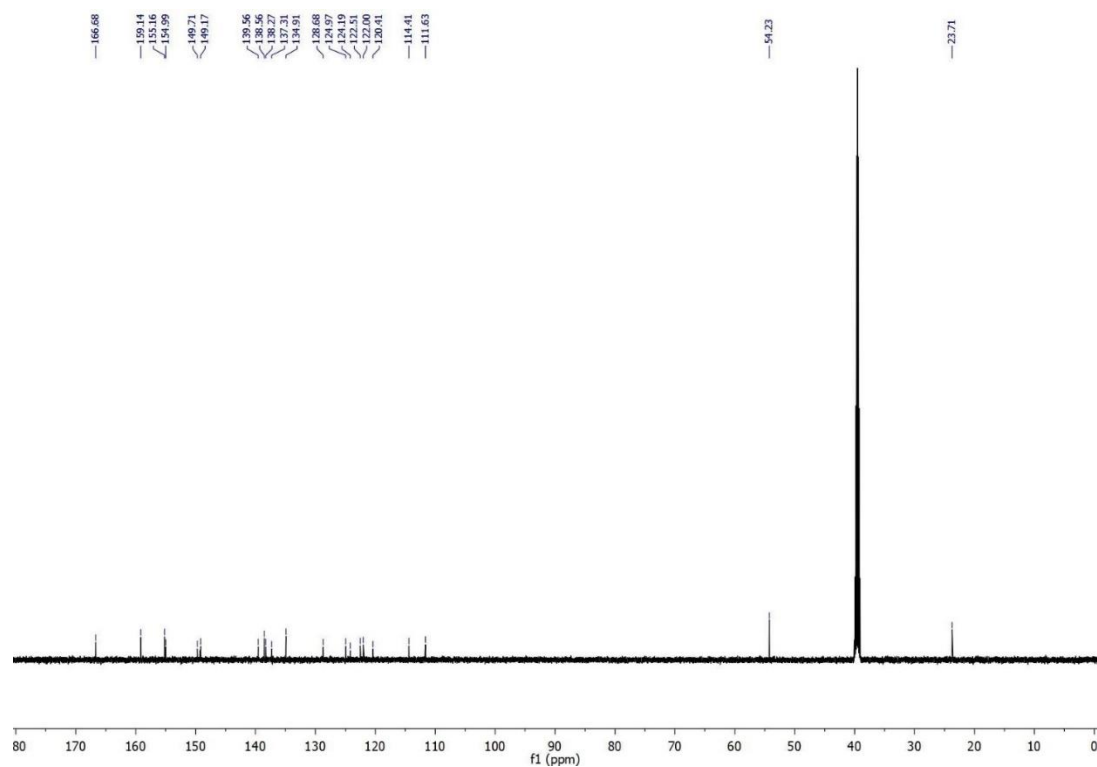


Figure S38:  $^{13}\text{C}$ -NMR of **6[Br]**,  $\text{DMSO-}d^6$ , 100 MHz.



## ESI-MS

Figure S39: ESI-MS of **1**[PF<sub>6</sub>], positive region ions, CH<sub>3</sub>CN.

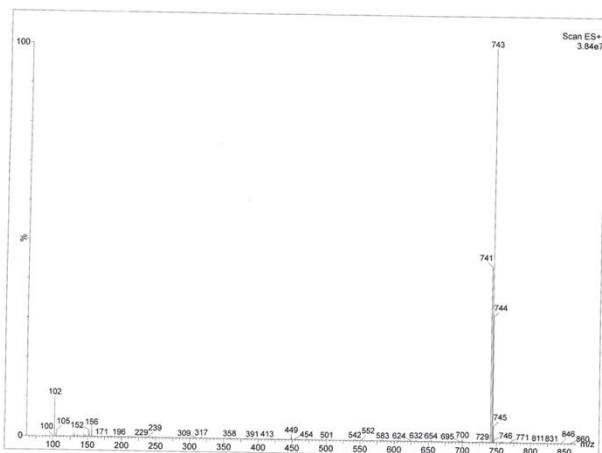


Figure S40: ESI-MS of **2**[PF<sub>6</sub>], positive region ions, CH<sub>3</sub>CN.

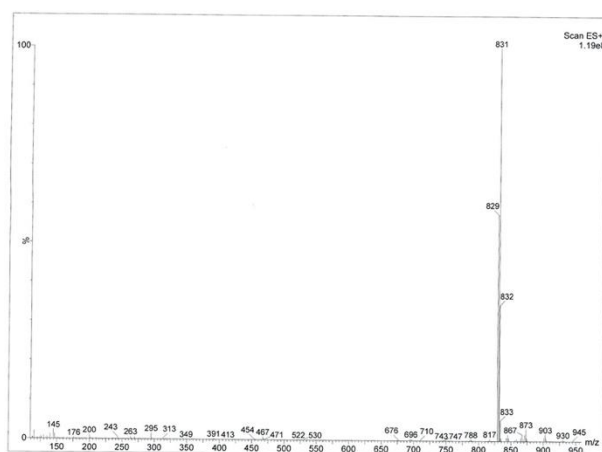


Figure S41: ESI-MS of **3**[PF<sub>6</sub>], positive region ions, CH<sub>3</sub>CN.

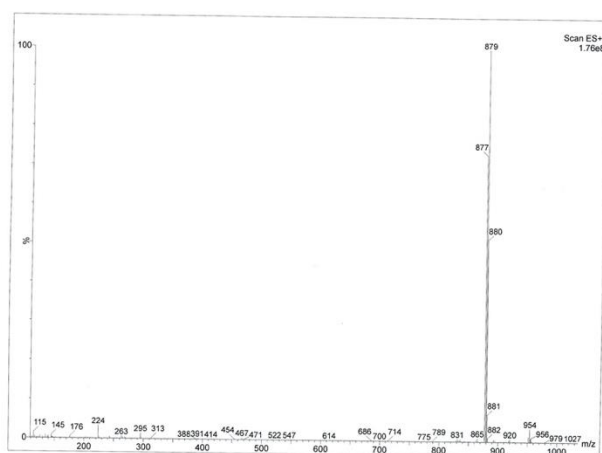


Figure S42: ESI-MS of **4**[PF<sub>6</sub>], positive region ions, CH<sub>3</sub>CN.

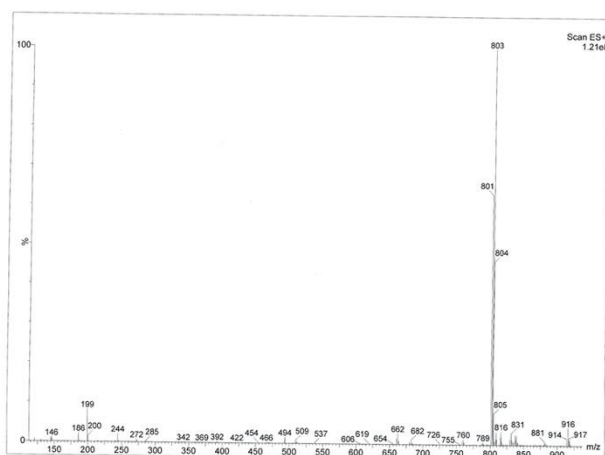


Figure S43: ESI-MS of **1**[BF<sub>4</sub>], positive and negative region ions, CH<sub>3</sub>CN.

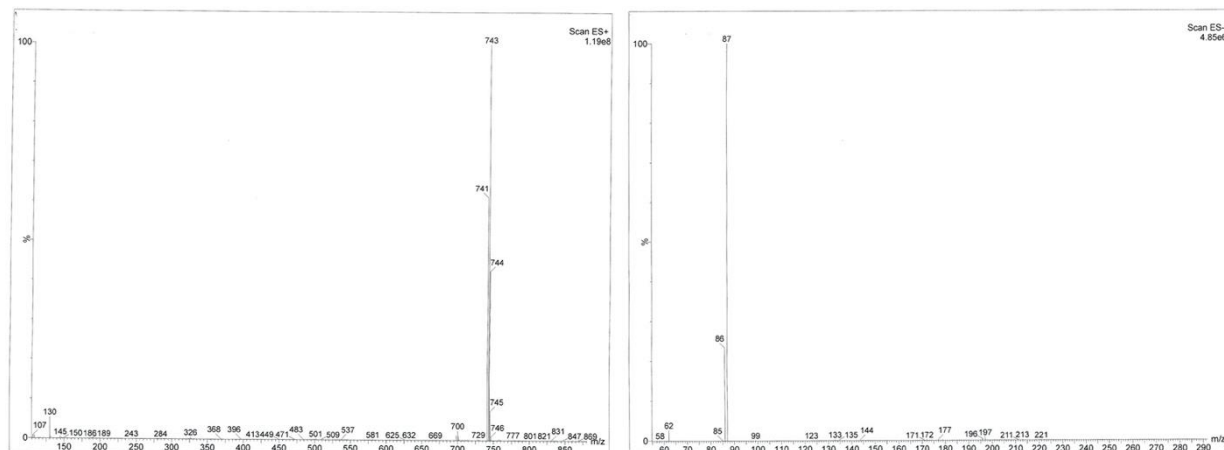


Figure S44: ESI-MS of **1**[Br], positive and negative region ions, CH<sub>3</sub>CN.

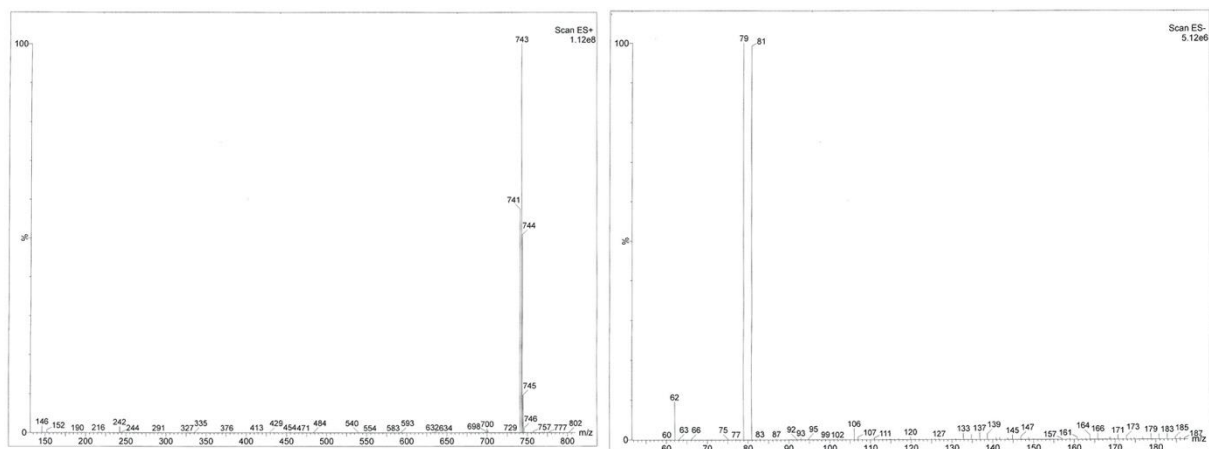


Figure S45: ESI-MS of **2[Br]**, positive and negative region ions, CH<sub>3</sub>CN.

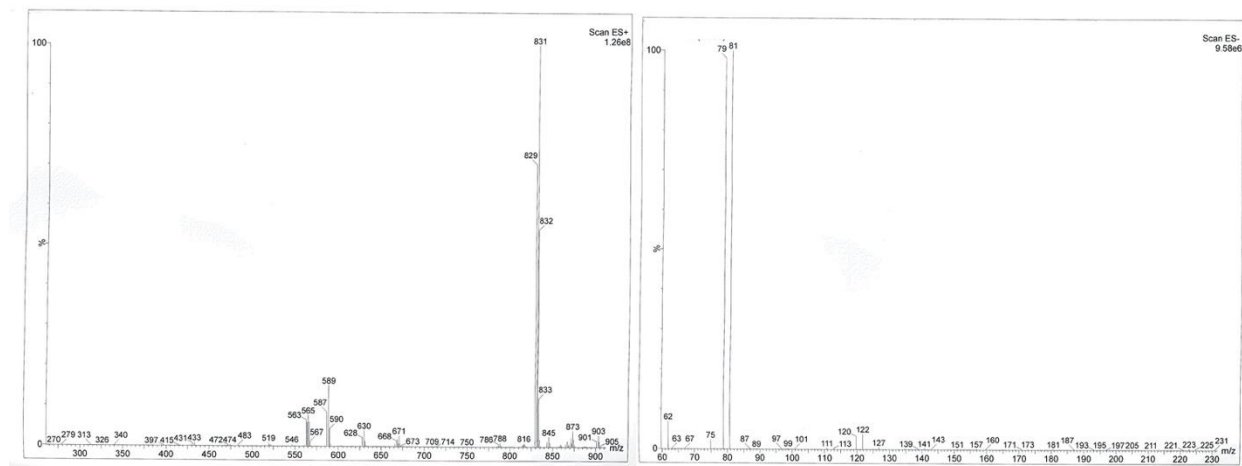


Figure S46: ESI-MS of **4[Br]**, positive and negative region ions, CH<sub>3</sub>CN.

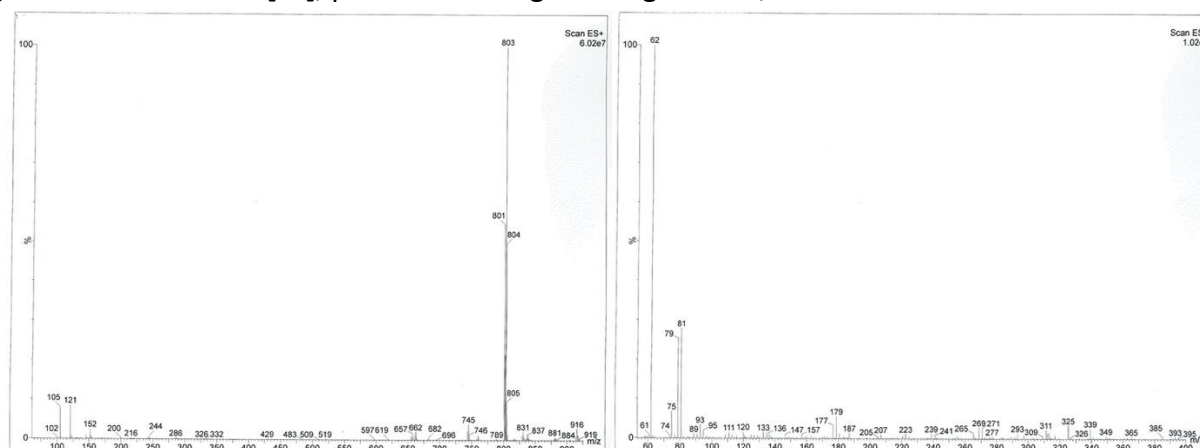


Figure S47: ESI-MS of **7[Br]**, positive and negative region ions, CH<sub>3</sub>CN.

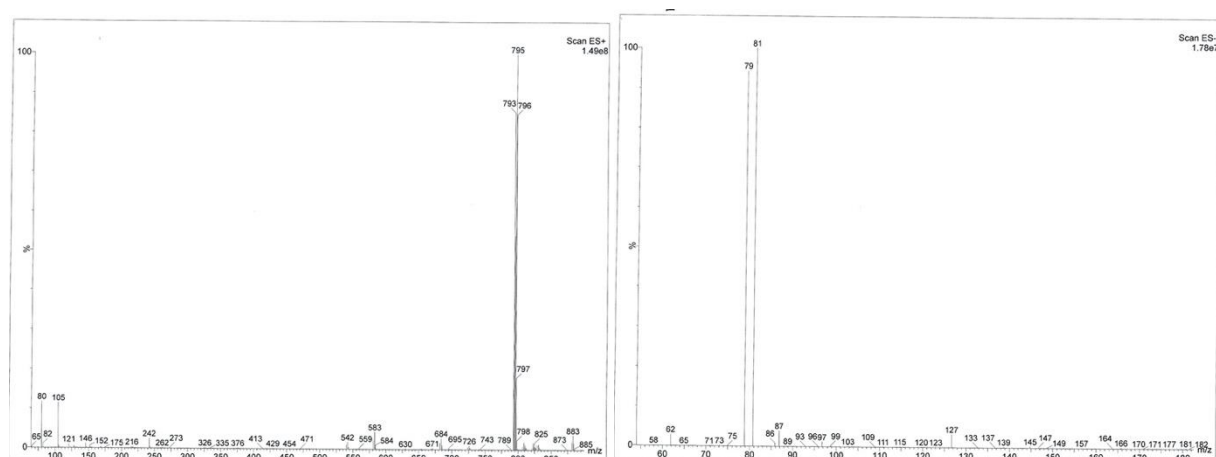


Figure S48: ESI-MS of **8[Br]**, positive and negative region ions, CH<sub>3</sub>CN.

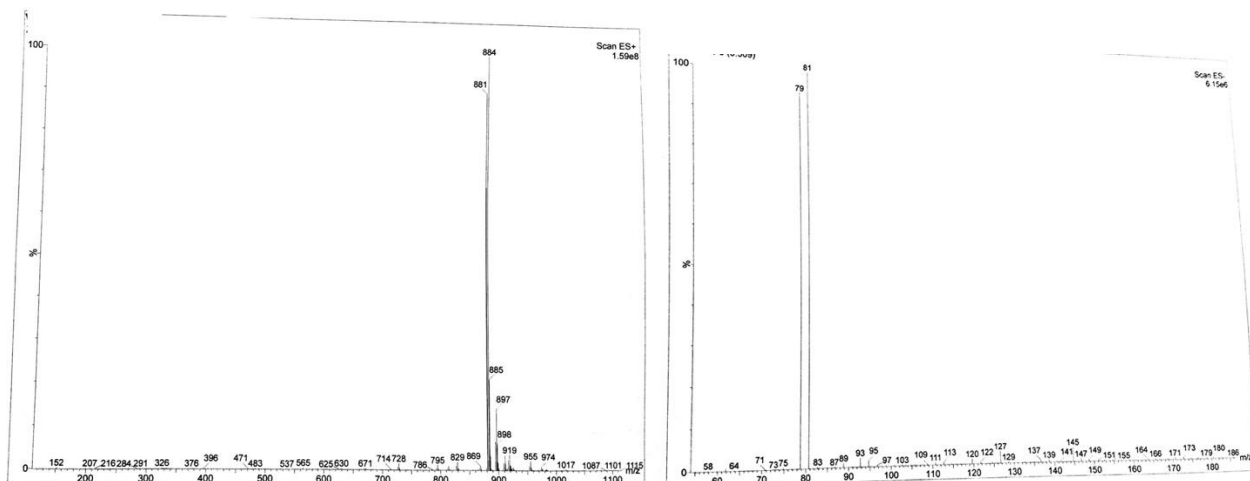


Figure S49: ESI-MS of **9[Br]**, positive and negative region ions, CH<sub>3</sub>CN.

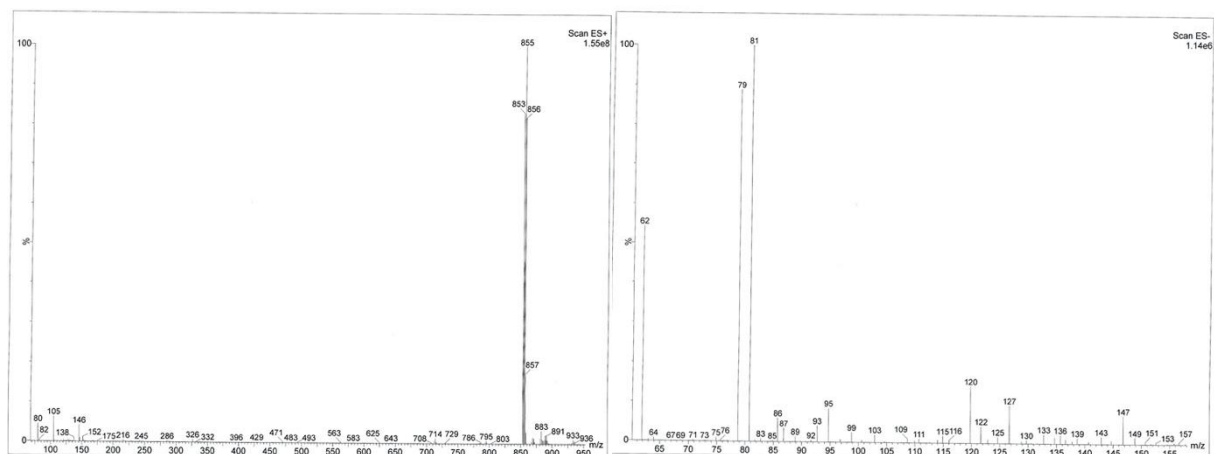


Figure S50: ESI-MS of **10[Br]**, positive and negative region ions, CH<sub>3</sub>CN.

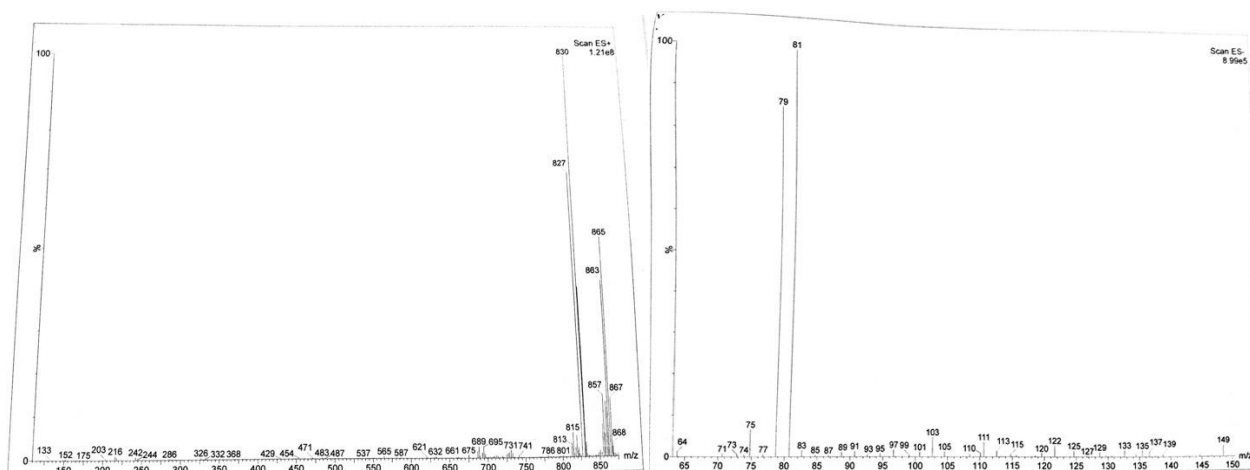




Figure S51: ESI-MS of **11[Br]**, positive and negative region ions, CH<sub>3</sub>CN.

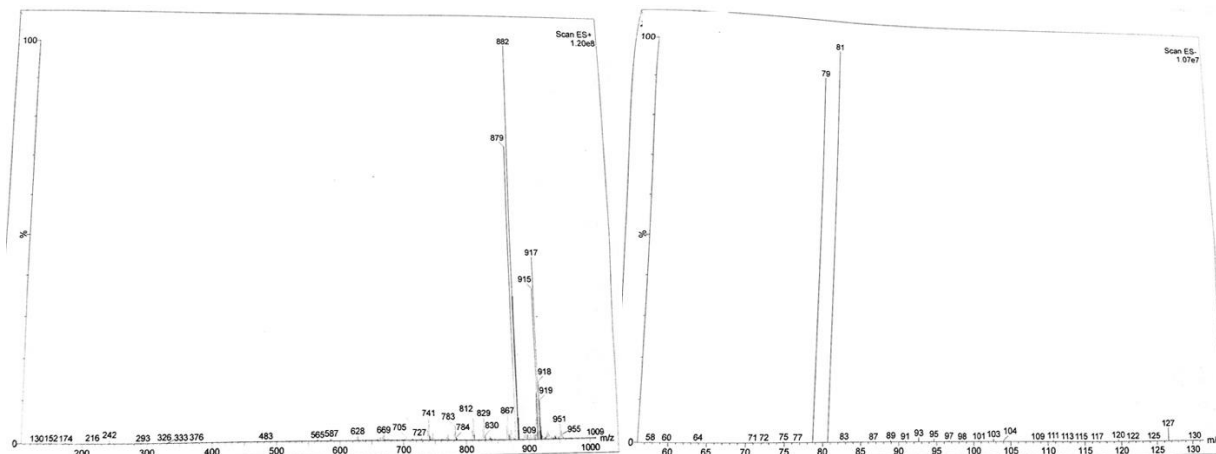


Figure S52: ESI-MS of **5[Br]**, positive and negative region ions, CH<sub>3</sub>CN.

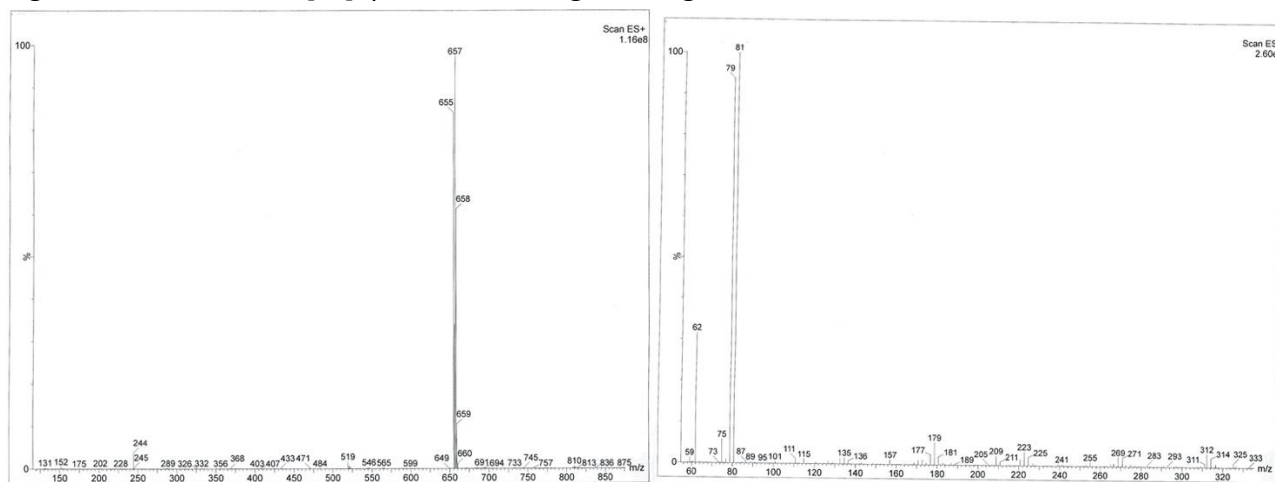
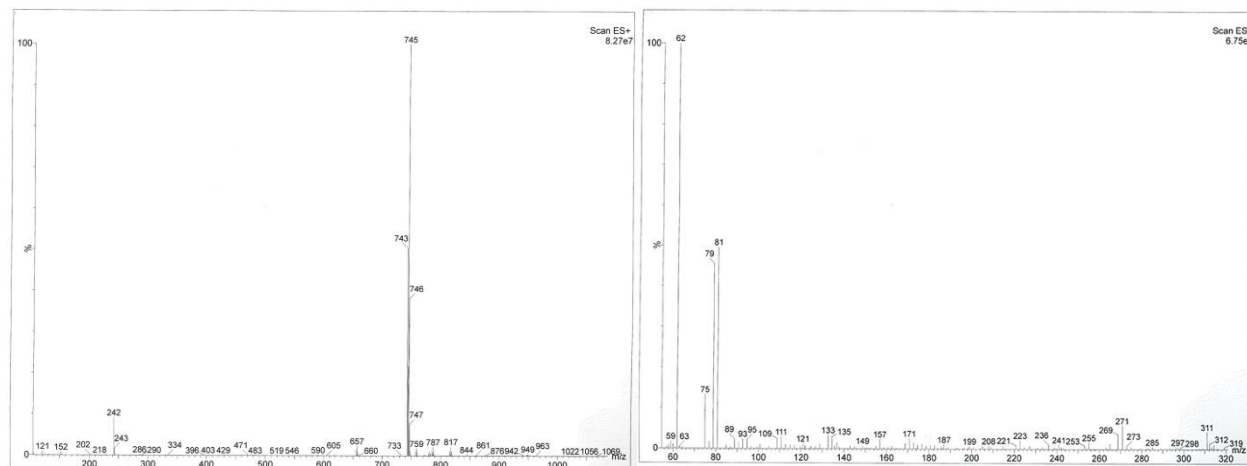


Figure S53: ESI-MS of **6[Br]**, positive and negative region ions, CH<sub>3</sub>CN.



## Cyclic Voltammetry

**Table S1:** Half-Wave redox potentials for all the reported Ir(III) species ( $10^{-3}$  M in anhydrous DMF, TBAPF<sub>6</sub> 0.1 M as the supporting electrolyte); SCE and Pt(II) as reference and working electrode, respectively. Scan rate 0.1 V/s; Excited States Redox Potentials; HOMO-LUMO energies.

Complex	oxidation vs SCE	reduction vs SCE	$E_{ox}^{*a}$ Ir(III)*/Ir(IV)	$E_{red}^{*a}$ Ir(II)/Ir(III)*	$E_{00}^b$	HOMO <sup>c</sup>	LUMO <sup>c</sup>	GAP
	E(V)	E ½ (V)	(eV)	(eV)	(eV)	(eV)	(eV)	
1[Br]	+1.22	-1.72	-1.32	+0.82	2.54	-5.62	-2.68	2.94
2[Br]	+1.18	-1.72	-1.20	+0.66	2.38	-5.58	-2.68	2.90
3[PF <sub>6</sub> ]	+1.64	-1.67	-0.98	+0.95	2.62	-6.04	-2.73	3.32
4[Br]	+1.21	-1.72	-1.20	+0.69	2.41	-5.61	-2.68	2.93
5[Br]	+1.30	-1.32	-0.78	+0.77	2.08	-5.70	-3.08	2.62
6[Br]	+1.36	-1.31	-0.67	+0.71	2.03	-5.76	-3.09	2.67
7[Br]	+1.24	-1.74	-1.32	+0.82	2.56	-5.64	-2.66	2.98
8[Br]	+1.14	-1.76	-1.42	+0.75	2.51	-5.54	-2.64	2.90
9[Br]	+1.19	-1.78	-1.37	+0.78	2.56	-5.59	-2.62	2.97
10[Br]	+0.79 +0.97 +1.14	-1.76	-1.41	+0.44	2.20	-5.19	-2.64	2.73
11[Br]	+0.93 +1.16	-1.80	-1.30	+0.43	2.23	-5.33	-2.60	2.73
(bpy-(NMe <sub>2</sub> ) <sub>2</sub> )	+1.20	-0.65 <sup>irr</sup> -1.08 <sup>irr</sup> -1.26 <sup>irr</sup>	/	/	/	/	/	/
(ppy-NMe <sub>2</sub> )	+1.28	-0.66	/	/	/	/	/	/
fac-[Ir(ppy) <sub>3</sub> ]	+0.70	-2.20	-1.73	+0.23	2.43	-5.10	-2.20	2.90
Fc/Fc <sup>+</sup>	+0.51	/	/	/	/	/	/	/

**Figure S54:** CV curves of (bpy-(NMe<sub>2</sub>)<sub>2</sub>)  $10^{-3}$  M in DMF/0.1 M TBAPF<sub>6</sub> vs SCE. (a) oxidation, (b) reduction.

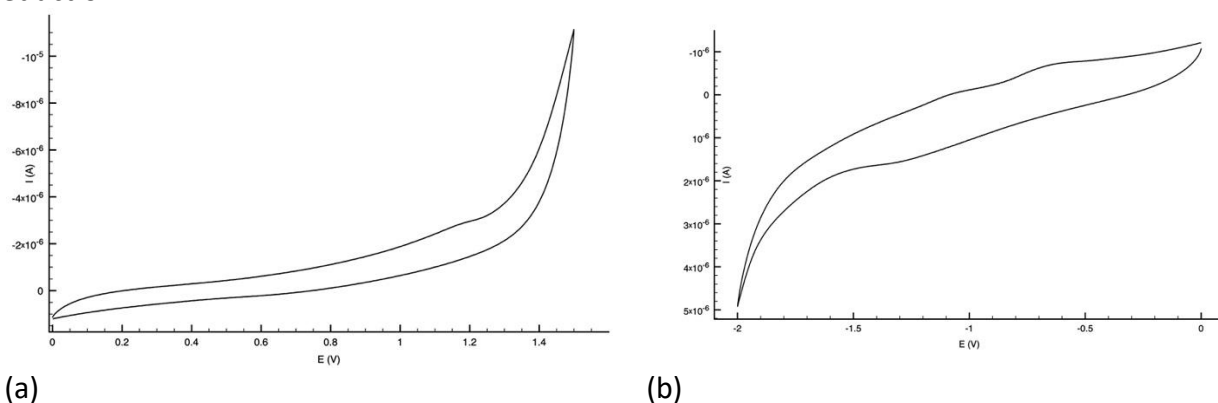


**Figure S55:** CV curves of **1[Br]**  $10^{-3}$ M in DMF/0.1 M TBAPF<sub>6</sub> vs SCE. (a) oxidation, (b) reduction.

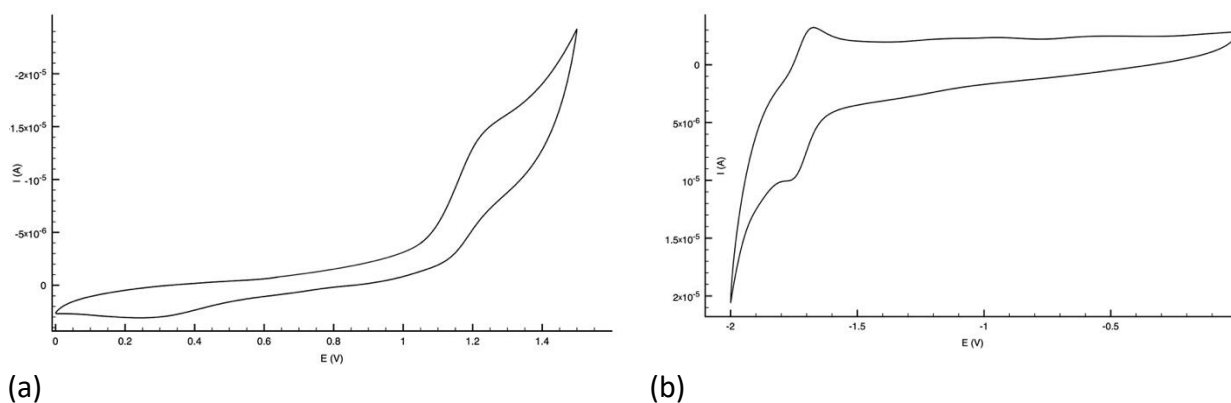


**Figure S56:** CV curves of **2[Br]**  $10^{-3}$ M in DMF/0.1 M TBAPF<sub>6</sub> vs SCE. (a) oxidation, (b) reduction.

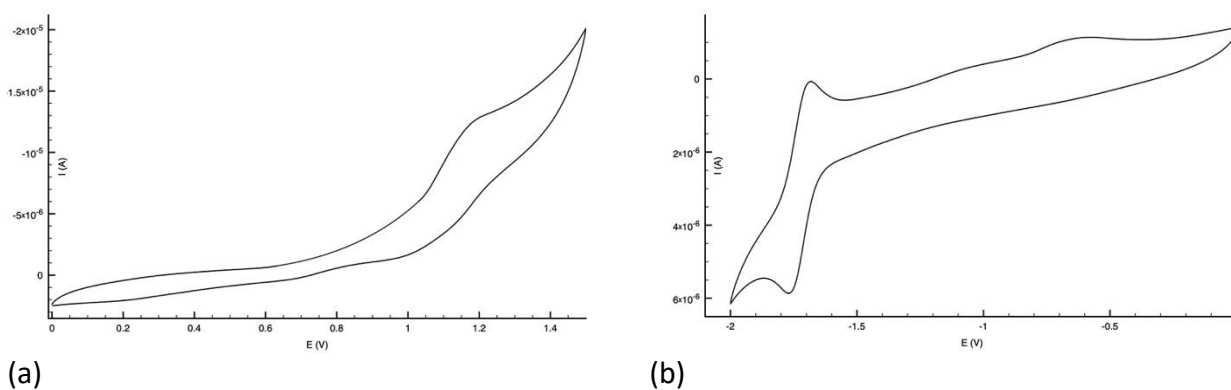


**Figure S57:** CV curves of **4[Br]**  $10^{-3}$ M in DMF/0.1 M TBAPF<sub>6</sub> vs SCE. (a) oxidation, (b) reduction.

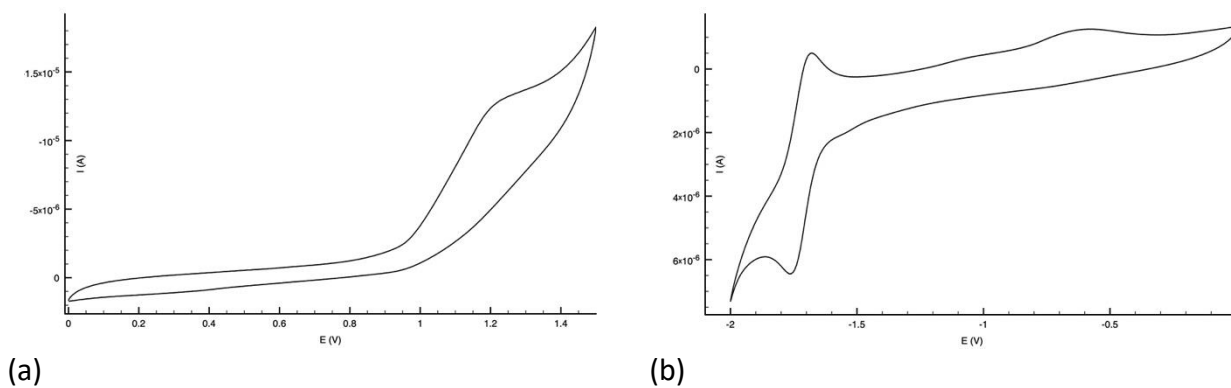


**Figure S58:** CV curves of **3**[PF<sub>6</sub>] 10<sup>-3</sup>M in DMF/0.1 M TBAPF<sub>6</sub> vs SCE. (a) oxidation, (b) reduction.

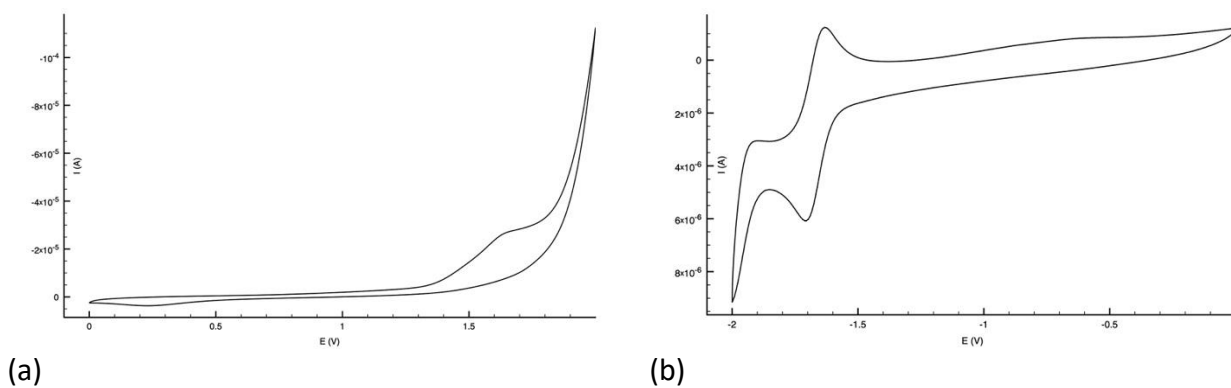


**Figure S59:** CV curves of **7**[Br] 10<sup>-3</sup>M in DMF/0.1 M TBAPF<sub>6</sub> vs SCE. (a) oxidation, (b) reduction.

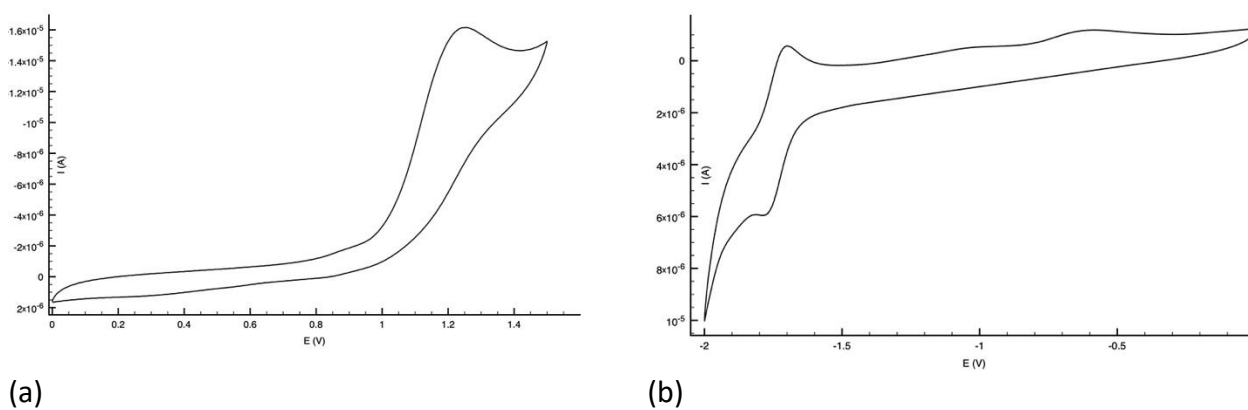


**Figure S60:** CV curves of **8**[Br] 10<sup>-3</sup>M in DMF/0.1 M TBAPF<sub>6</sub> vs SCE. (a) oxidation, (b) reduction.

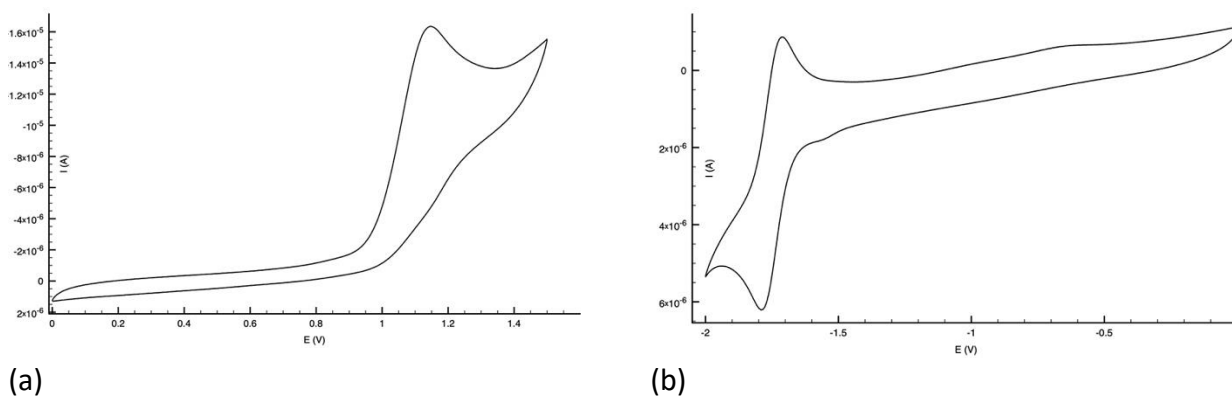


**Figure S61:** CV curves of **9[Br]**  $10^{-3}$ M in DMF/0.1 M TBAPF<sub>6</sub> vs SCE. (a) oxidation, (b) reduction.

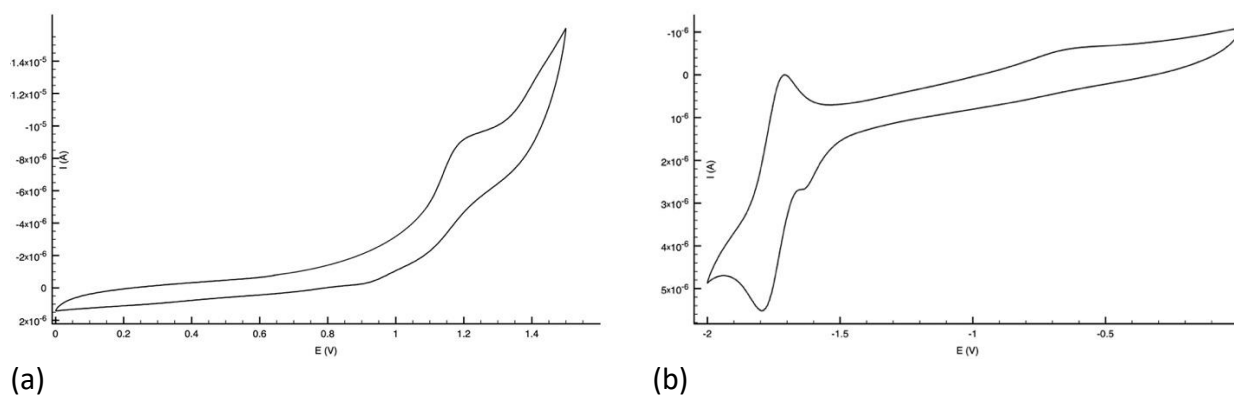


**Figure S62:** CV curves of **(ppy-NMe<sub>2</sub>)**  $10^{-3}$ M in DMF/0.1 M TBAPF<sub>6</sub> vs SCE. (a) oxidation, (b) reduction.

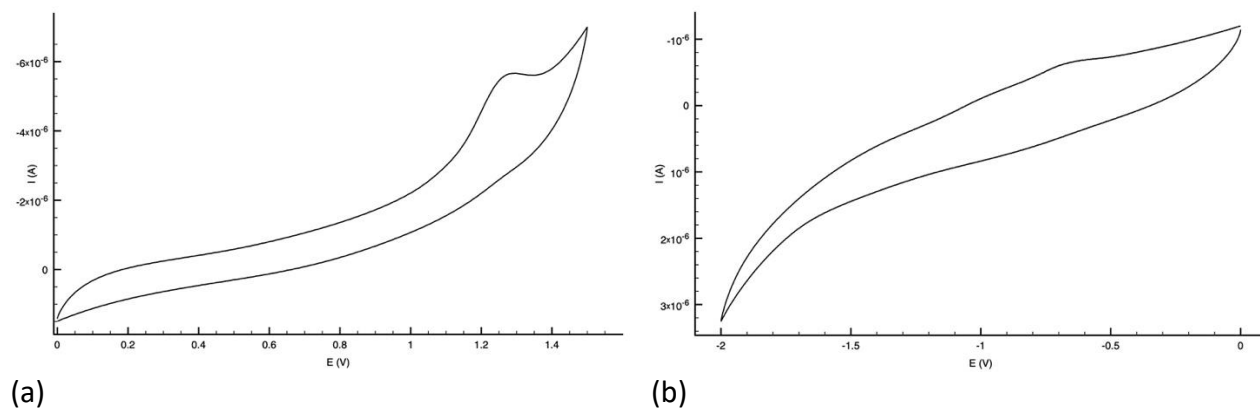


**Figure S63:** CV curves of **10[Br]**  $10^{-3}$ M in DMF/0.1 M TBAPF<sub>6</sub> vs SCE. (a) oxidation, (b) reduction.

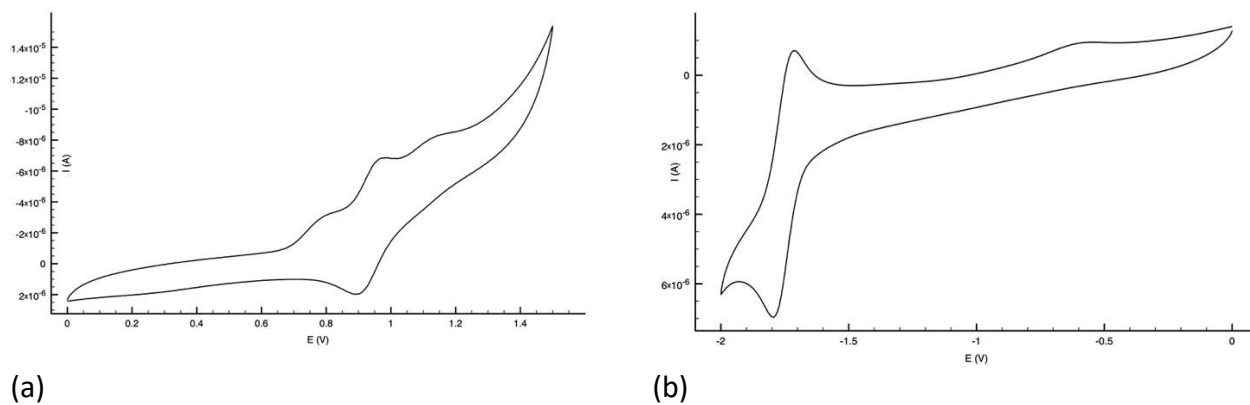


**Figure S64:** CV curves of **11[Br]**  $10^{-3}$ M in DMF/0.1 M TBAPF<sub>6</sub> vs SCE. (a) oxidation, (b) reduction.

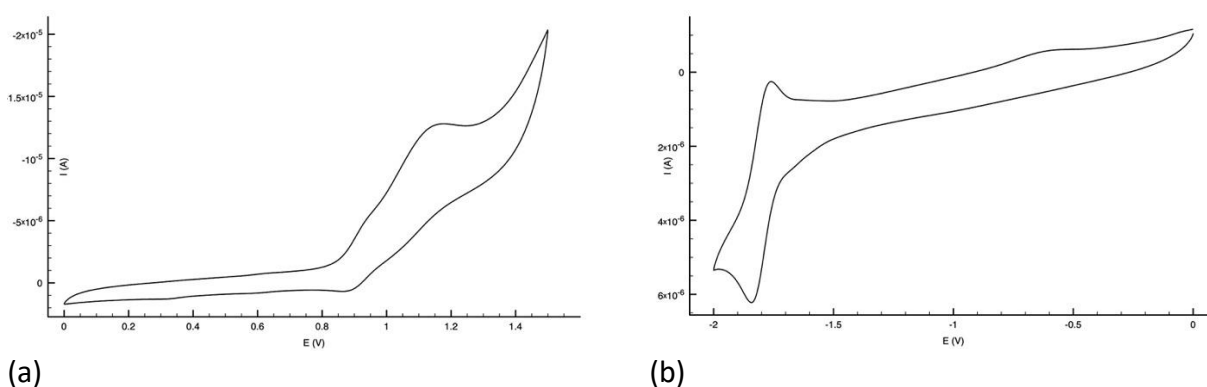


**Figure S65:** CV curves of **5[Br]**  $10^{-3}$ M in DMF/0.1 M TBAPF<sub>6</sub> vs SCE. (a) oxidation, (b) reduction.

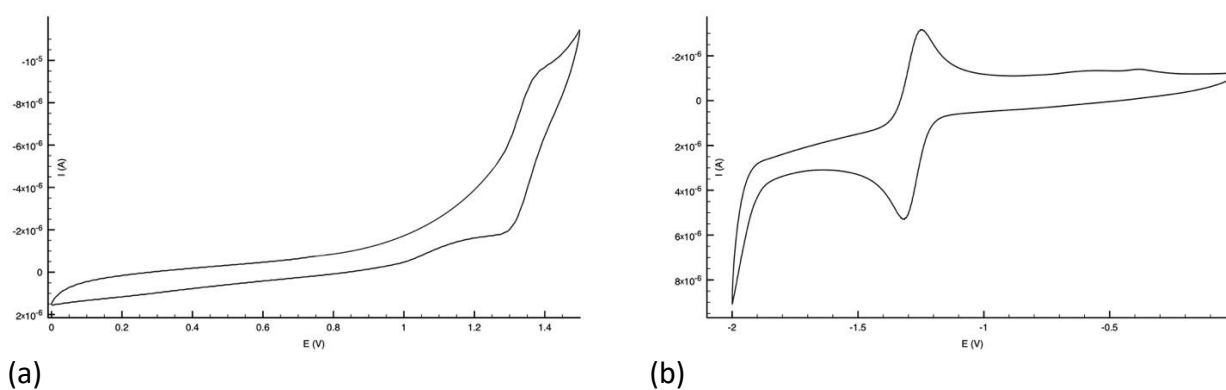
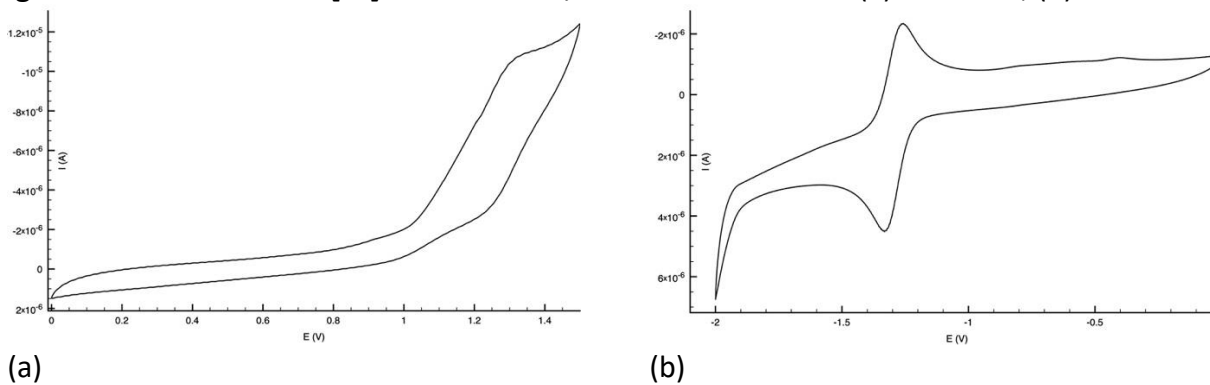


**Figure S66:** CV curves of **6[Br]**  $10^{-3}$ M in DMF/0.1 M TBAPF<sub>6</sub> vs SCE. (a) oxidation, (b) reduction.



## Photophysics and Stern Volmer quenching studies

**Table S2:** Photophysical Characterization of Ir(III) catalysts

Complex	Absorption	Emission 298 K <sup>a, b</sup>				Emission 77 K <sup>c</sup>		
CH <sub>2</sub> Cl <sub>2</sub> as the solvent, 10 <sup>-5</sup> M	$\lambda$ (nm) 10 <sup>-4</sup> $\epsilon$ (cm <sup>-1</sup> M <sup>-1</sup> )	$\lambda_{em}$ (nm)	$\tau_{ox}$ ( $\mu$ s)	$\tau_{deox}$ ( $\mu$ s)	$\Phi_{ox}$ (%)	$\Phi_{deox}$ (%)	$\lambda_{em}$ (nm)	$\tau$ ( $\mu$ s)
<b>1[PF<sub>6</sub>]</b>	268 (4.68), 358 (0.62), 425 (0.14)	486, 516	0.08	1.3	2	10	484, 516	3.0
<b>1[BF<sub>4</sub>]</b>	266 (5.41), 361 (0.77), 426 (0.76)	488, 518	0.08	1.1	2	12	488, 524	1.6
<b>1[Br]</b>	268 (2.87), 366 (0.54), 432 (0.23)	488, 518	0.09	1.5	3	14	486, 524	2.1
<b>2[PF<sub>6</sub>]</b>	268 (9.98), 282 (8.81), 363 (2.14), 422 (0.60)	522	0.08	0.8	4.9	49	484, 518	2.7
<b>2[Br]</b>	267 (8.59), 282 (7.60), 370 (1.59)	522	0.10	1.2	4	35	482, 514	2.9
<b>3[PF<sub>6</sub>]</b>	267 (7.57), 354 (1.21), 386 (0.85), 420 (0.26)	474, 502	0.18	2.2	5.2	60	472, 508	3.4
<b>4[PF<sub>6</sub>]</b>	265 (10.6), 284 (9.48), 352 (2.56), 412 (0.22)	512	0.07	1.1	2	27	482, 516	1.8
<b>4[Br]</b>	268 (8.20), 289 (7.35), 365 (1.47)	514	0.10	1.6	5	35	476, 512	2.7
<b>7[Br]</b>	268 (4.79), 360 (0.88), 430 (0.30)	486, 516	0.08	1.1	2	34	490, 512, 550	2.3
<b>8[Br]</b>	268 (3.08), 287 (2.66), 370 (0.80), 420 (0.37)	516	0.07	1.0	2	25	498	2.8
<b>9[Br]</b>	268 (4.61), 293 (4.16), 356 (1.14), 400 (0.49)	482, 512	0.08	0.7	2	22	478, 514, 552	3.4
<b>10[Br]</b>	270 (5.39), 317 (1.93), 360 (0.94), 427 (0.26)	564	0.08	1.0	2	32	516, 548	5.6
<b>11[Br]</b>	271 (5.47), 316 (1.98), 360 (0.96), 424 (0.25)	556	0.07	1.0	3	36	528	4.5
<b>5[Br]</b>	256 (9.30), 268 (9.17), 380 (1.05), 410 (0.54)	598	0.19	0.5	8	16	514, 548	3.5
<b>6[Br]</b>	279 (8.08), 309 (4.05), 332 (2.65), 380 (0.76)	610	0.15	0.3	10	25	522, 550	3.9
<i>fac</i> -[Ir(ppy) <sub>3</sub> ]	243 (3.30), 283 (3.23), 381 (0.65)	522	0.05	0.7	1.9	25.6	512, 548	4.4

<sup>a</sup>: "ox" = air equilibrated solutions, "deox" = deoxygenated solutions under argon atmosphere; <sup>b</sup>: vs [Ru(bpy)<sub>3</sub>]Cl<sub>2</sub>/H<sub>2</sub>O ( $\Phi_r = 0.028$ )<sup>11</sup>; <sup>c</sup>: in frozen CH<sub>2</sub>Cl<sub>2</sub>.

**Table S3:** Stern Volmer quenching studies data summary

Complex	Emission 298 K		K <sub>D</sub>	K <sub>q</sub>
DMF as solvent, EBPA as quencher $\lambda_{exc}$ = 370 nm	$\lambda_{em}$ (nm)	$\tau_0$ ( $\mu$ s)	L*mol <sup>-1</sup>	L*mol <sup>-1</sup> *s <sup>-1</sup>
1[Br]	492, 518	0.096	6.2	6.4*10 <sup>7</sup>
2[Br]	492, 518	0.122	14.1	1.2*10 <sup>8</sup>
4[Br]	484, 512	0.110	9.1	8.2*10 <sup>7</sup>
7[Br]	484, 518	0.087	8.8	1.0*10 <sup>8</sup>
8[Br]	494, 516	0.084	14.3	1.7*10 <sup>8</sup>
9[Br]	484, 514	0.085	7.8	9.2*10 <sup>7</sup>
10[Br]	566	0.164	32.6	2.0*10 <sup>8</sup>
11[Br]	562	0.150	42.1	2.8*10 <sup>8</sup>

**Figure S67: Photophysical Characterization of  $1[\text{PF}_6]$**

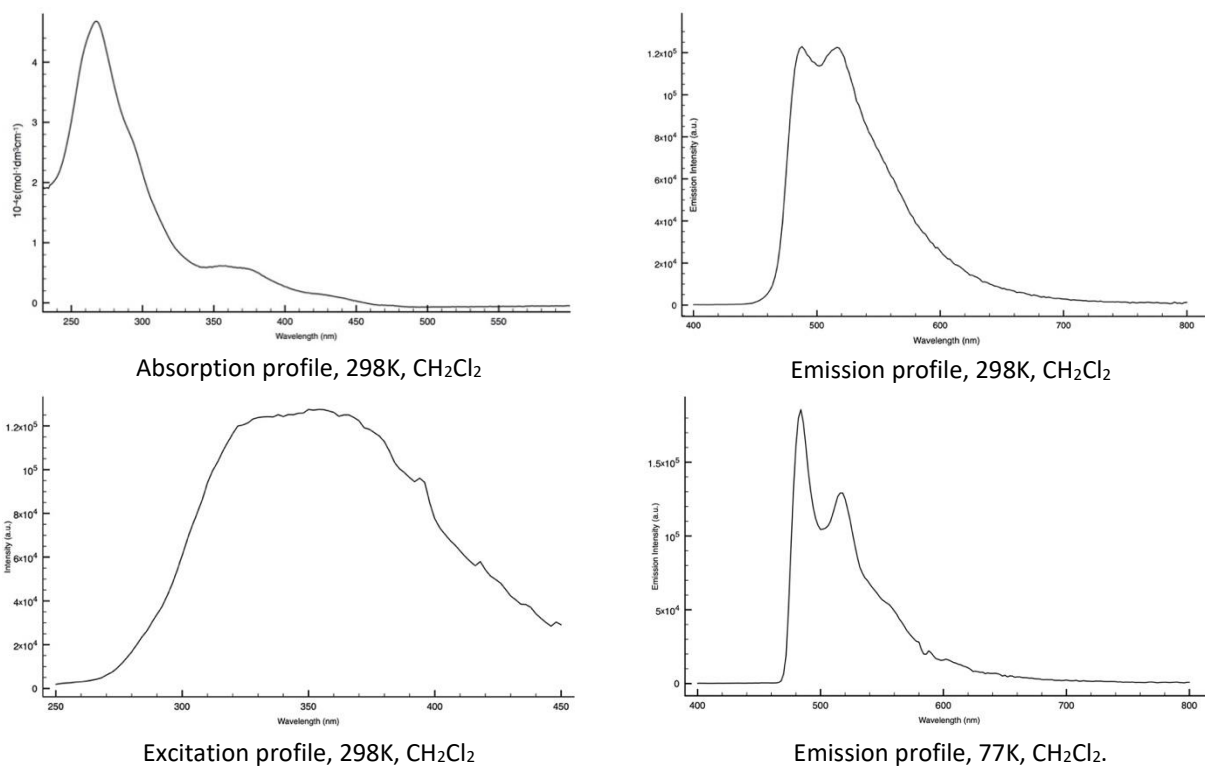


**Figure S68: Photophysical Characterization of  $1[\text{BF}_4]$**

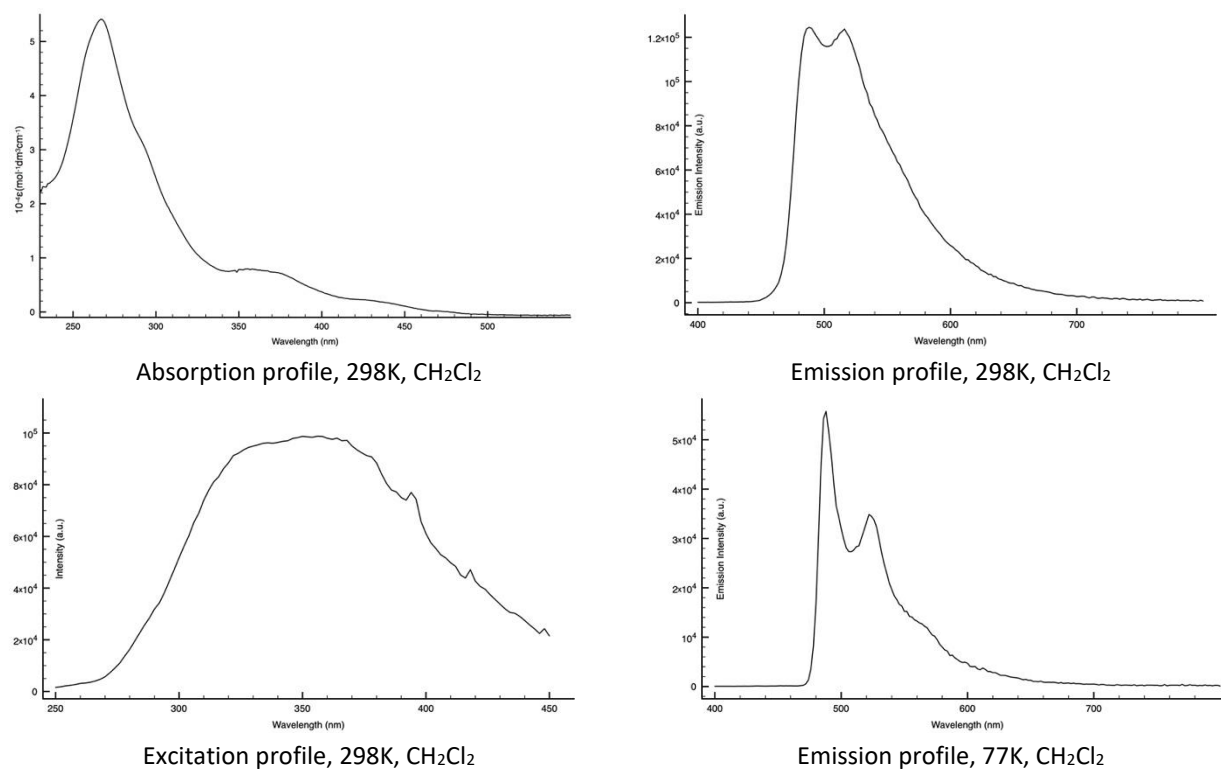




**Figure S69: Photophysical Characterization of 1[Br]**

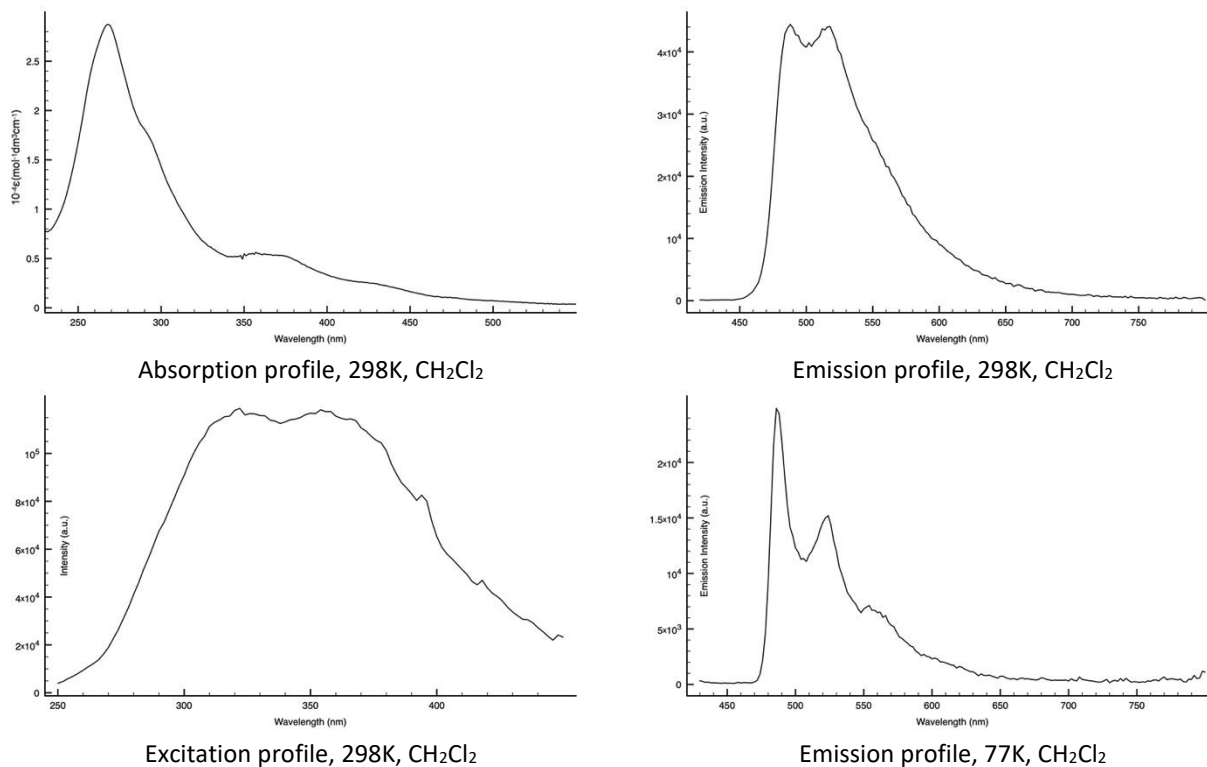


**Figure S70: Stern Volmer Quenching Studies of 1[Br] ( $M = 1.22 \cdot 10^{-4}$  in DMF) vs EBPA ( $9 \times 5 \mu\text{L}$ ).**

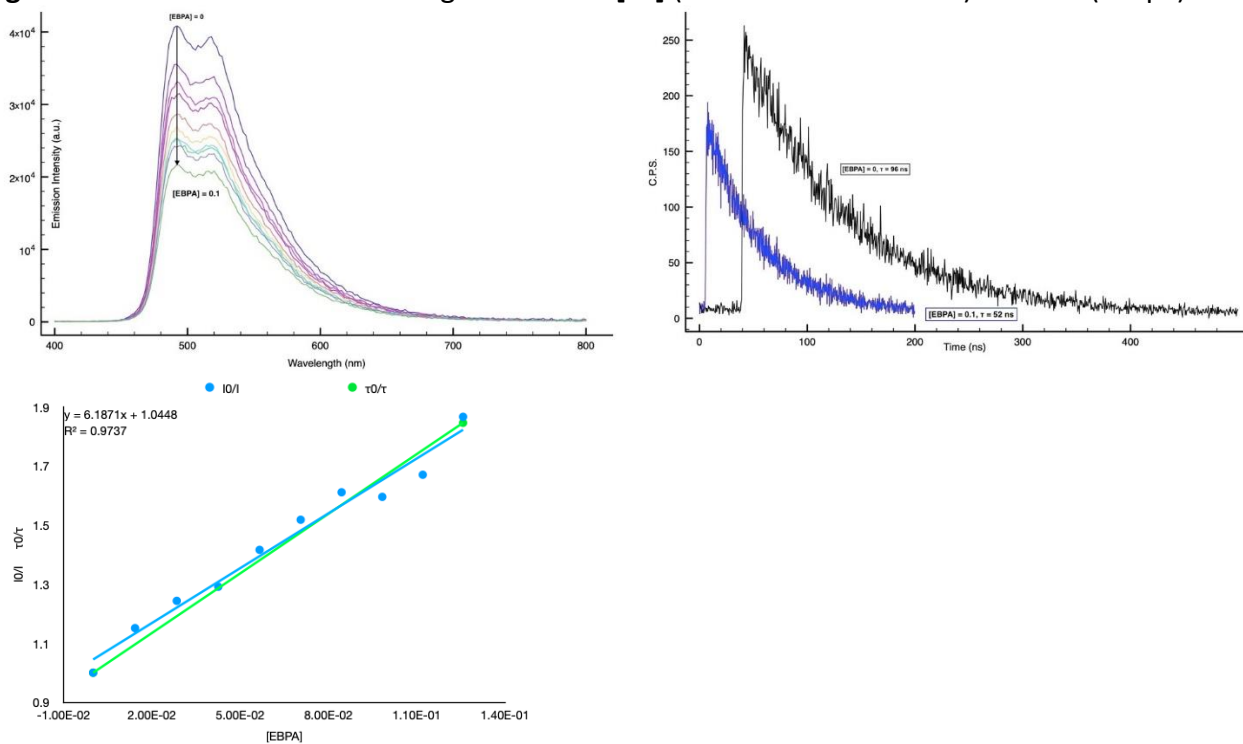
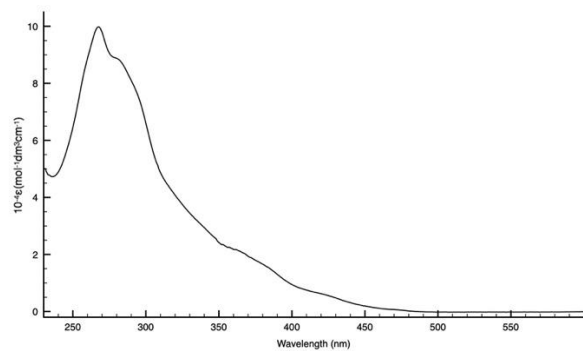
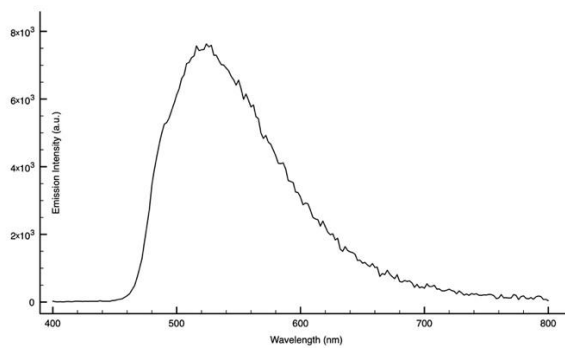


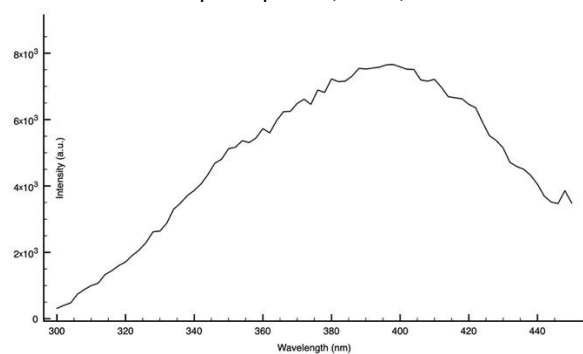
**Figure S71: Photophysical Characterization of 2[PF<sub>6</sub>]**



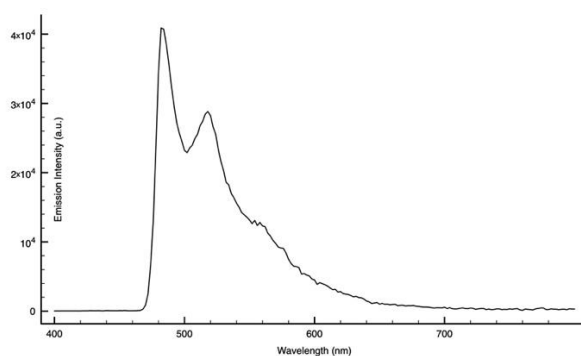
Absorption profile, 298K, CH<sub>2</sub>Cl<sub>2</sub>



Emission profile, 298K, CH<sub>2</sub>Cl<sub>2</sub>

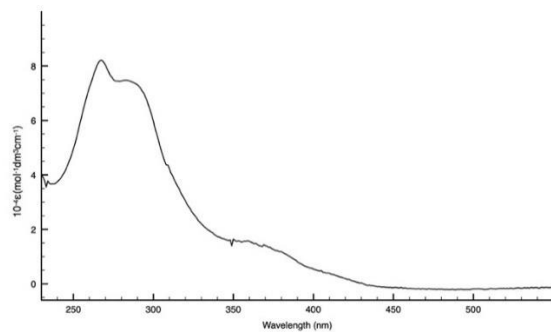


Excitation profile, 298K, CH<sub>2</sub>Cl<sub>2</sub>

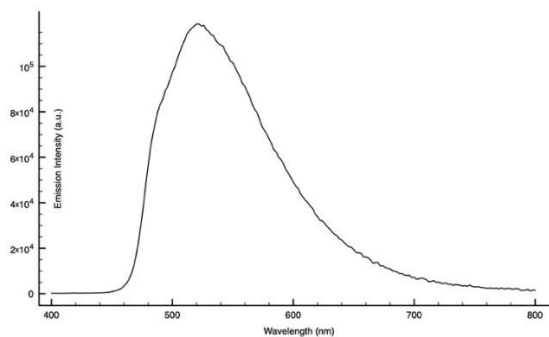


Emission profile, 77K, CH<sub>2</sub>Cl<sub>2</sub>

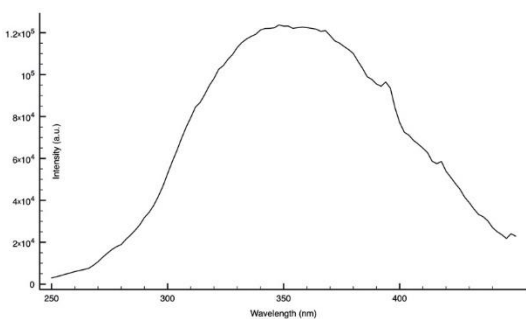
**Figure S72: Photophysical Characterization of 2[Br]**



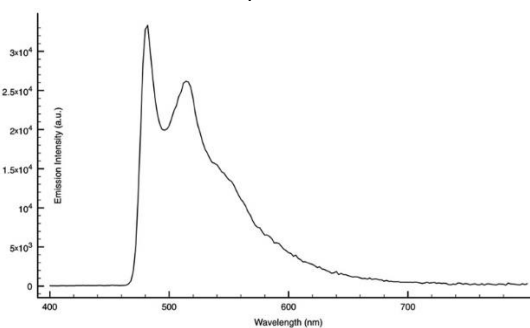
Absorption profile, 298K, CH<sub>2</sub>Cl<sub>2</sub>



Emission profile, 298K, CH<sub>2</sub>Cl<sub>2</sub>



Excitation profile, 298K, CH<sub>2</sub>Cl<sub>2</sub>



Emission profile, 77K, CH<sub>2</sub>Cl<sub>2</sub>

**Figure S73:** Stern Volmer Quenching Studies of **2[Br]** ( $M = 1.09 \times 10^{-4}$  in DMF) vs EBPA ( $9 \times 5 \mu\text{L}$ ).

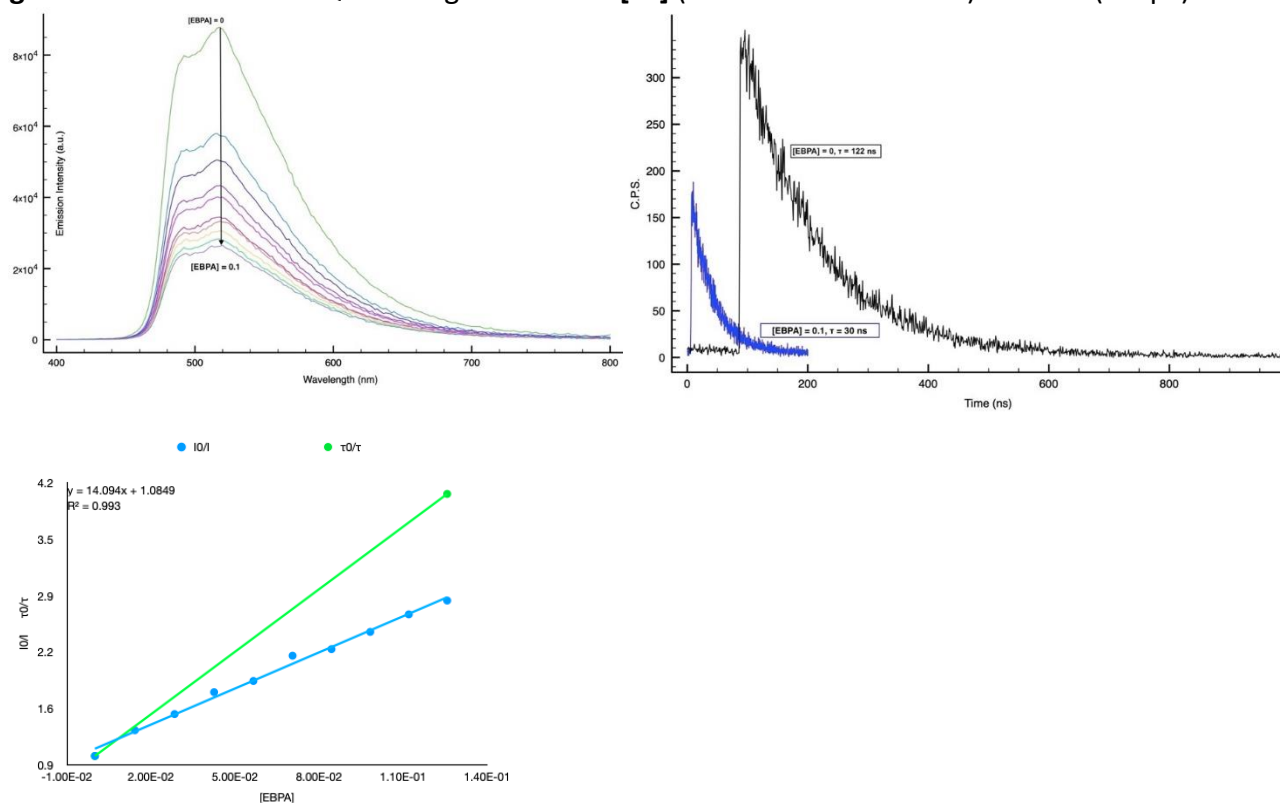


**Figure S74:** Photophysical Characterization of **4[PF<sub>6</sub>]**

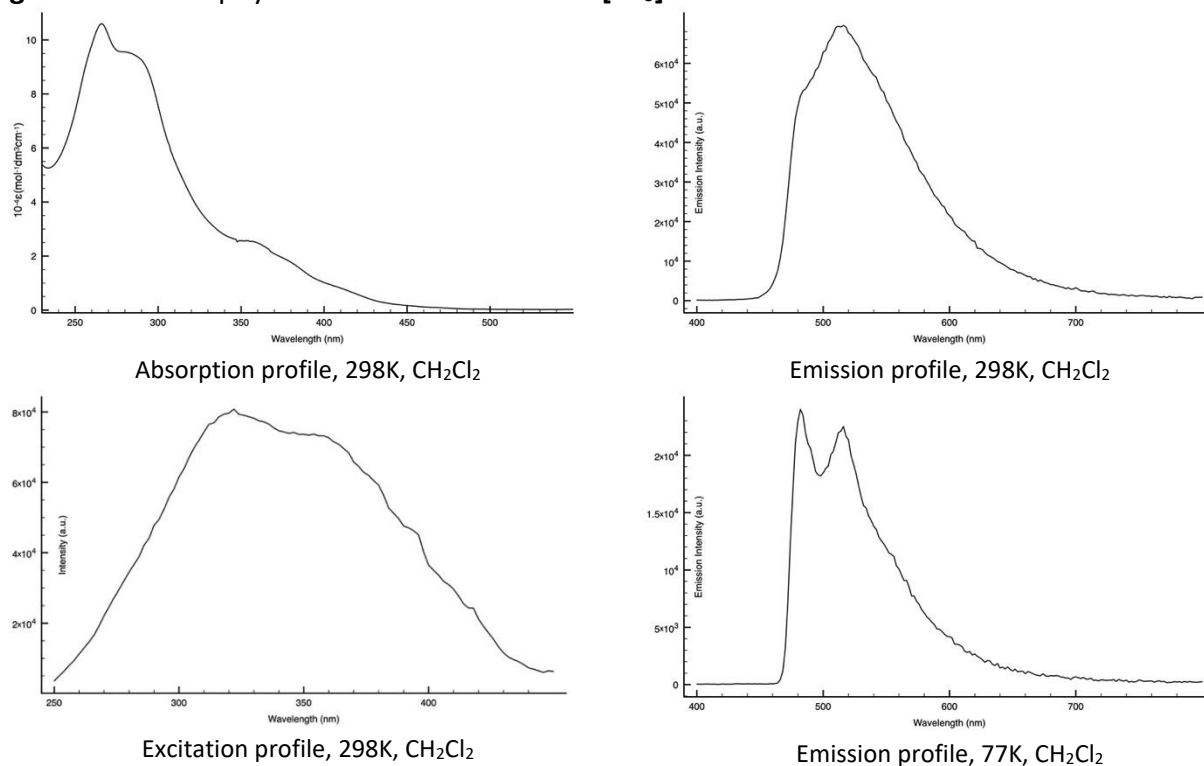


**Figure S75: Photophysical Characterization of 4[Br]**

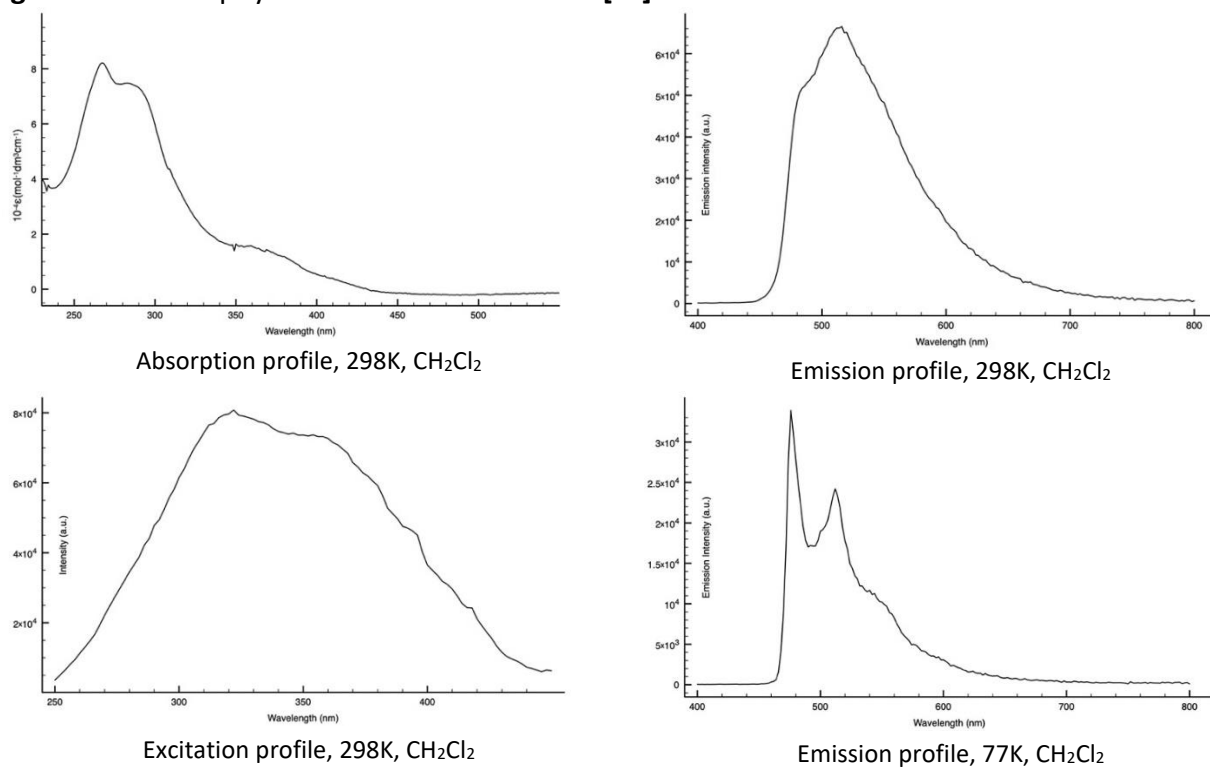


**Figure S76: Stern Volmer Quenching Studies of 4[Br] ( $M = 1.09 \times 10^{-4}$  in DMF) vs EBPA ( $9 \times 5 \mu\text{L}$ ).**

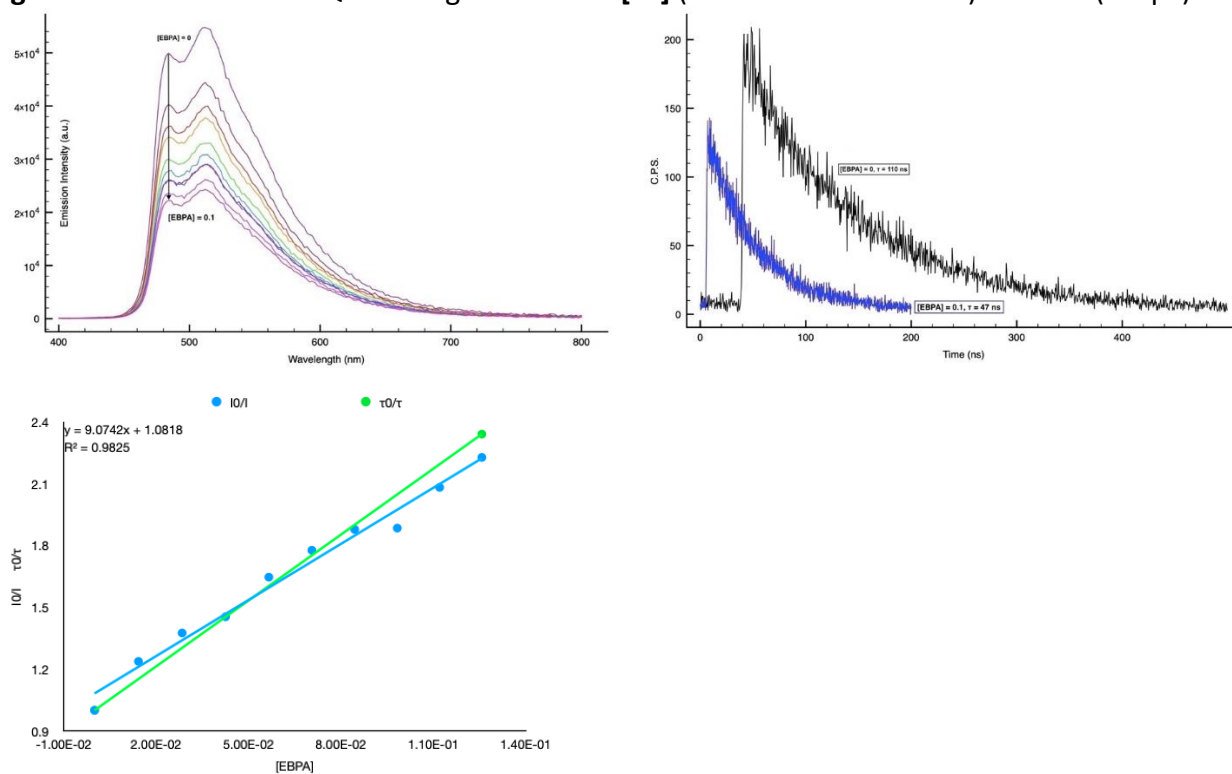


**Figure S77: Photophysical Characterization of 3[PF<sub>6</sub>]**

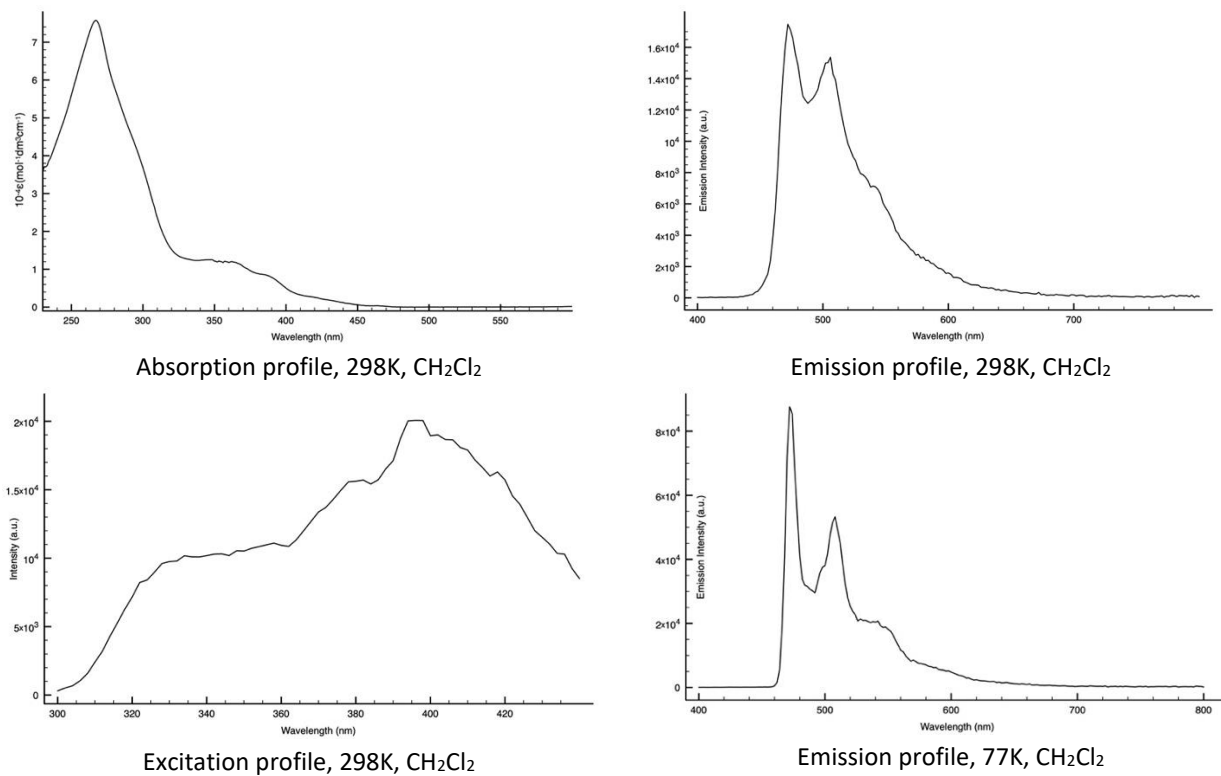


**Figure S78: Photophysical Characterization of 7[Br]**

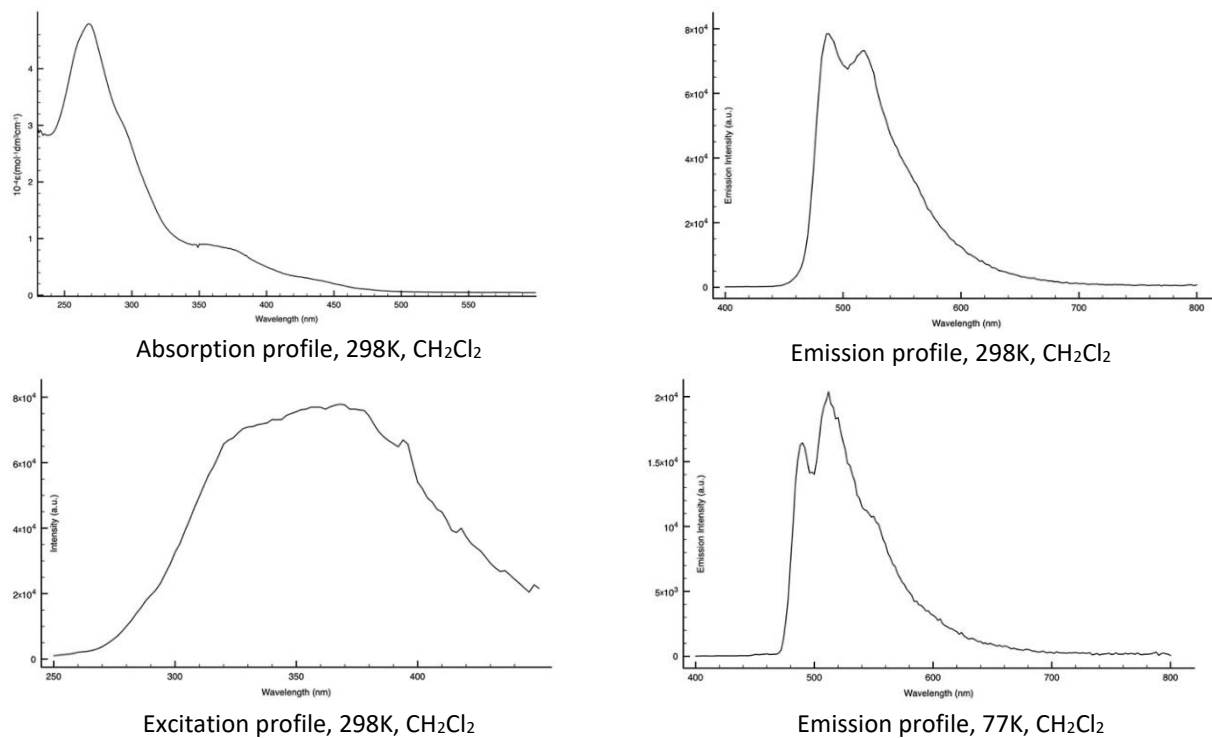


**Figure S79:** Stern Volmer Quenching Studies of **7[Br]** ( $M = 1.14 \times 10^{-4}$  in DMF) vs EBPA ( $9 \times 5 \mu\text{L}$ ).

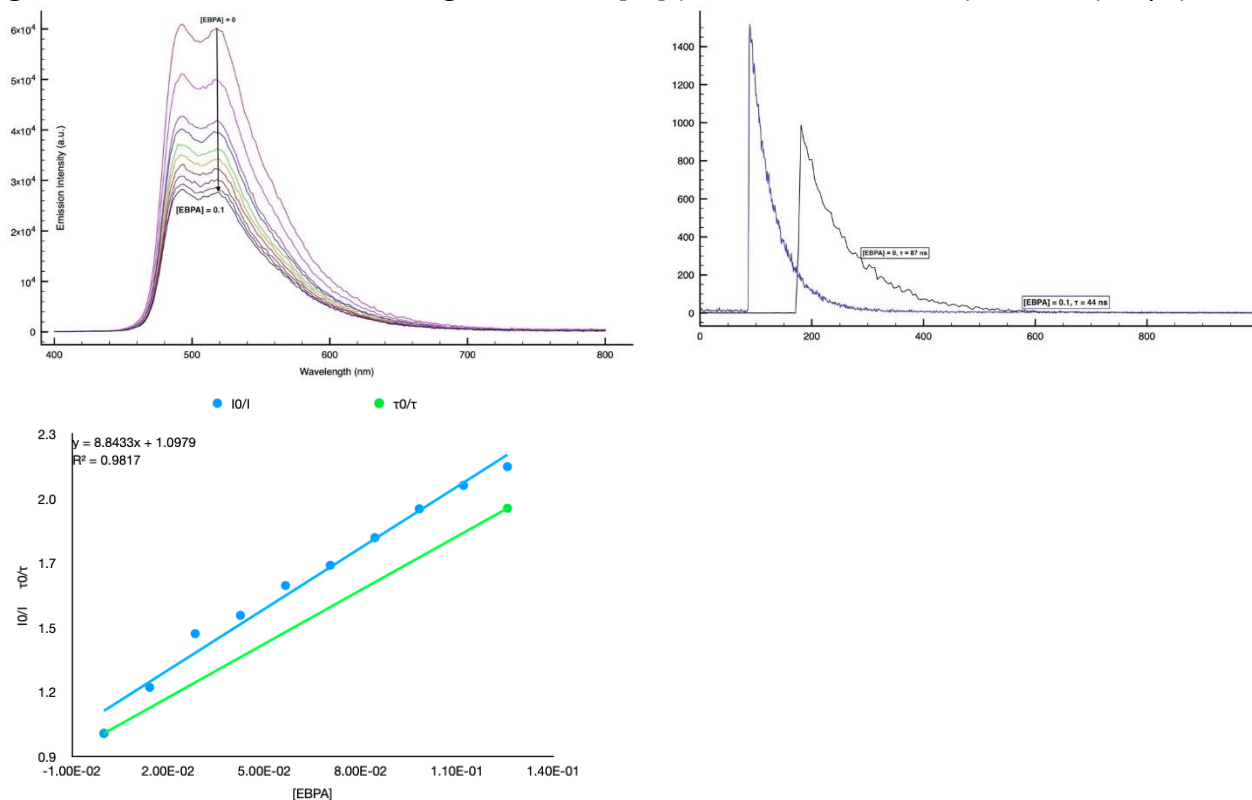


**Figure S80:** Photophysical Characterization of **8[Br]**

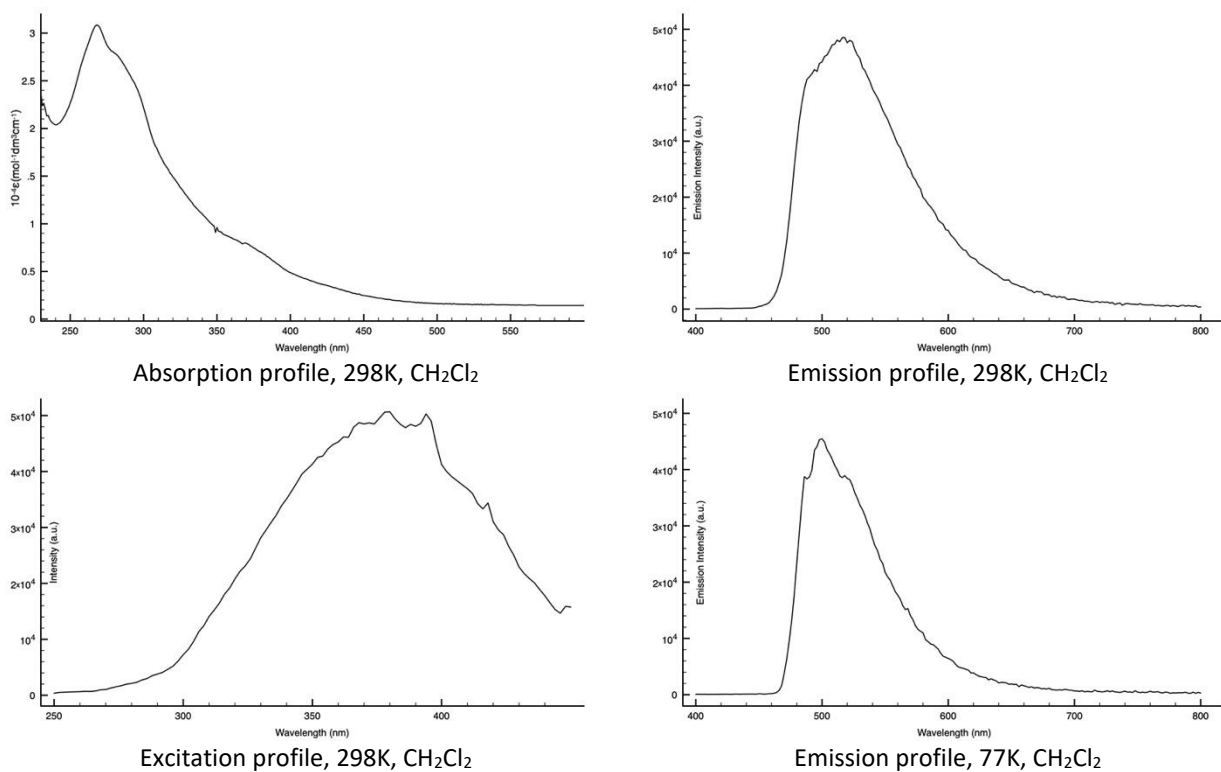


**Figure S81:** Stern Volmer Quenching Studies of **8[Br]** ( $M = 1.04 \times 10^{-4}$  in DMF) vs EBPA (9x5 $\mu$ L).

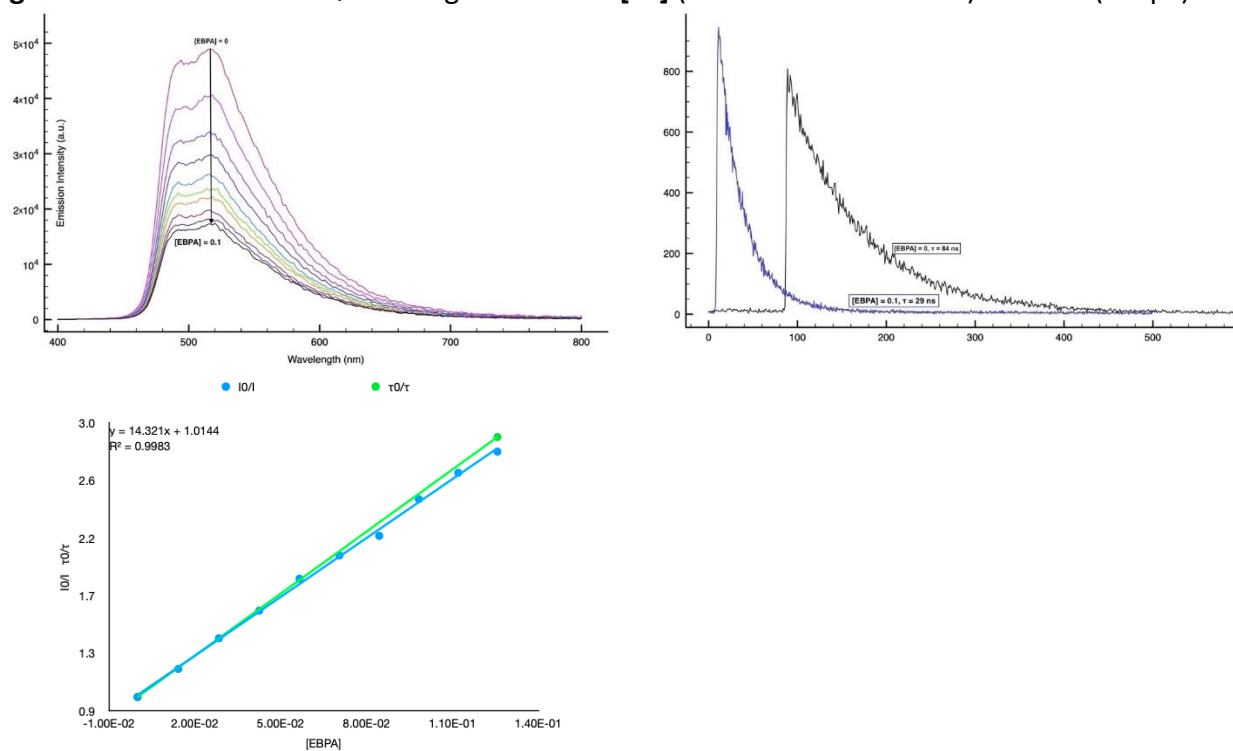


**Figure S82:** Photophysical Characterization of **9[Br]**

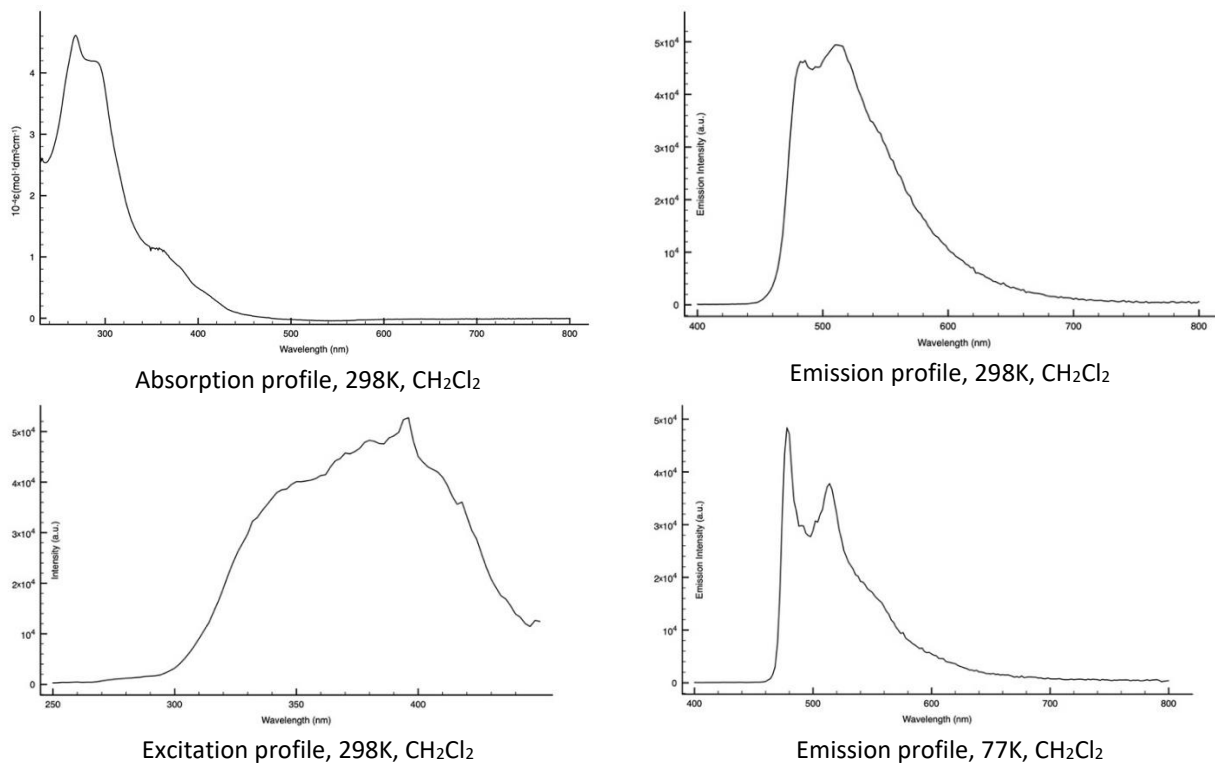


**Figure S83:** Stern Volmer Quenching Studies of **9[Br]** ( $M = 1.07 \times 10^{-4}$  in DMF) vs EBPA ( $9 \times 5 \mu\text{L}$ ).

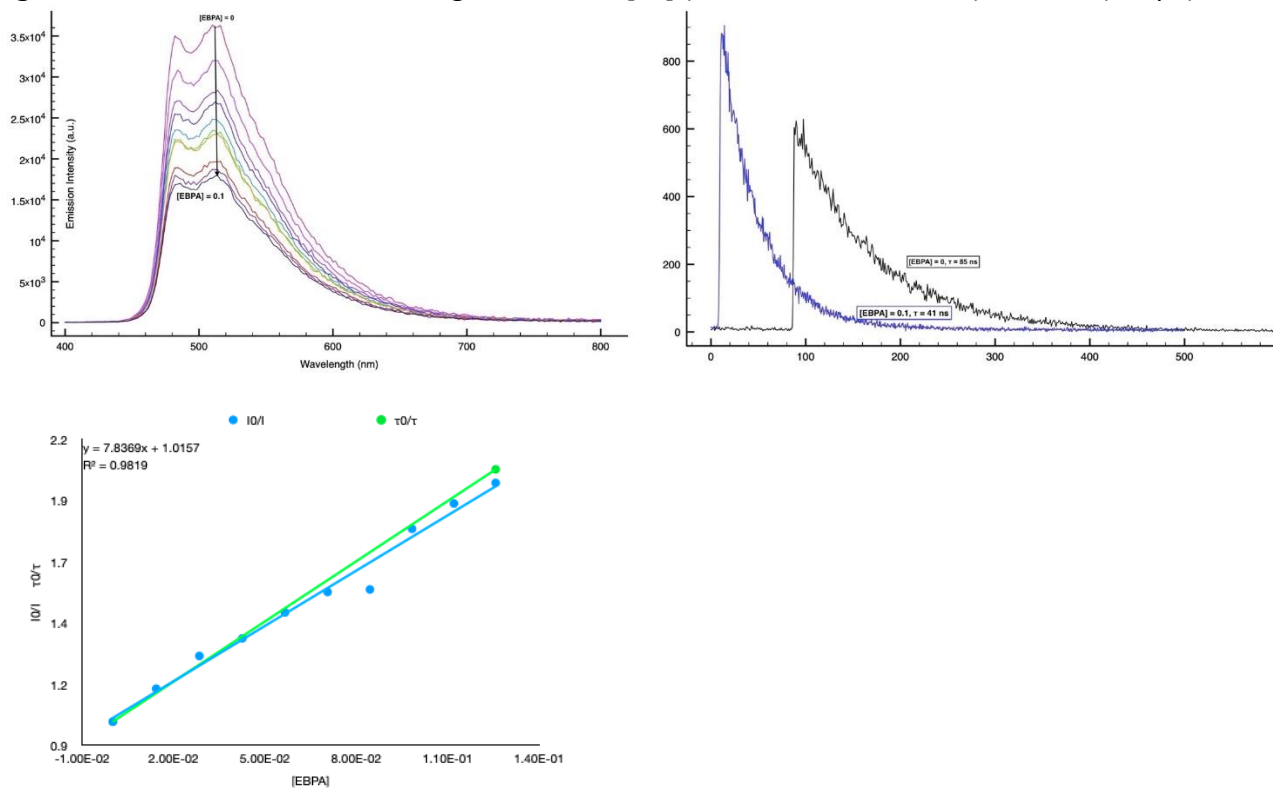


**Figure S84:** Photophysical Characterization of **10[Br]**

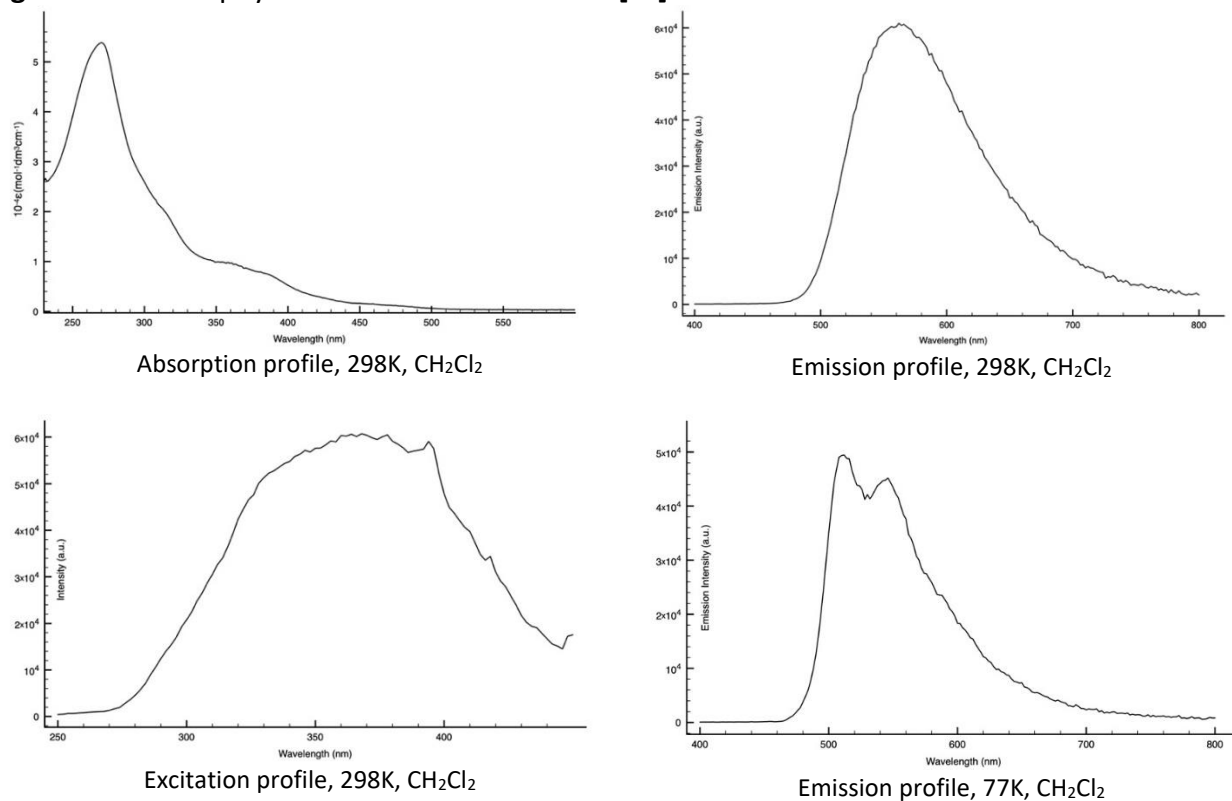




**Figure S85: Stern Volmer Quenching Studies of 10[Br] ( $M = 1.10 \times 10^{-4}$  in DMF) vs EBPA (9x5 $\mu$ L).**

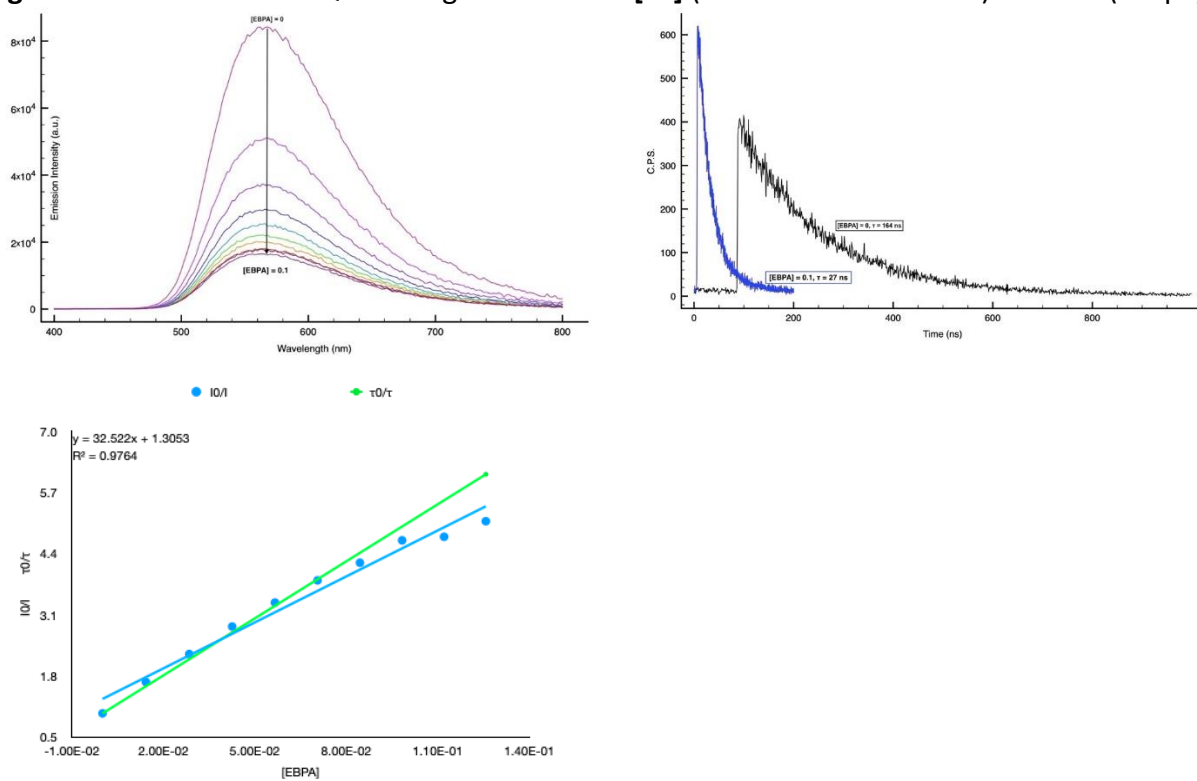


**Figure S86: Photophysical Characterization of 11[Br]**

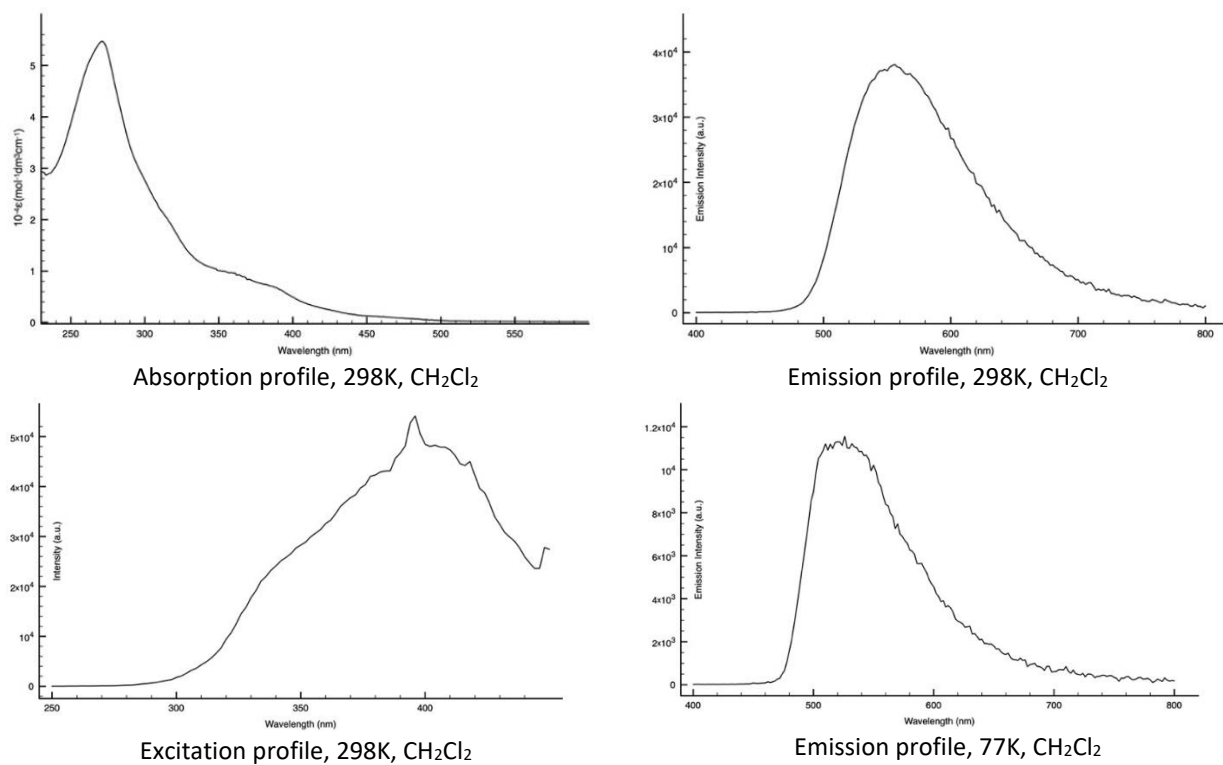


**Figure S87:** Stern Volmer Quenching Studies of **11[Br]** ( $M = 1.04 \times 10^{-4}$  in DMF) vs EBPA ( $9 \times 5 \mu\text{L}$ ).

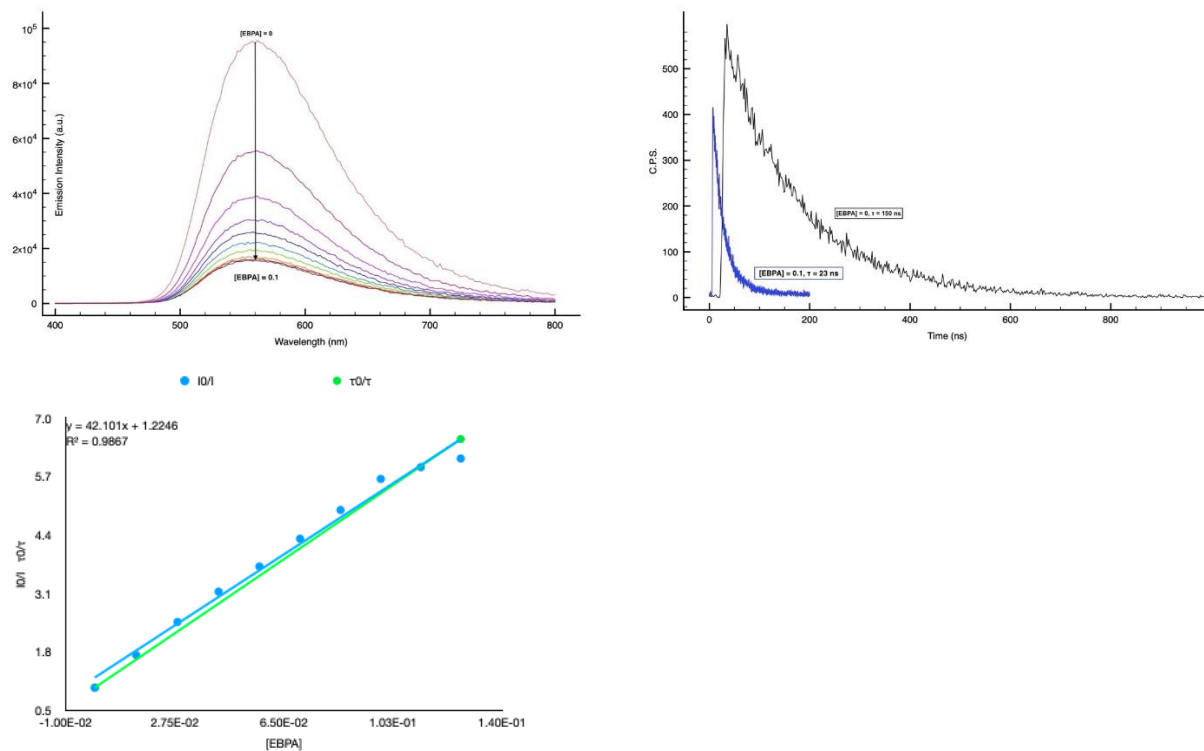


**Figure S88:** Photophysical Characterization of **5[Br]**

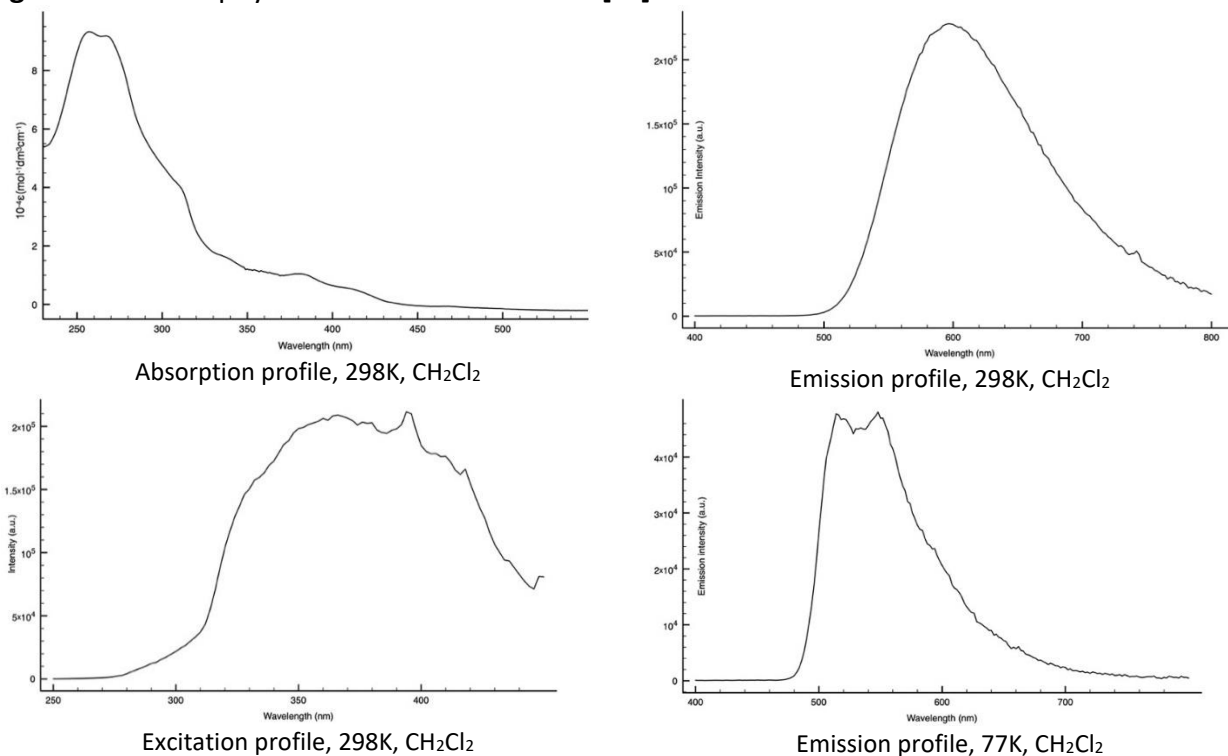


**Figure S89:** Photophysical Characterization of **6[Br]**

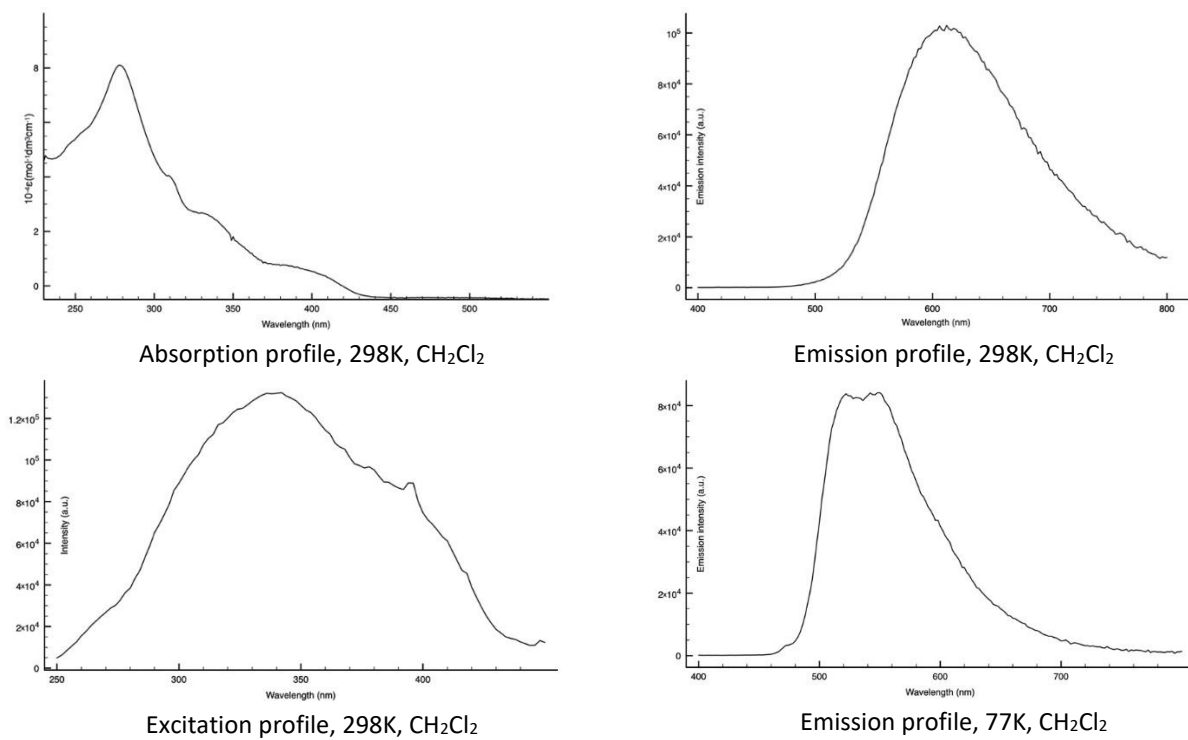
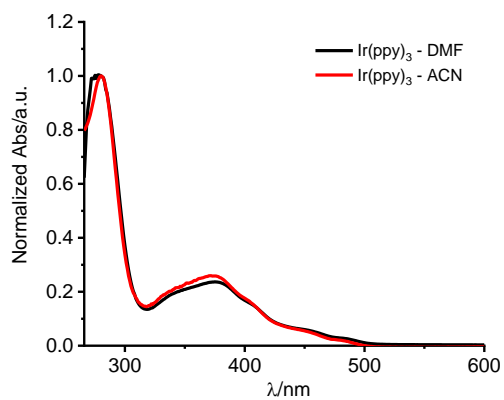


**Figure S90:** Comparison of the absorption spectra of the standard **Ir(ppy)<sub>3</sub>** in DMF and in ACN solutions



## X-Ray Crystallography

**Table S4.** Crystal data and measurement details for [1][BF<sub>4</sub>] $\cdot$ solv and [2][PF<sub>6</sub>] $\cdot$ CH<sub>2</sub>Cl<sub>2</sub>.

	[1][BF <sub>4</sub> ] $\cdot$ solv	[2][PF <sub>6</sub> ] $\cdot$ CH <sub>2</sub> Cl <sub>2</sub>
Formula	C <sub>36</sub> H <sub>34</sub> BF <sub>4</sub> IrN <sub>6</sub>	C <sub>41</sub> H <sub>44</sub> Cl <sub>2</sub> F <sub>6</sub> IrN <sub>6</sub> O <sub>2</sub> P
FW	829.70	1060.89
T, K	100(2)	100(2)
$\lambda$ , Å	0.71073	0.71073
Crystal system	Monoclinic	Triclinic
Space group	<i>P</i> 2 <sub>1</sub> / <i>c</i>	<i>P</i> $\bar{1}$
<i>a</i> , Å	15.3253(5)	8.5899(4)
<i>b</i> , Å	16.2114(5)	14.3850(8)
<i>c</i> , Å	15.8400(5)	17.2373(9)
$\alpha$ , °	90	71.361(2)
$\beta$ , °	105.9080(10)	84.697(2)
$\gamma$ , °	90	88.999(2)
Cell Volume, Å <sup>3</sup>	3784.6(2)	2009.42(18)
Z	4	2
<i>D<sub>c</sub></i> , g·cm <sup>-3</sup>	1.456	1.753
$\mu$ , mm <sup>-1</sup>	3.579	3.569
F(000)	1640	1056
Crystal size, mm	0.16×0.14×0.12	0.16×0.14×0.11
$\theta$ limits, °	1.834-26.000	1.494-27.000
Reflections collected	71196	41035
Independent reflections	7440 [ <i>R</i> <sub>int</sub> = 0.0702]	8755 [ <i>R</i> <sub>int</sub> = 0.0987]
Data / restraints / parameters	7440 / 75 / 433	8755 / 110 / 547
Goodness on fit on F <sup>2</sup>	1.115	1.104
<i>R</i> <sub>1</sub> ( <i>I</i> > 2 $\sigma$ ( <i>I</i> ))	0.0407	0.0339
<i>wR</i> <sub>2</sub> (all data)	0.0972	0.0804
Largest diff. peak and hole, e Å <sup>-3</sup>	1.903 / -1.717	1.853 / -1.022

## General Procedure for the photopolymerization of MMA

All the polymerizations were conducted following a slightly modified procedure by Fors *et al.*<sup>ref</sup> DMF (anhydrous, 99.8%) was thoroughly degassed with several freeze pump thaw cycles until no further gas evolution was observed; MMA was distilled before use. EBPA was stored in the dark under an argon atmosphere once opened. A two neck 5 mL flask under argon atmosphere was charged with MMA (0.4 mL, 3.75 mmol), Ir catalyst (0.01-0.02 mol%), DMF (1.4 mL) and 0.004 equivalent of EBPA. The reaction was stirred within a crystallization dish (Figure XX) equipped with an adhered 5-meter LED strip or with two CFL Households lamps (6500 K, 12 W, Osram). The MMA conversion was measured by <sup>1</sup>H-NMR in CDCl<sub>3</sub> by integration of the -OCH<sub>3</sub> singlet (3.71 ppm) of MMA vs -OCH<sub>3</sub> backbone (3.56 ppm) of PMMA. Number average molecular weights (M<sub>n</sub>) and PDI of the samples were determined by GPC.

**Figure S91:** (sx) Emission profile of the led strip used as light source,  $\lambda_{exc} = 370$  nm. (dx): photoreactor setup: crystallization dish (136 × 70 mm) equipped with an adhered 5-meter LED strip and a fan.

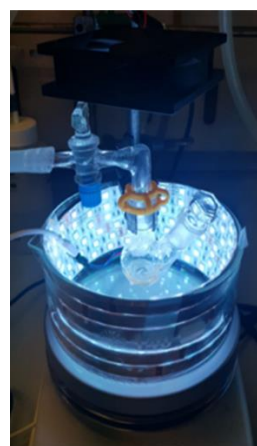
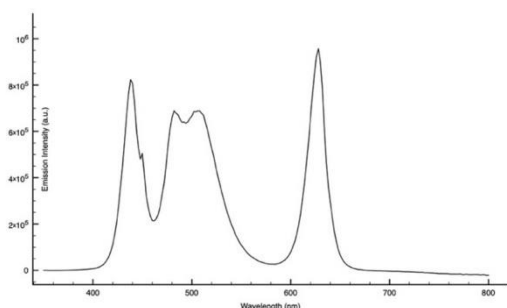


**Figure S92:** photoreactor setup with two CFL Households lamps (6500 K, 12 W, Osram) and a fan.



### First-order kinetic plots, $M_n$ and PDI versus conversion

**Figure S93:** (sx)  $M_n$  and PDI versus conversion (dx) First-order kinetic plot of Entry 1 **1**[PF<sub>6</sub>] 0.01% mol, LED.

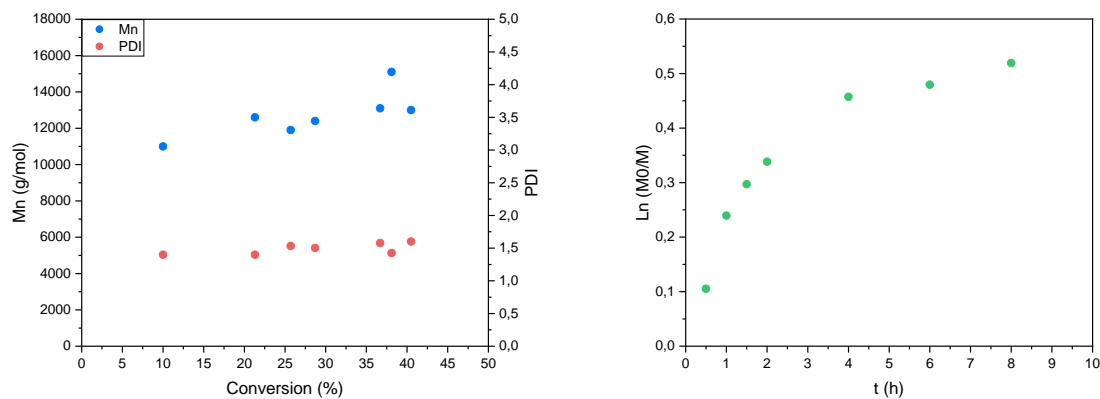


**Figure S94:** (sx)  $M_n$  and PDI versus conversion (dx) First-order kinetic plot of Entry 2 **1**[BF<sub>4</sub>] 0.01% mol, LED

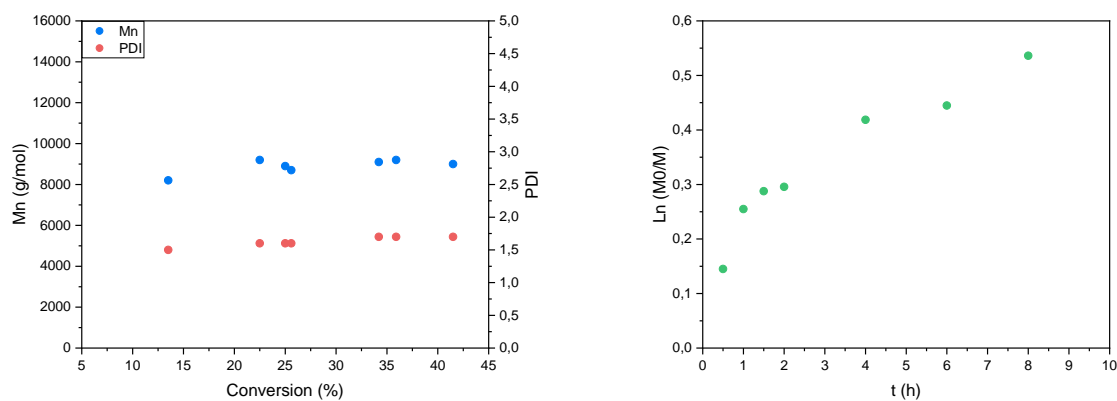


**Figure S95:** (sx)  $M_n$  and PDI versus conversion (dx) First-order kinetic plot of Entry 3 **1**[Br] 0.01% mol, LED

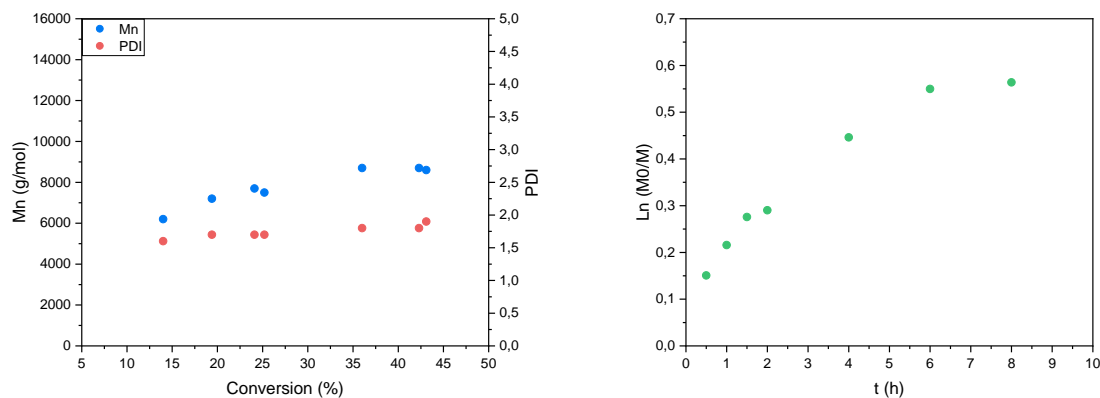


**Figure S96:** (sx)  $M_n$  and PDI versus conversion (dx) First-order kinetic plot of Entry 4 **1[Br]** 0.01% mol, CFL

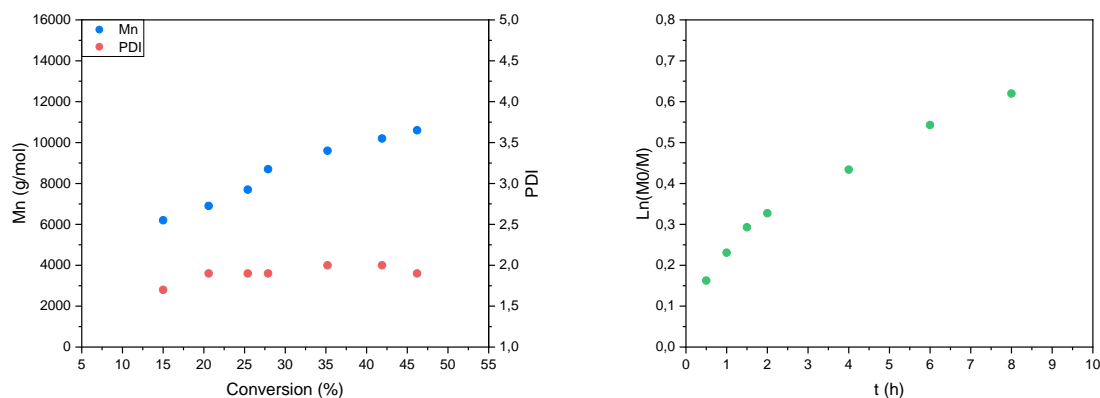


**Figure S97:** (sx)  $M_n$  and PDI versus conversion (dx) First-order kinetic plot of Entry 5 **1[Br]** 0.0125% mol, CFL

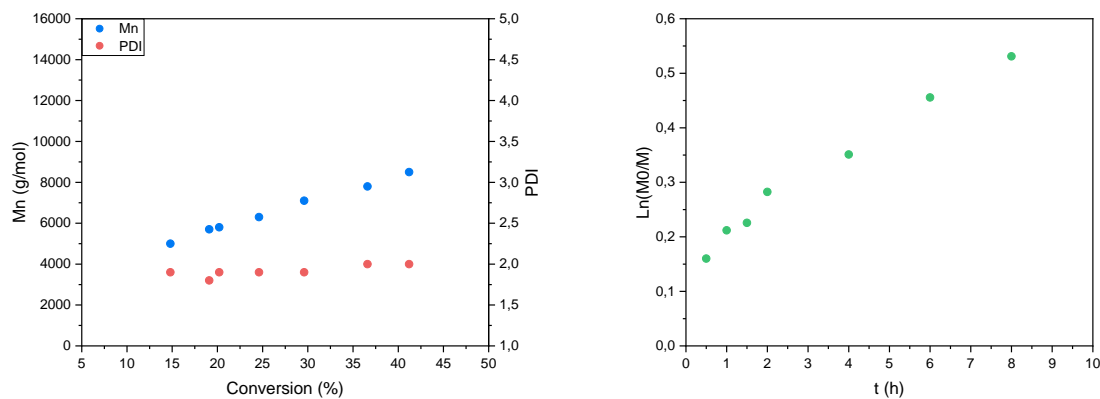


**Figure S98:** (sx)  $M_n$  and PDI versus conversion (dx) First-order kinetic plot of Entry 6 **1[PF<sub>6</sub>]** 0.015% mol, LED

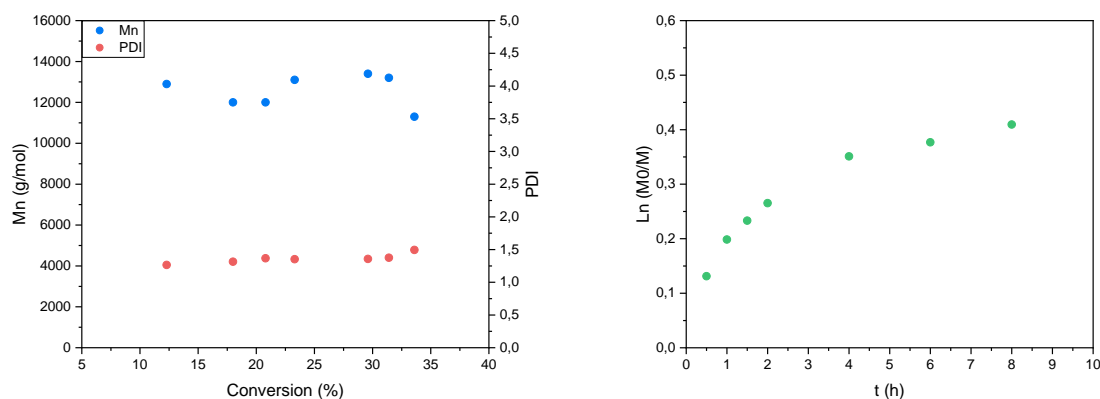


**Figure S99:** (sx)  $M_n$  and PDI versus conversion (dx) First-order kinetic plot of Entry 7 **1[Br]** 0.015 mol, LED

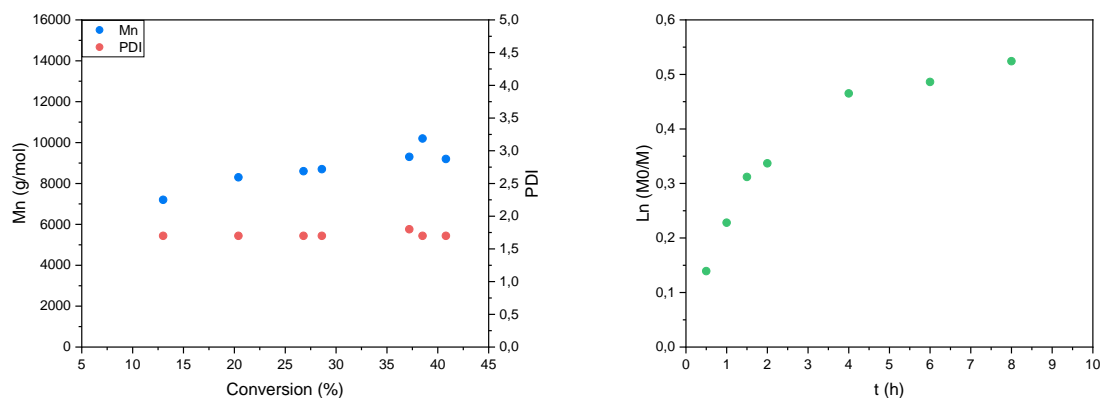


**Figure S100:** (sx)  $M_n$  and PDI versus conversion (dx) First-order kinetic plot of Entry 8 **1[Br]** 0.015% mol, CFL

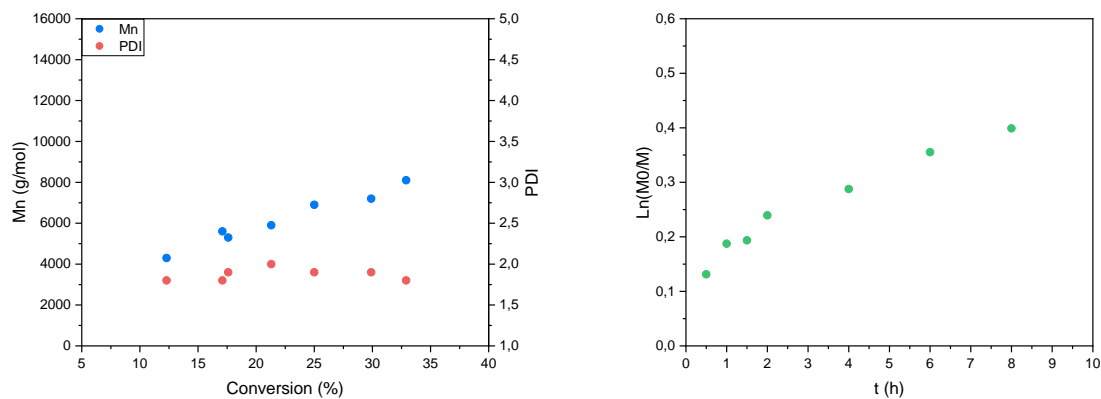


**Figure S101:** (sx)  $M_n$  and PDI versus conversion (dx) First-order kinetic plot of Entry 9 **1[Br]** 0.02% mol, CFL

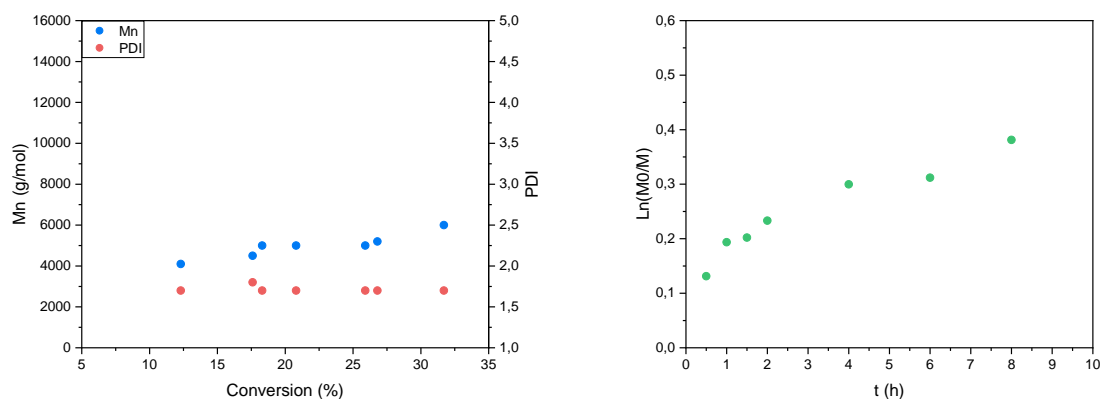




**Figure S102:** (sx)  $M_n$  and PDI versus conversion (dx) First-order kinetic plot of Entry 10 **2**[PF<sub>6</sub>] 0.01% mol, LED

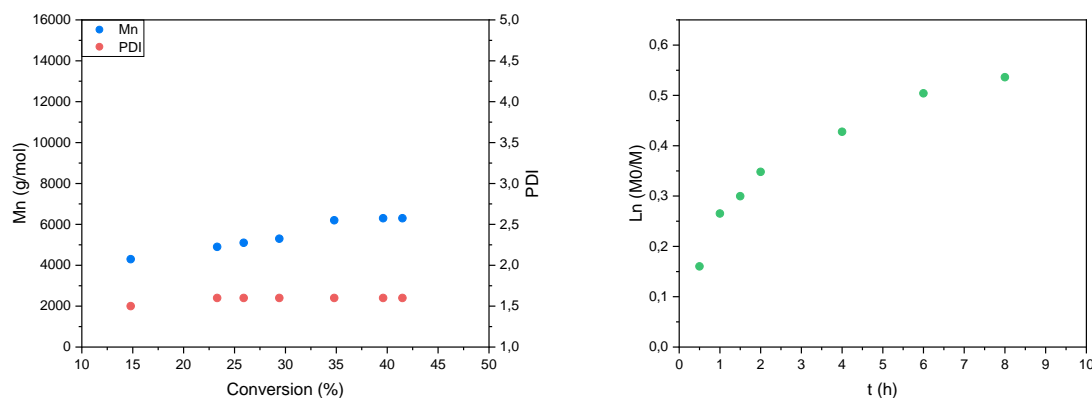


**Figure S103:** (sx)  $M_n$  and PDI versus conversion (dx) First-order kinetic plot of Entry 11 **2**[Br] 0.01% mol, LED

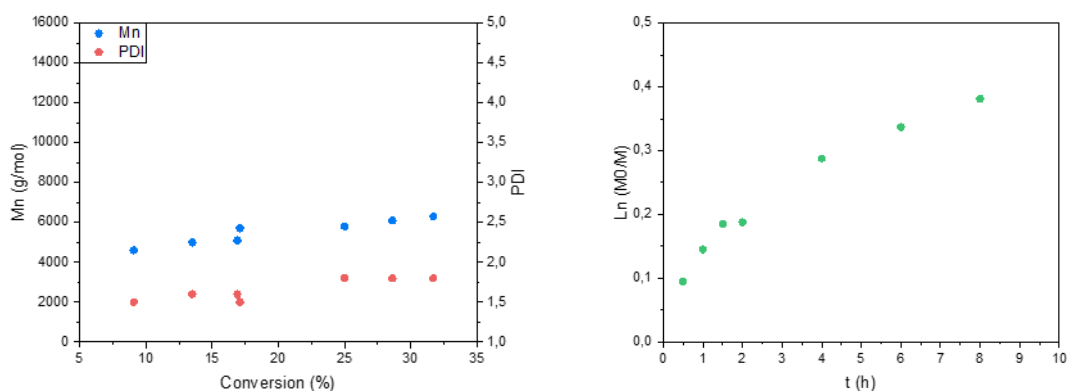


**Figure S104:** (sx)  $M_n$  and PDI versus conversion (dx) First-order kinetic plot of Entry 12 **2**[Br] 0.01% mol, CFL

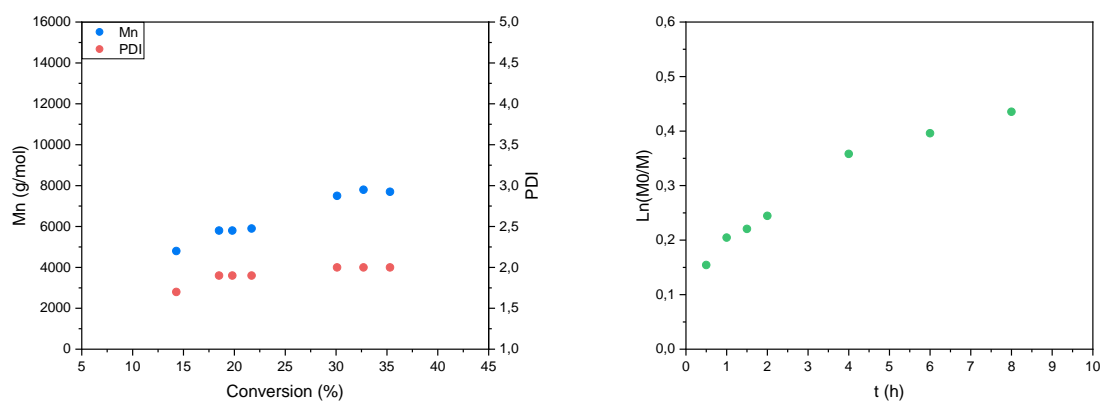


**Figure S105:** (sx)  $M_n$  and PDI versus conversion (dx) First-order kinetic plot of Entry 13 **2[Br]** 0.0125% mol, CFL

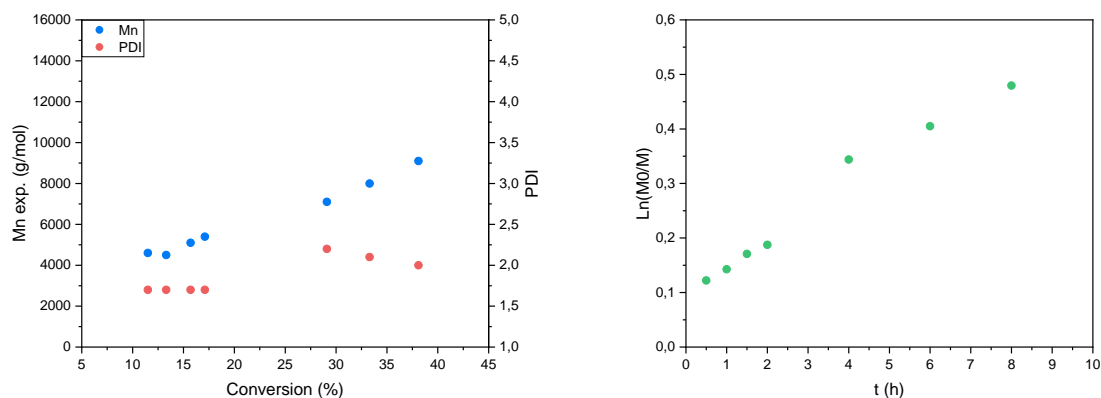


**Figure S106:** (sx)  $M_n$  and PDI versus conversion (dx) First-order kinetic plot of Entry 14 **2[Br]** 0.015% mol, LED

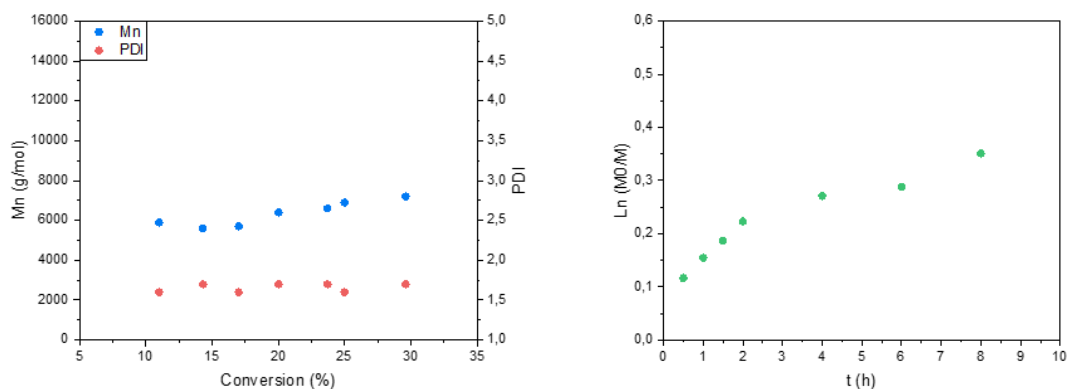


**Figure S107:** (sx)  $M_n$  and PDI versus conversion (dx) First-order kinetic plot of Entry 15 **2[Br]** 0.02% mol, LED

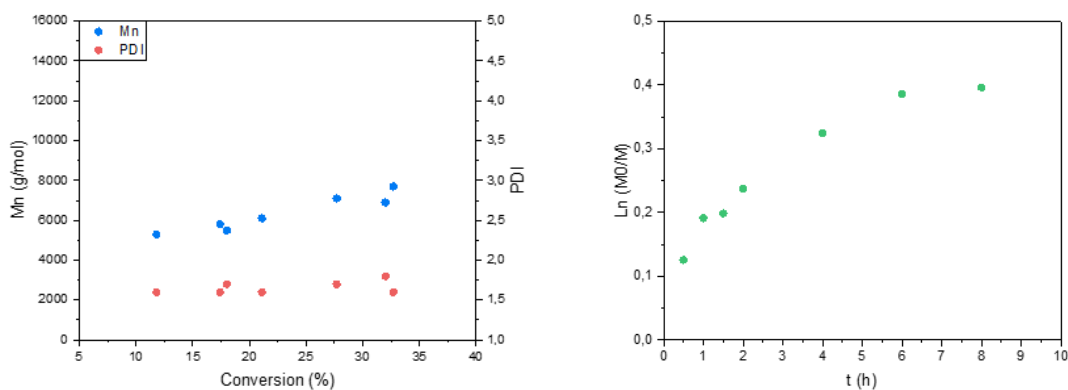


**Figure S108:** (sx)  $M_n$  and PDI versus conversion (dx) First-order kinetic plot of Entry 16 **3**[PF<sub>6</sub>] 0.01% mol, LED

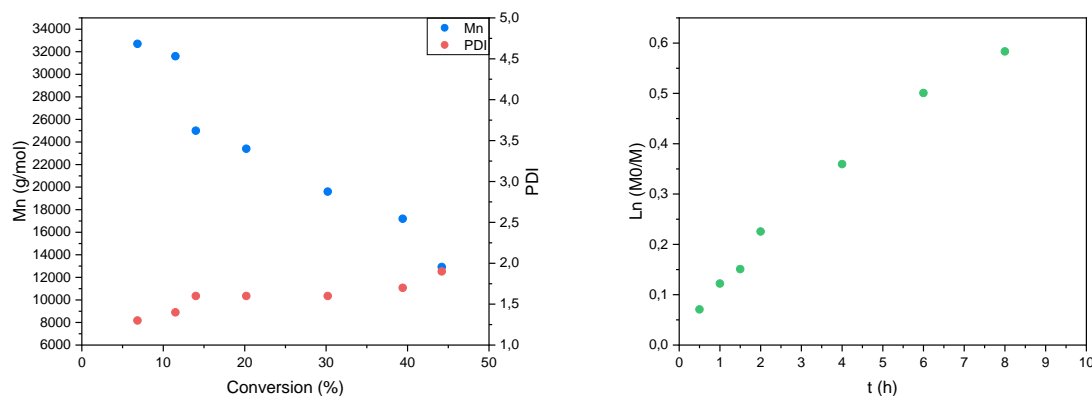


**Figure S109:** (sx)  $M_n$  and PDI versus conversion (dx) First-order kinetic plot of Entry 17 **4**[PF<sub>6</sub>] 0.01% mol, LED

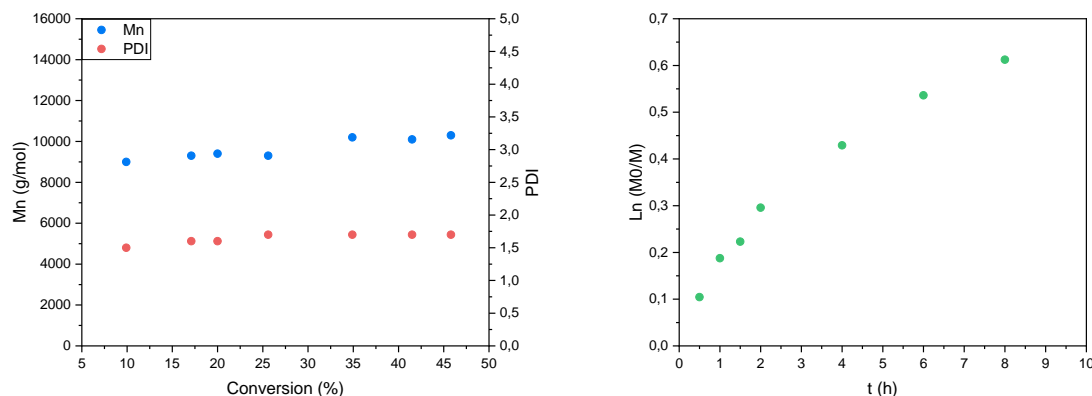


**Figure S110:** (sx)  $M_n$  and PDI versus conversion (dx) First-order kinetic plot of Entry 18 **4**[Br] 0.01% mol, LED

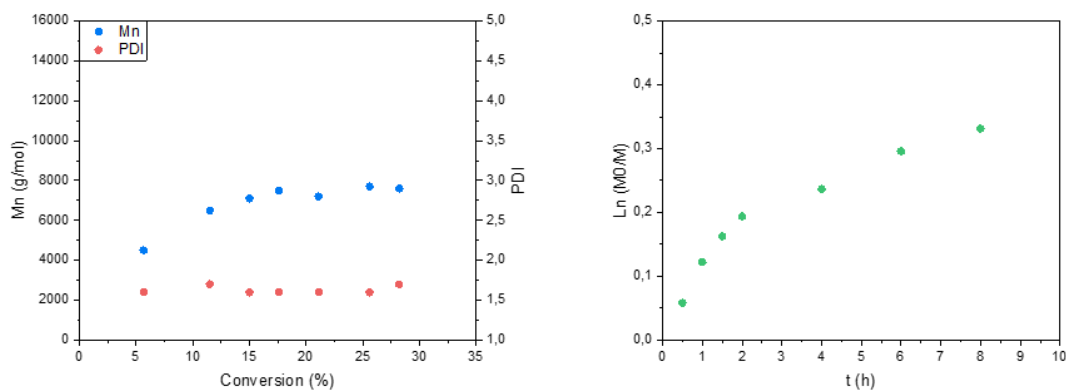


**Figure S111:** (sx) *Mn* and PDI versus conversion (dx) First-order kinetic plot of Entry 19 **4[Br]** 0.01% mol, CFL

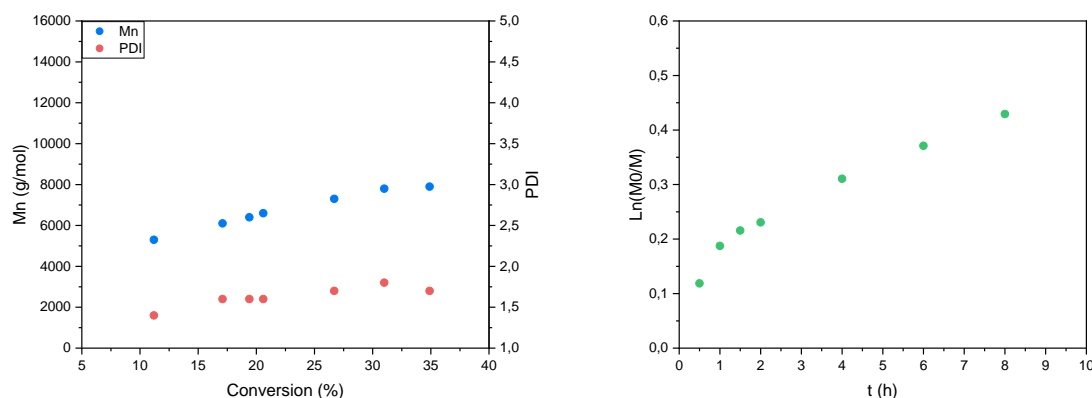


**Figure S112:** (sx) *Mn* and PDI versus conversion (dx) First-order kinetic plot of Entry 20 **4[Br]** 0.015% mol, CFL

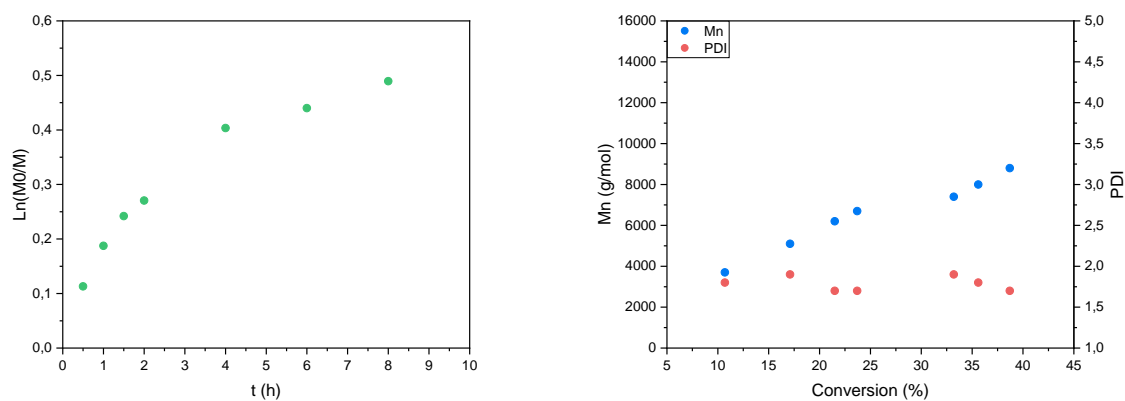


**Figure S113:** (sx) *Mn* and PDI versus conversion (dx) First-order kinetic plot of Entry 21 **4[Br]** 0.02% mol, CFL

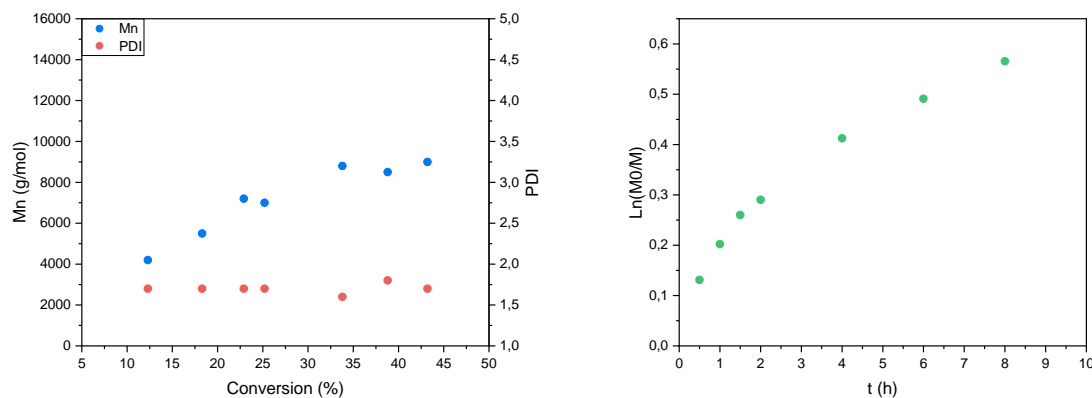


**Figure S114:** (sx) *Mn* and PDI versus conversion (dx) First-order kinetic plot of Entry 22 **7[Br]** 0.015% mol, CFL

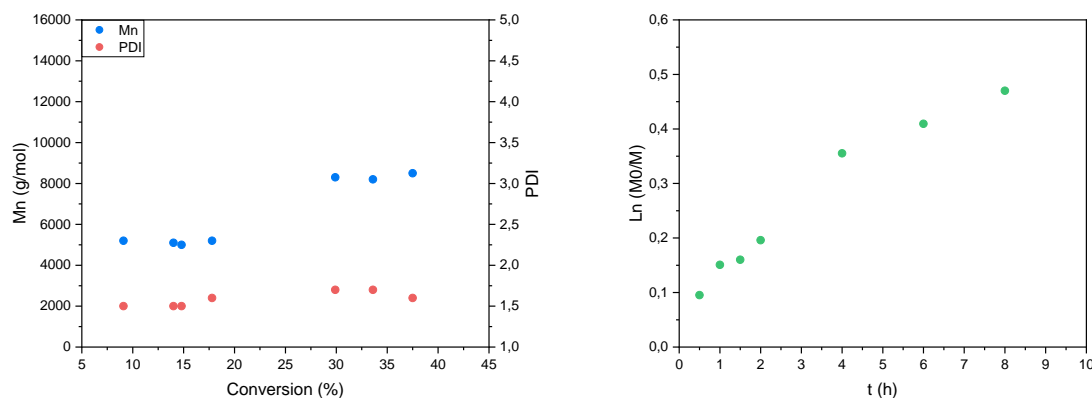


**Figure S115:** (sx) *Mn* and PDI versus conversion (dx) First-order kinetic plot of Entry 23 **7[Br]** 0.02% mol, CFL

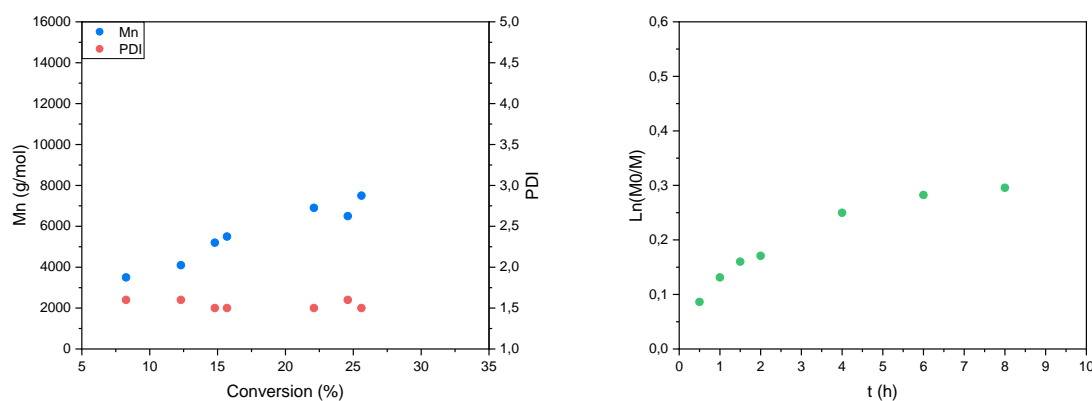


**Figure S116:** (sx) *Mn* and PDI versus conversion (dx) First-order kinetic plot of Entry 24 **8[Br]** 0.015% mol, CFL

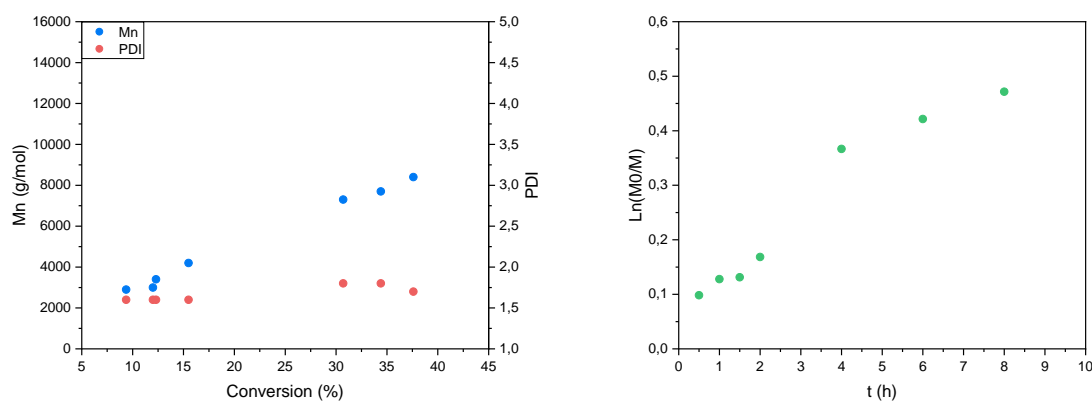


**Figure S117:** (sx)  $M_n$  and PDI versus conversion (dx) First-order kinetic plot of Entry 25 **8[Br]** 0.02% mol, CFL

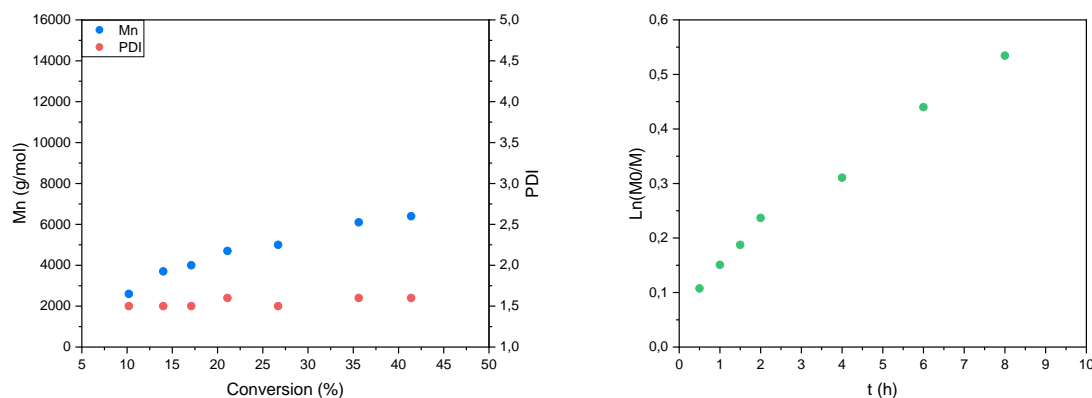


**Figure S118:** (sx)  $M_n$  and PDI versus conversion (dx) First-order kinetic plot of Entry 26 **9[Br]** 0.015% mol, CFL

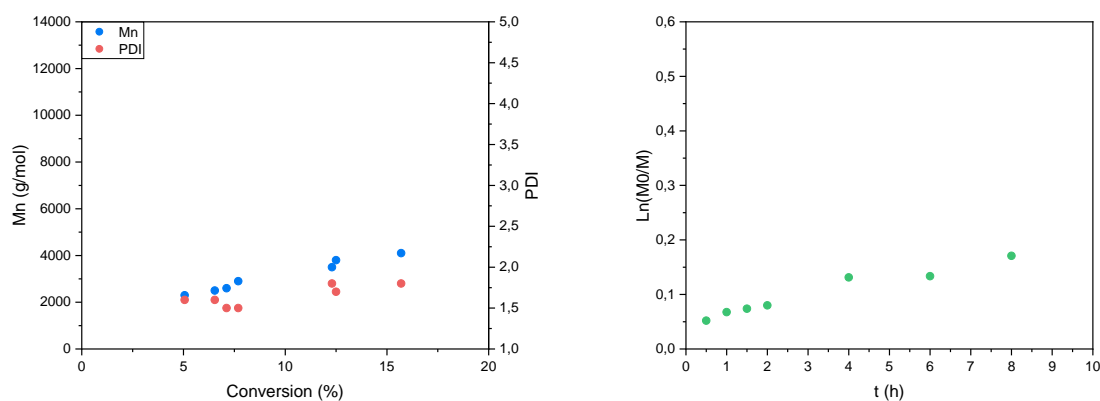


**Figure S119:** (sx)  $M_n$  and PDI versus conversion (dx) First-order kinetic plot of Entry 27 **9[Br]** 0.02% mol, CFL

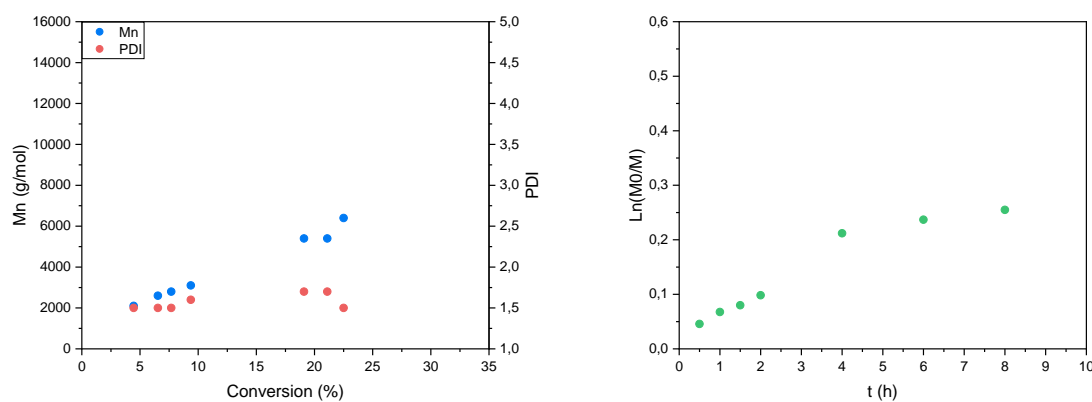


**Figure S120:** (sx)  $M_n$  and PDI versus conversion (dx) First-order kinetic plot of Entry 28 **10[Br]** 0.01% mol, CFL

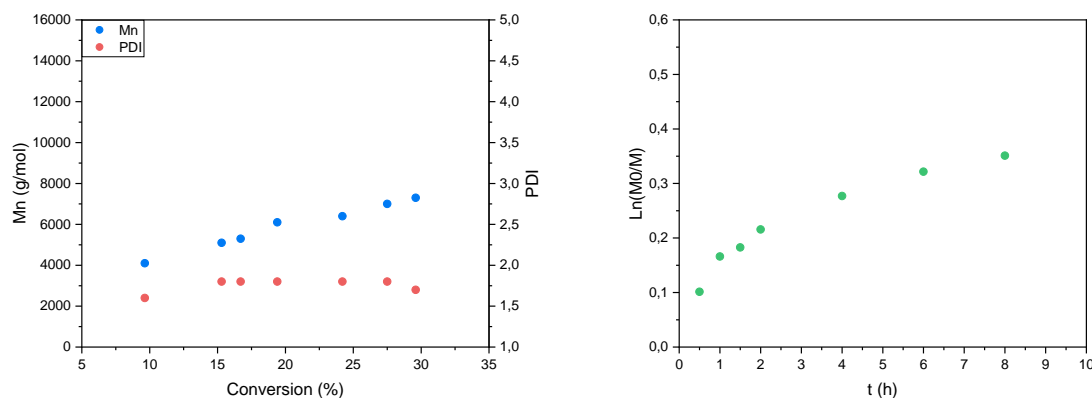


**Figure S121:** (sx)  $M_n$  and PDI versus conversion (dx) First-order kinetic plot of Entry 29 **10[Br]** 0.0125% mol, CFL

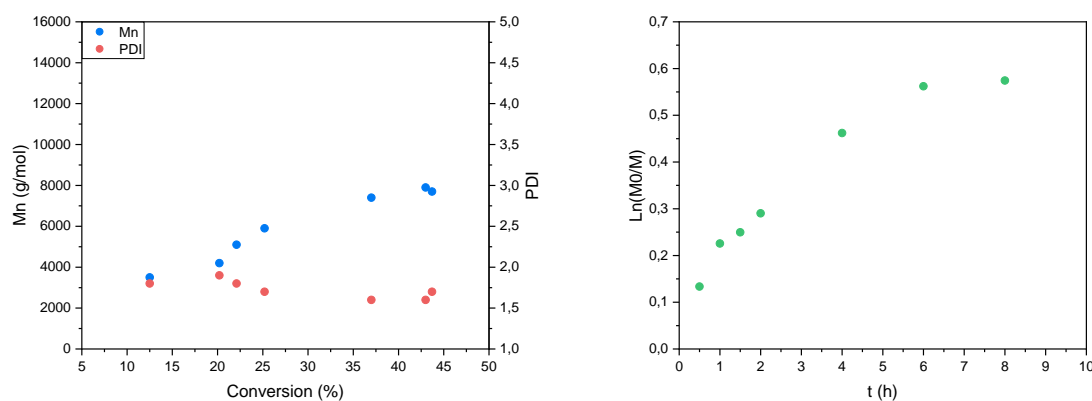


**Figure S122:** (sx)  $M_n$  and PDI versus conversion (dx) First-order kinetic plot of Entry 30 **10[Br]** 0.015% mol, CFL

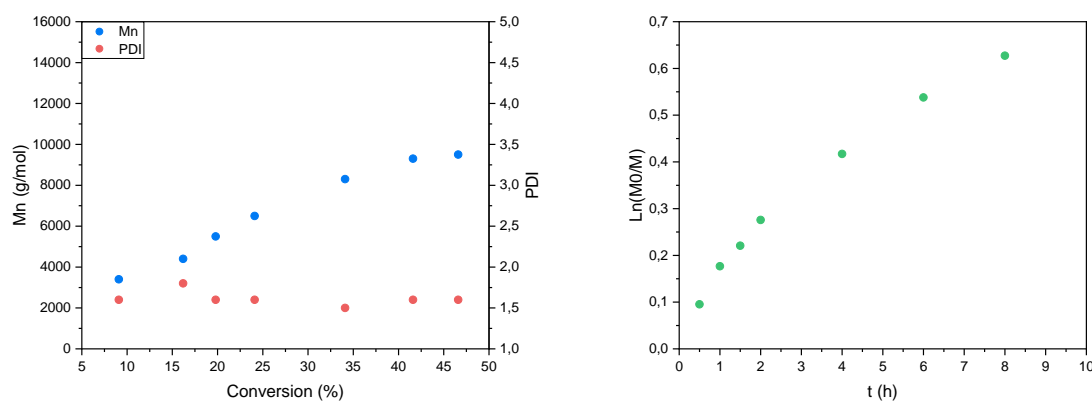


**Figure S123:** (sx)  $M_n$  and PDI versus conversion (dx) First-order kinetic plot of Entry 31 **10[Br]** 0.02% mol, CFL

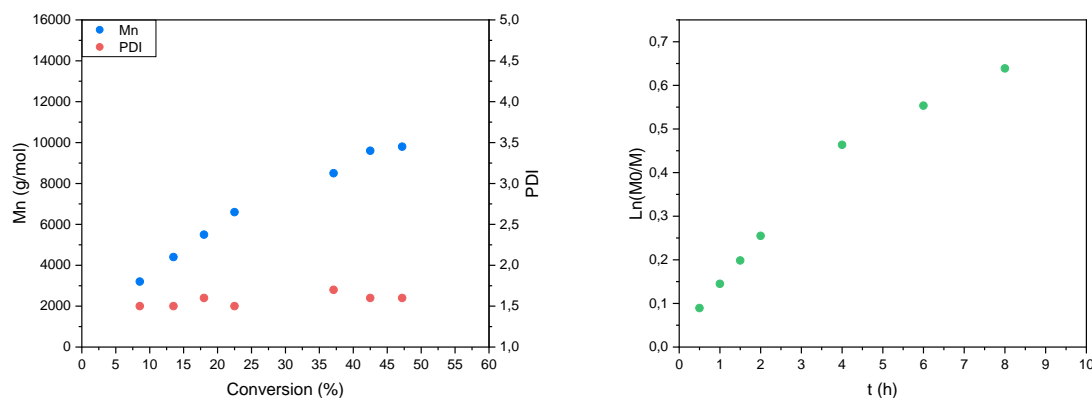


**Figure S124:** (sx)  $M_n$  and PDI versus conversion (dx) First-order kinetic plot of Entry 32 **10[Br]** 0.02% mol, LED

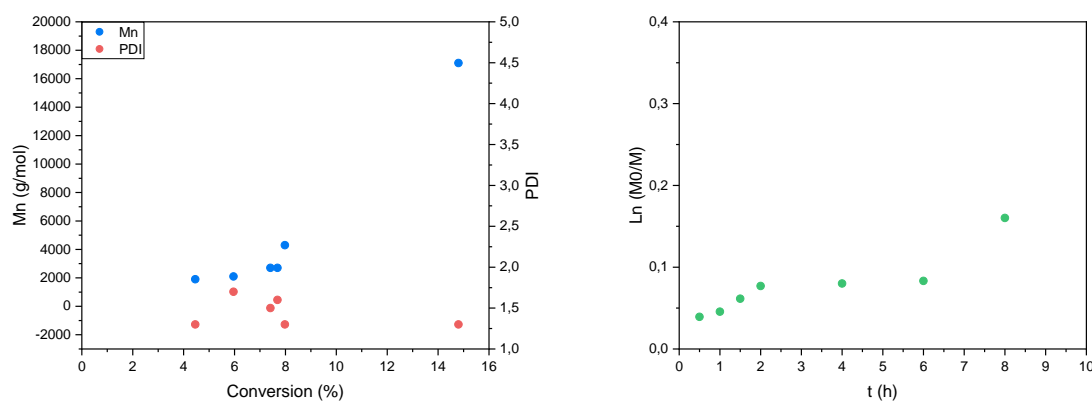


**Figure S125:** (sx)  $M_n$  and PDI versus conversion (dx) First-order kinetic plot of Entry 33 **11[Br]** 0.01% mol, CFL

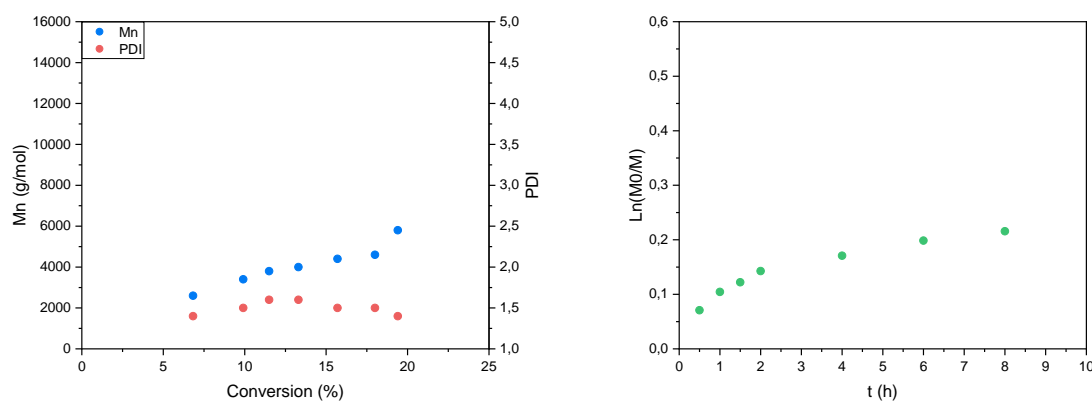




**Figure S126:** (sx)  $M_n$  and PDI versus conversion (dx) First-order kinetic plot of Entry 34 **11[Br]** 0.015% mol, CFL

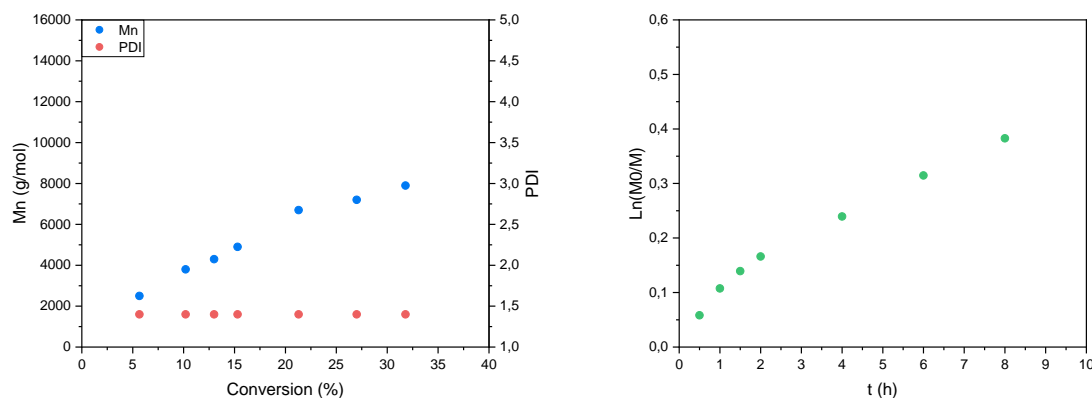
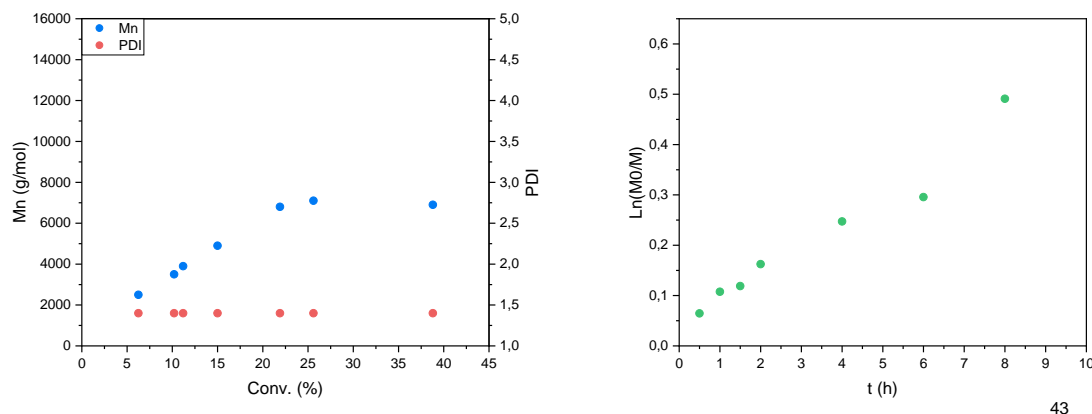
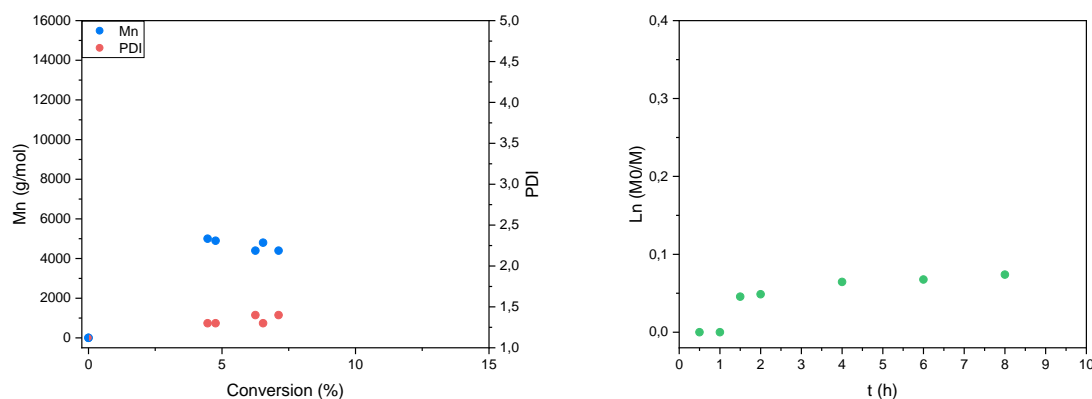


**Figure S127:** (sx)  $M_n$  and PDI versus conversion (dx) First-order kinetic plot of Entry 35 **11[Br]** 0.02% mol, CFL



43

**Figure S128:** (sx)  $M_n$  and PDI versus conversion (dx) First-order kinetic plot of Entry 36 **11[Br]** 0.02% mol, LED



## Synthesis of poly(methyl methacrylate-*b*-hexyl methacrylate) using PMMA as macroinitiator

### *First step*

A two neck 5 mL flask under argon atmosphere was charged with MMA (2.4 mL, 22.5 mmol), catalyst **10 [Br]** (0.02 % mol), DMF (1.4 mL) and 0.004 equivalent of EBPA. The reaction was stirred for 4 hours under irradiation of two CFL Households lamps 6500K, 12 W, Osram. The solution was added dropwise to a cold mixture of MeOH/H<sub>2</sub>O (3:1, 300 mL) leading to a white precipitate. The solid was filtered, redissolved in the minimum amount of CH<sub>2</sub>Cl<sub>2</sub> and precipitated in a cold mixture of MeOH/H<sub>2</sub>O (3:1, 300 mL) as a white powder (350 mg). The MMA conversion was measured by <sup>1</sup>H-NMR in CDCl<sub>3</sub> by integration of the -OCH<sub>3</sub> singlet (3.71 ppm) of MMA vs -OCH<sub>3</sub> backbone (3.56 ppm) of PMMA. Number average molecular weight (M<sub>n</sub>) and PDI were determined by GPC. M<sub>n</sub>= 9800 g/mol, PDI= 1.5.

### *Second step*

A two neck 5 mL flask under argon atmosphere was charged with HMA (0.740 mL, 3.75 mmol), catalyst **10 [Br]** (0.02 % mol), DMF (1.4 mL) and 0.004 equivalent of macroinitiator PMMA (147 mg). The reaction was stirred for 8 hours under irradiation of two CFL Households lamps 6500K, 12 W, Osram. The solution was added dropwise to a cold mixture of MeOH/H<sub>2</sub>O (10:1, 200 mL) leading to a white precipitate. The solid was filtered, redissolved in the minimum amount of CH<sub>2</sub>Cl<sub>2</sub> and precipitated in a cold mixture of MeOH/H<sub>2</sub>O (10:1, 200 mL) as a white powder (177 mg). The p(MMA-*b*-HMA) conversion was measured by <sup>1</sup>H-NMR in CDCl<sub>3</sub> by integration of the -OCH<sub>2</sub>- triplet (4.13 ppm) of HMA vs -OCH<sub>2</sub>- backbone (3.93 ppm) of PHMA. Number average molecular weight (M<sub>n</sub>) and PDI were determined by GPC. M<sub>n</sub>=16700 g/mol, PDI= 1.3

### **ON/OFF controllability experiment**

A two neck 5 mL flask under argon atmosphere was charged with MMA (1.2 mL, 11.25 mmol), catalyst **10 [Br]** (0.02 % mol), DMF (1.4 mL) and 0.004 equivalent of EBPA. The reaction was stirred for 7 hours, alternating dark periods of 1 hour and light exposure of 2 hours (two CFL Households lamps 6500K, 12 W, Osram). The MMA conversion was measured by <sup>1</sup>H-NMR in CDCl<sub>3</sub> by integration of the -OCH<sub>3</sub> singlet (3.71 ppm) of MMA vs -OCH<sub>3</sub> backbone (3.56 ppm) of PMMA. Number average molecular weights (M<sub>n</sub>) and PDI of the samples were determined by GPC.

## Transient Spectroscopy

**Figure S129:** Transient absorption spectra of the DMF solutions of (a)  $\text{Ir(ppy)}_3$ , (b)  $\text{Ir(ppy)}_3$  + EBPA, (c)  $\text{Ir(ppy)}_3$  + EBPA + MMA,  $t=0\text{h}$  of polymerization and (d)  $\text{Ir(ppy)}_3$  + EBPA + MMA,  $t=2\text{h}$  of polymerization

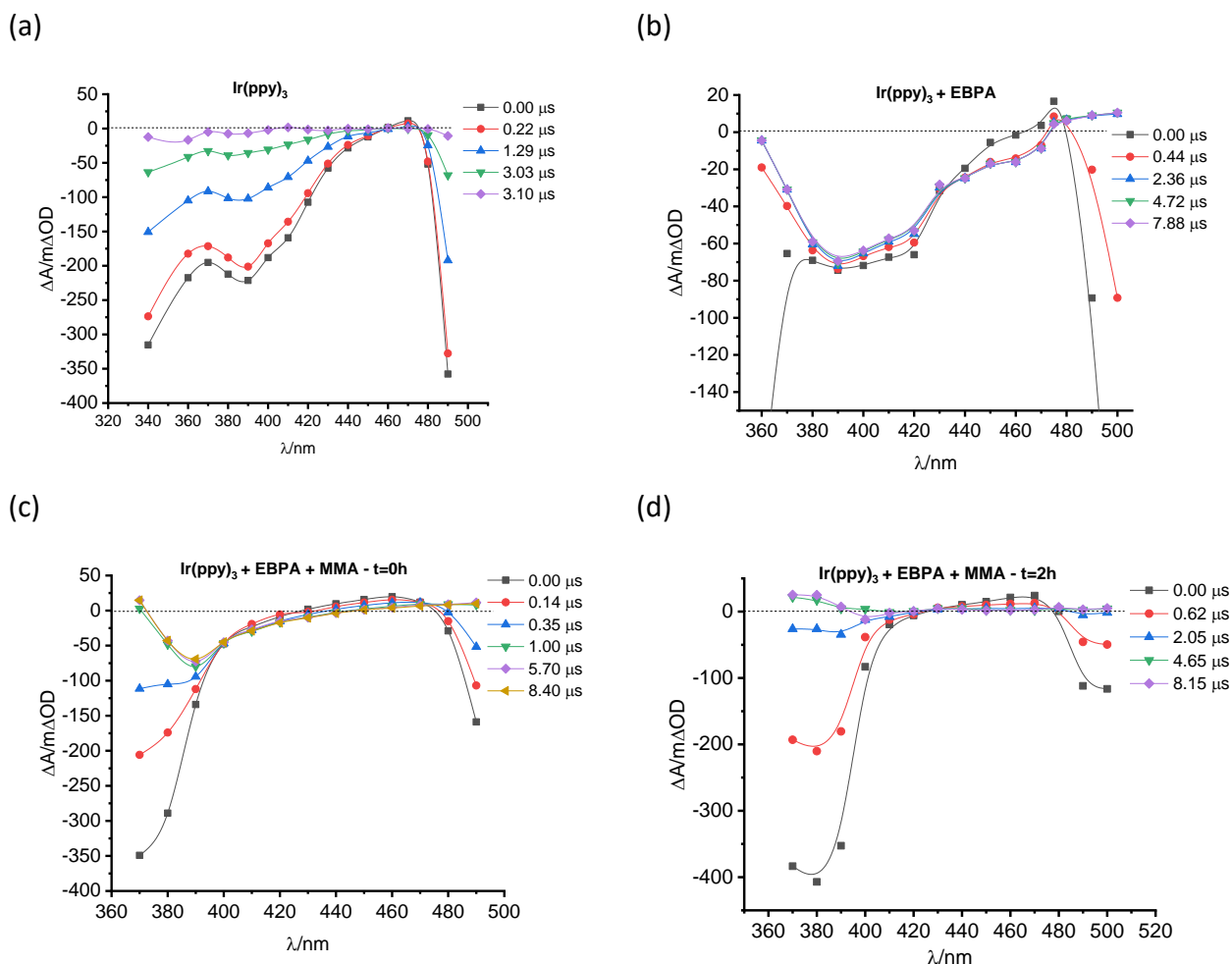


**Figure S130:** Transient absorption spectra of the DMF solution of  $1[\text{Br}]$  + EBPA at the best resolution of our spectrometer (FWHM=7-10 ns)

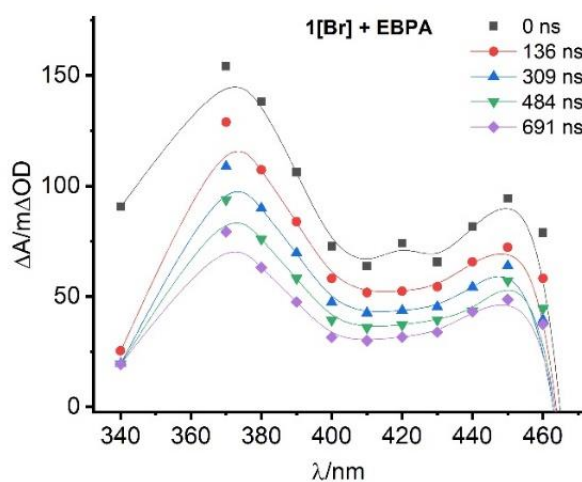


**Figure S131:** Comparison of the kinetics with and without the excess of EBPA (40:1) for (a)  $\text{Ir(ppy)}_3$ , (b)  $1[\text{Br}]$ , (c)  $5[\text{Br}]$ , (d)  $10[\text{Br}]$  at 400nm and (e)  $10[\text{Br}]$  at 420 nm

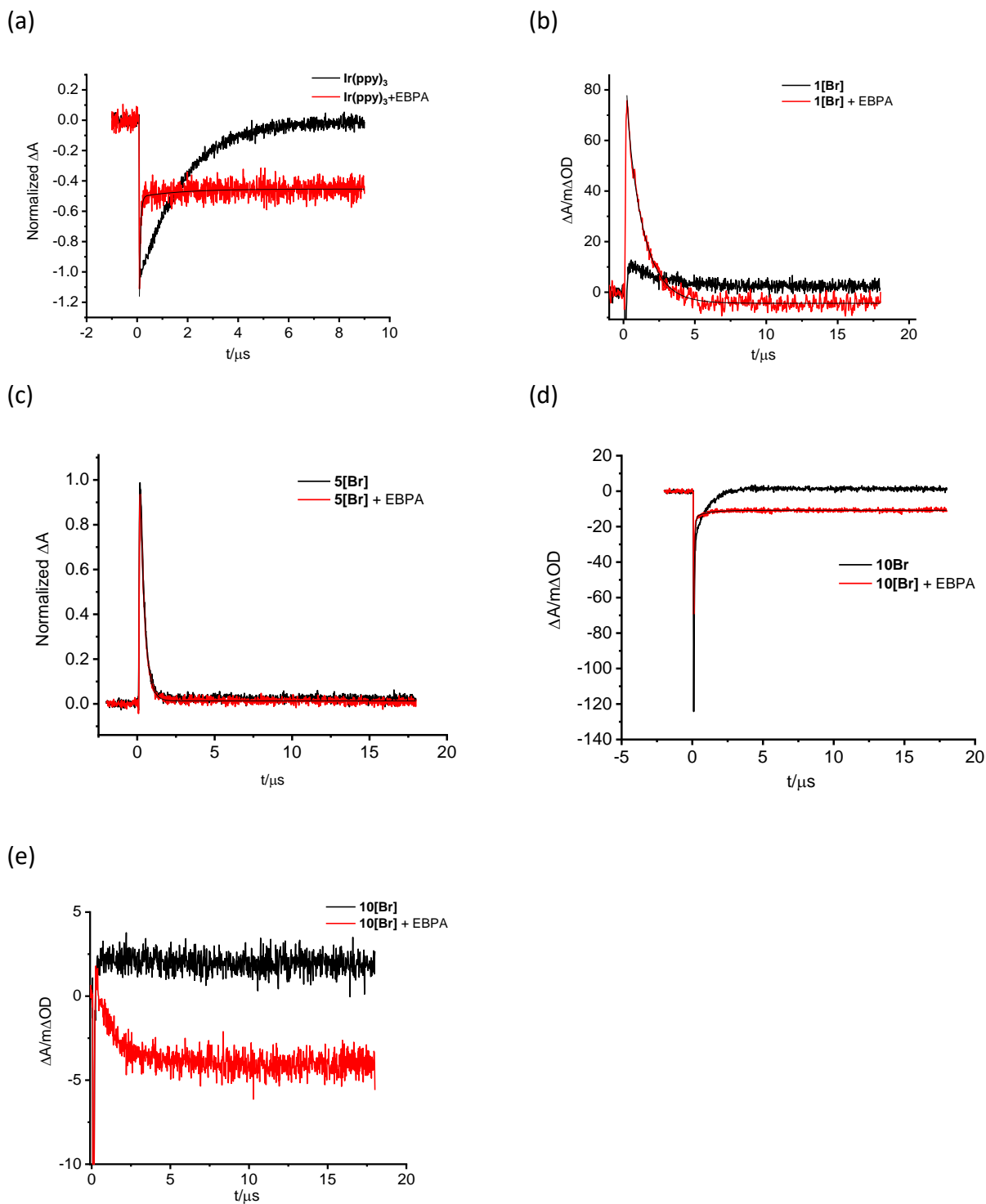
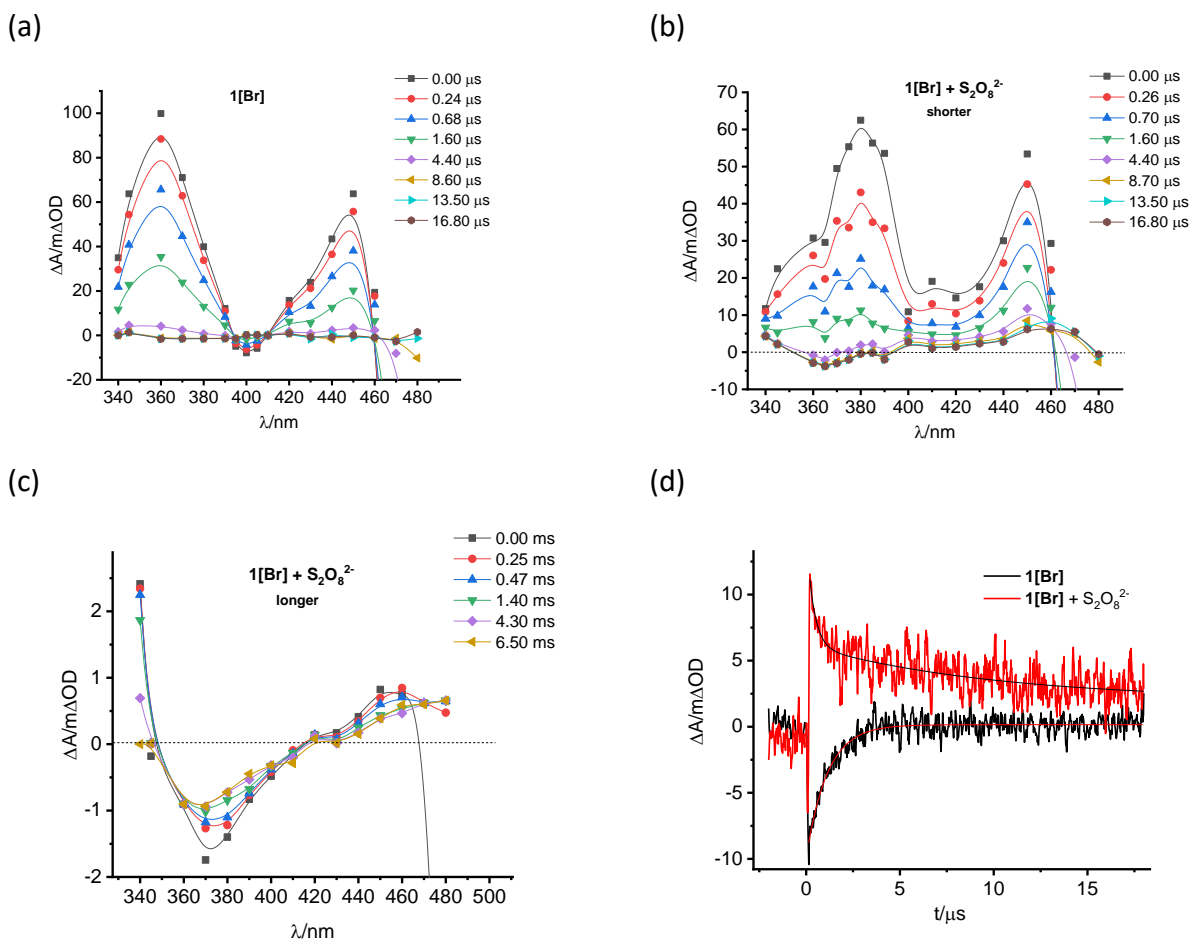
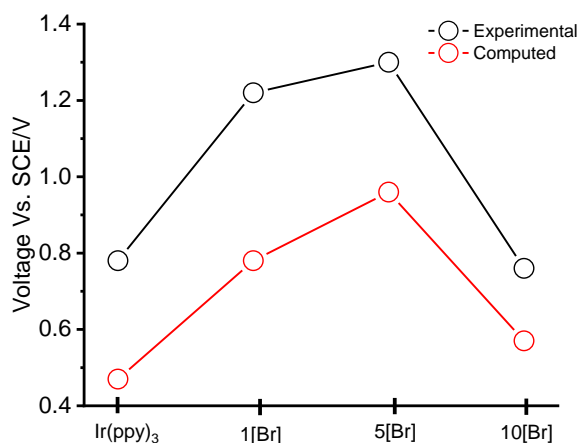


**Figure S132:** Transient absorption spectra of the acetonitrile solution of (a) **1[Br]** and (b) and (c) **1[Br]** +  $\text{S}_2\text{O}_8^{2-}$  at shorter and longer timescale respectively. (d) Comparison of the 360 nm kinetics decay of **1[Br]** and **1[Br]** in the presence of an excess of 240 equivalents of  $\text{S}_2\text{O}_8^{2-}$



## TDDFT calculations

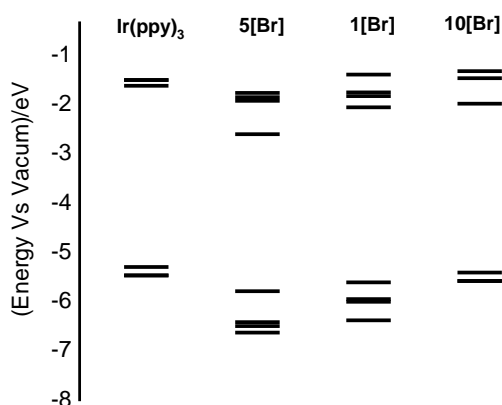
**Figure S133:** Comparison of the experimental and calculated HOMO energy for **Ir(ppy)<sub>3</sub>**, **1[Br]**, **5[Br]** and **10[Br]**



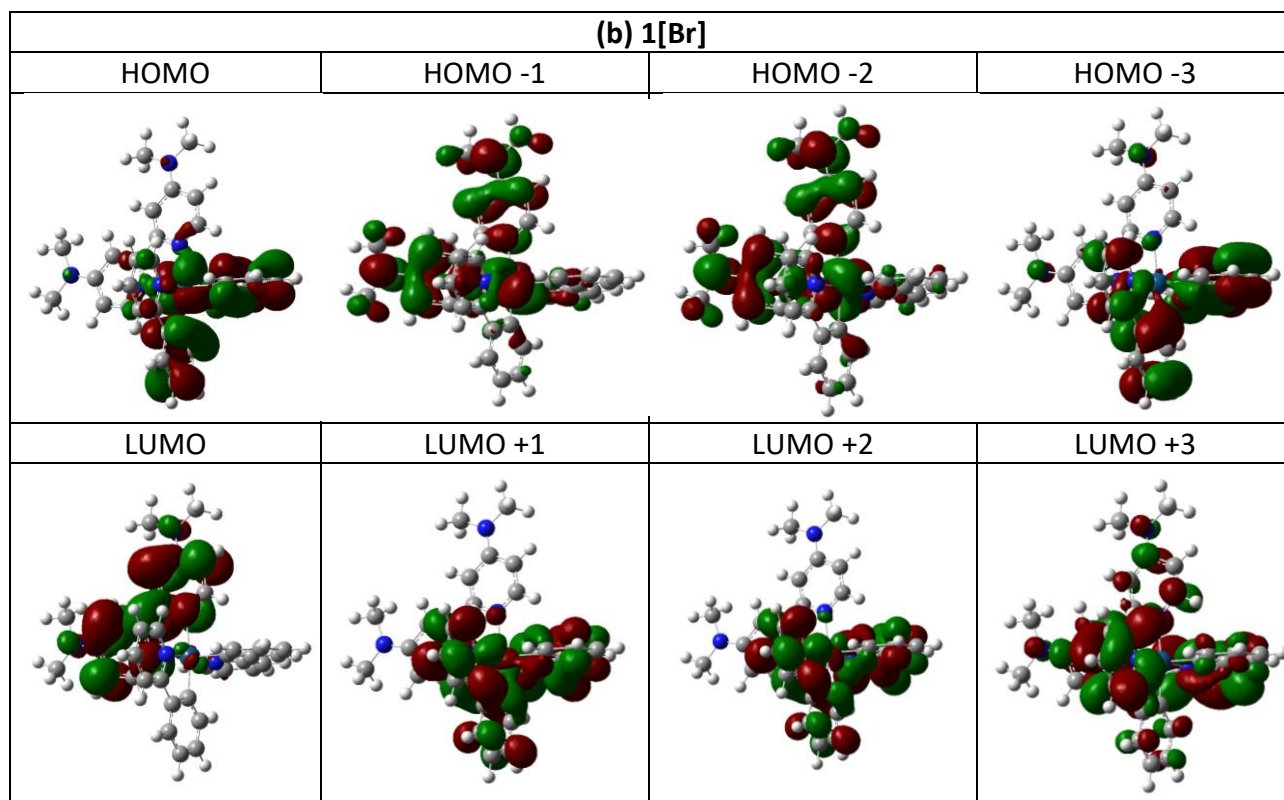
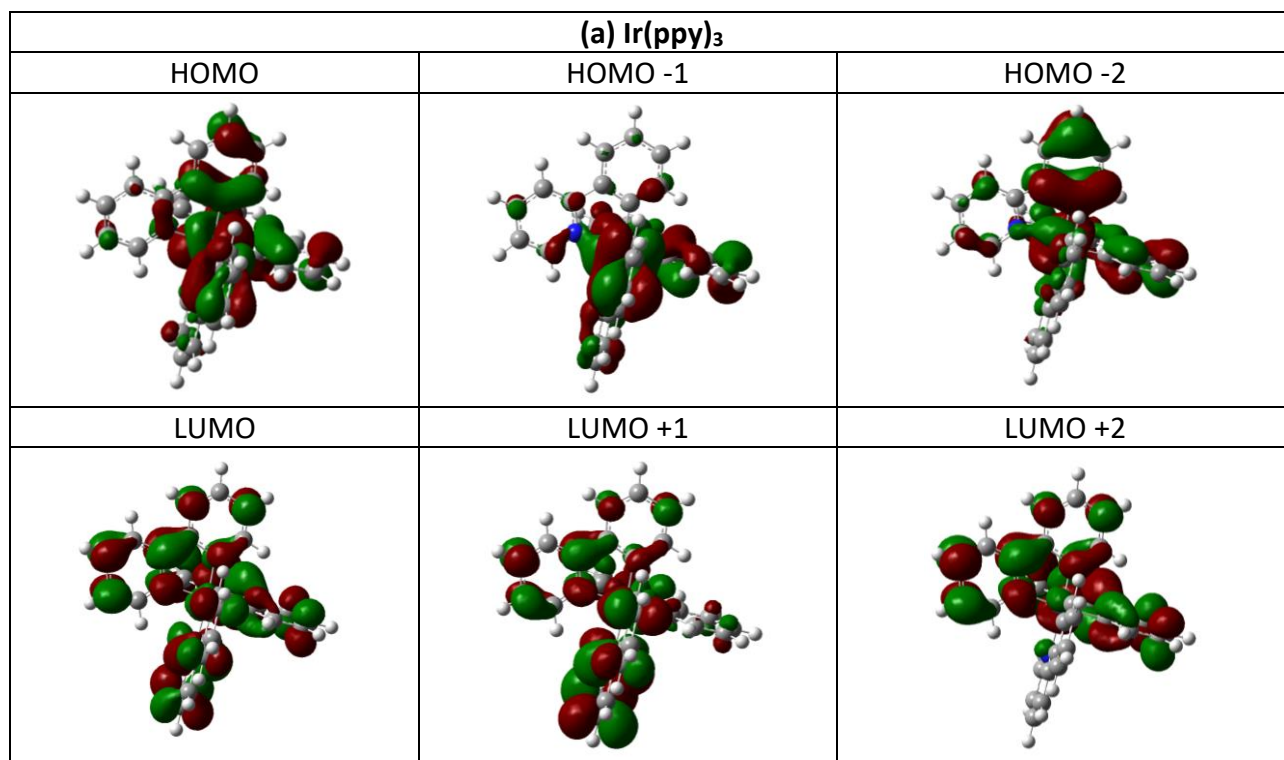
**Table S5:** Comparison of the computed and experimental electrochemical parameters of the Ir catalysts

	$E_{ox}$ Vs SCE	$E_{red}$ Vs SCE	$E_{red} - E_{ox}$	$E_{HOMO}$ cal	$E_{LUMO}$ cal	$\Delta E$ cal	$E_{ox}$ cal Vs NHE	$E_{red}$ cal Vs NHE	$E_{ox}$ cal Vs SCE	$E_{red}$ cal Vs SCE
<b>Ir(ppy)<sub>3</sub></b>	0.78	<2	>2.78	-5.31	-1.63	3.68	0.71	-2.97	0.47	-2.97
<b>1[Br]</b>	1.22	-1.72	2.94	-5.62	-2.07	3.55	1.02	-2.53	0.78	-2.77
<b>5[Br]</b>	1.30	-1.32	2.62	-5.80	-2.61	3.19	1.20	-1.99	0.96	-2.23
<b>10[Br]</b>	0.76	-1.76	2.52	-5.41	-1.99	3.42	0.81	-2.61	0.57	-2.85

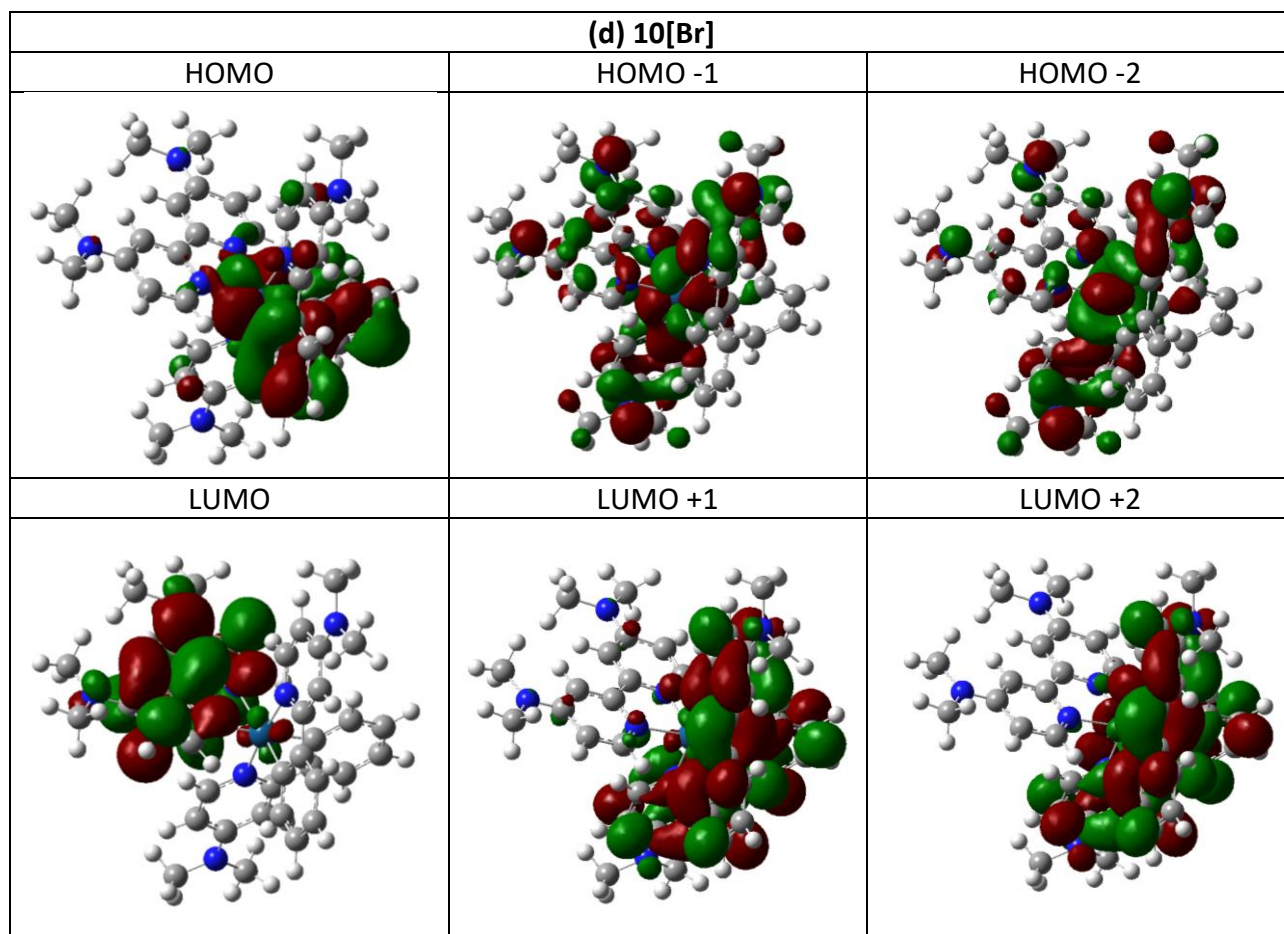
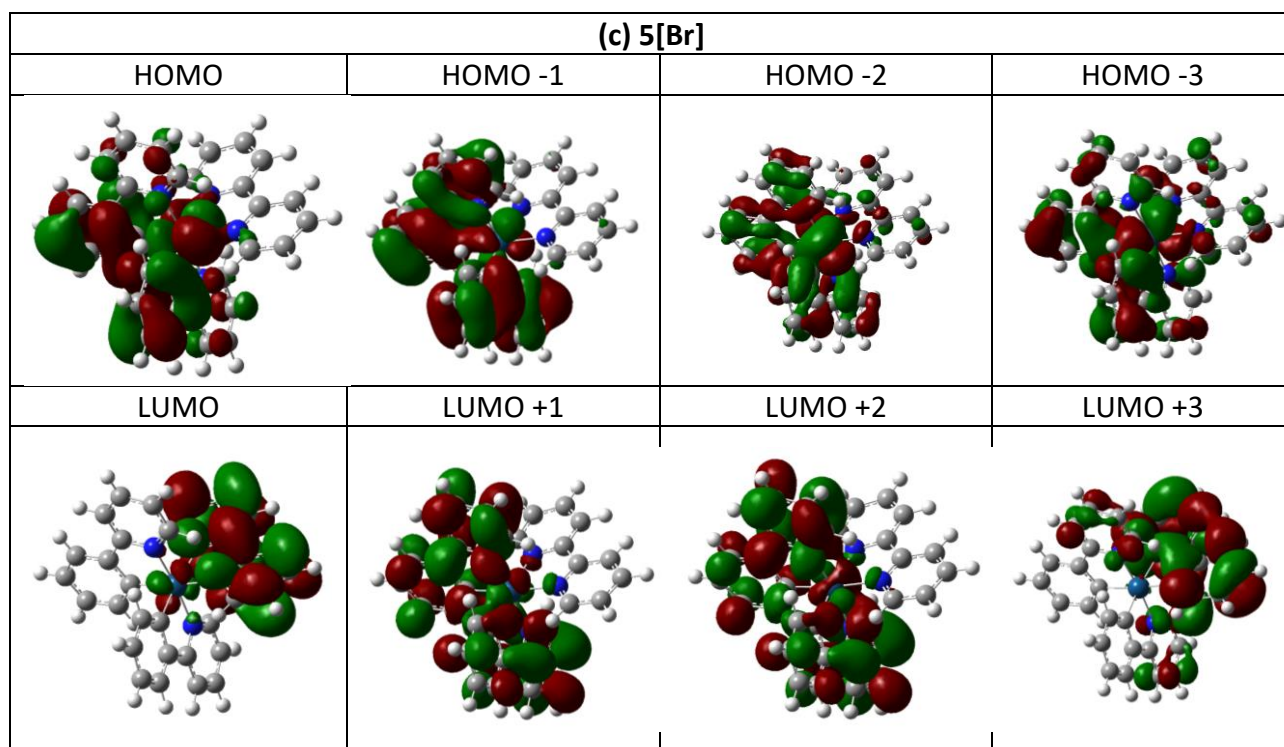
**Figure S134:** Energy levels of the KS orbitals for all the Ir(III) synthesized family compared to the standard **Ir(ppy)<sub>3</sub>** computed in ACN



**Figure S135:** Isodensity surfaces of the KS orbitals contributing to the vertical transitions reported in **Figure S134**

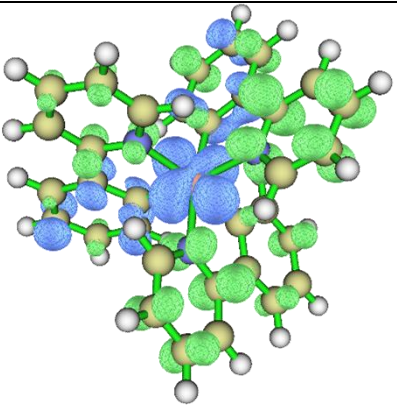
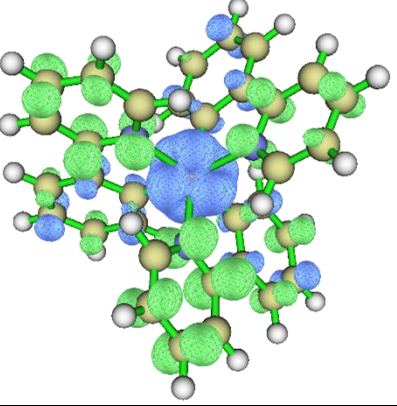
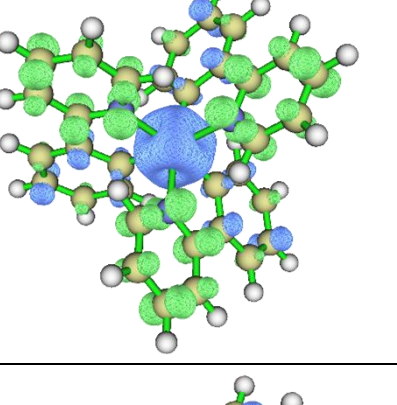
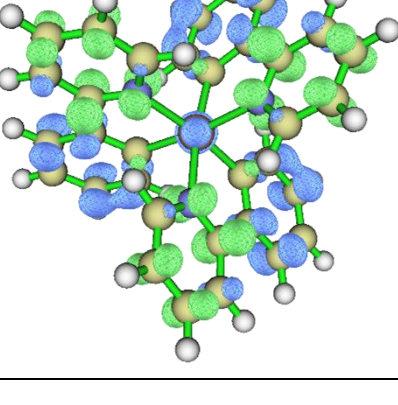




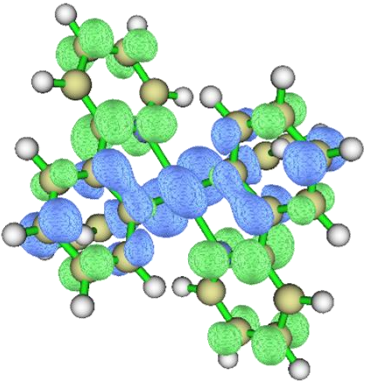
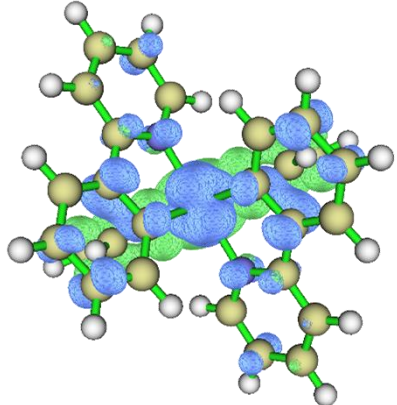
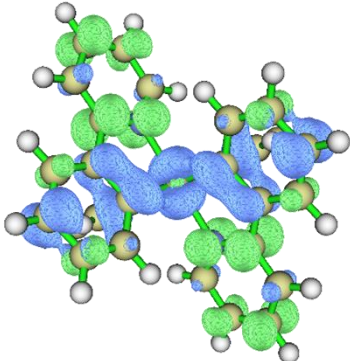
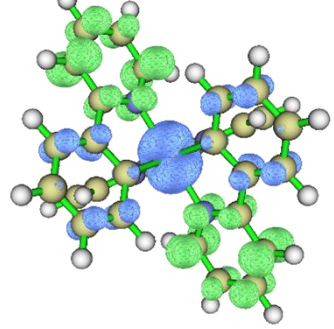




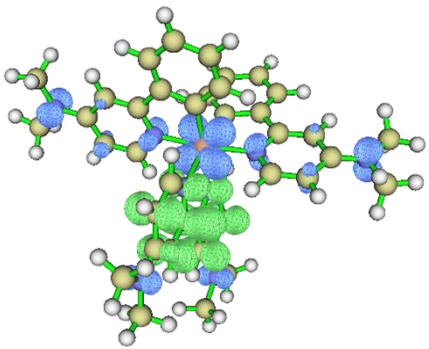
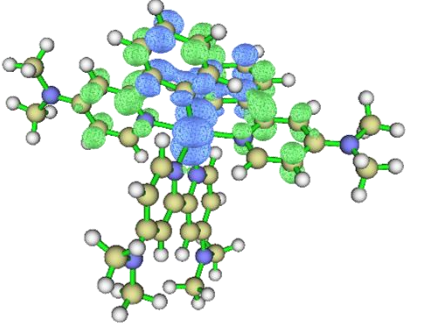
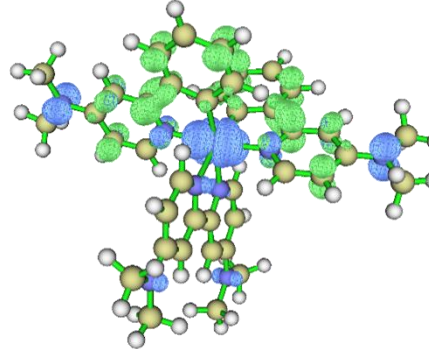
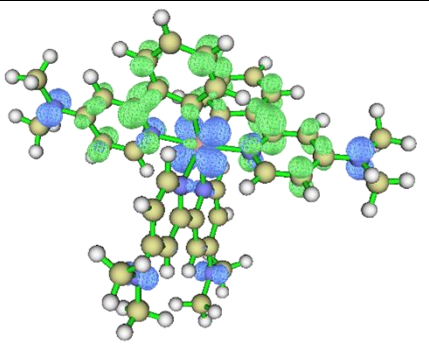
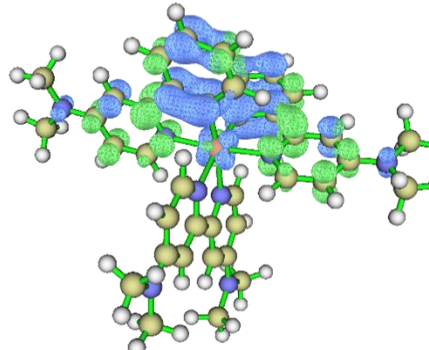
**Figure S136:** Electron Density Difference Maps of *fac*-[Ir(ppy)<sub>3</sub>]

Ir(ppy) <sub>3</sub>		
eV	f	EDDM
3.1528	0.0479	
3.2621	0.0682	
3.4762	0.0858	
4.3724	0.3073	

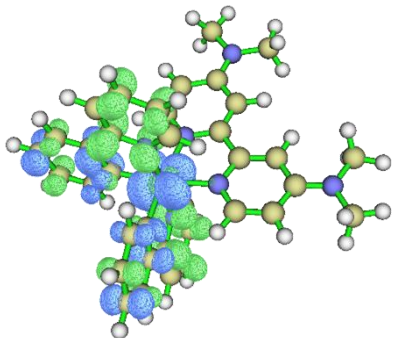
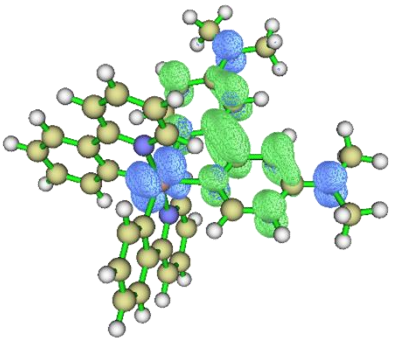
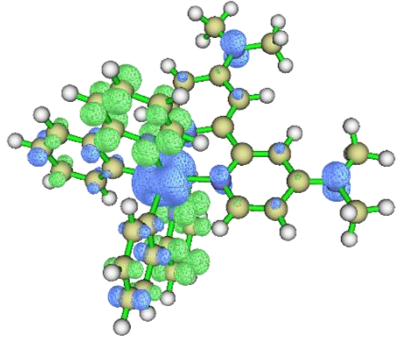
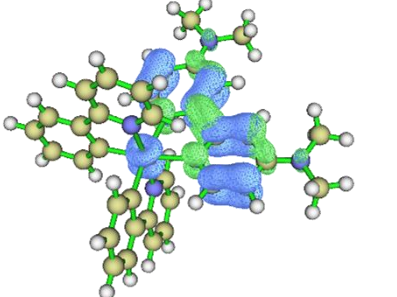
**Figure S137:** Electron Density Difference Maps of **5[Br]**

<b>5[Br]</b>		
<b>eV</b>	<b>f</b>	<b>EDDM</b>
3.1073	0.0537	
3.2305	0.0545	
4.0871	0.0156	
4.5946	0.4529	

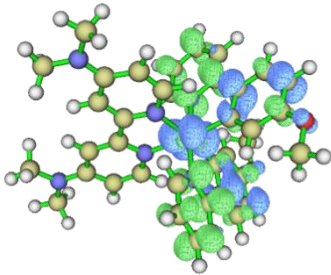
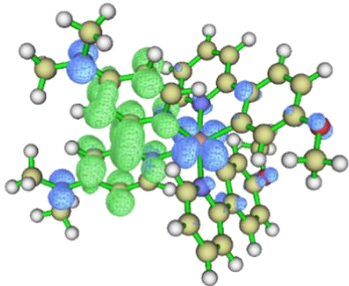
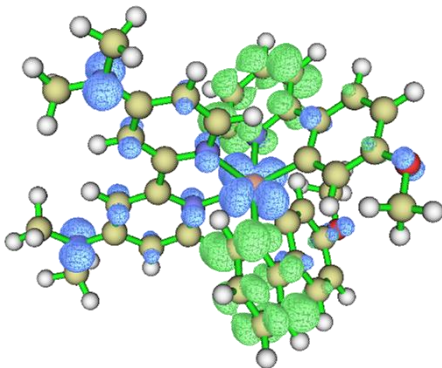
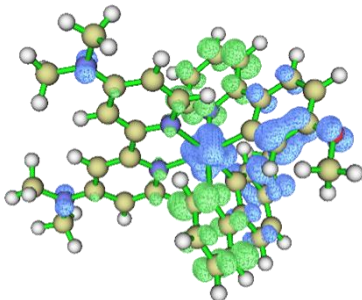
**Figure S138:** Electron Density Difference Maps of **10[Br]**

eV	f	EDDM
3.0041	0.1083	
3.2241	0.0779	
3.4629	0.0994	
3.5905	0.0867	
4.3446	0.4962	

**Figure S139:** Electron Density Difference Maps of **1[Br]**

eV	f	EDDM
3.0135	0.0445	
3.2966	0.1728	
3.5645	0.1060	
4.7408	0.7051	

**Figure S140:** Electron Density Difference Maps of **4[Br]**

eV	f	EDDM
3.0977	0.0581	
3.2771	0.1469	
4.1699	0.1786	
4.3908	0.1884	

[<sup>i</sup>] A. Pannwitz, A. Prescimone, O. S. Wenger, *Eur. J. Inorg. Chem.*, **2017**, 609 – 615.

[<sup>ii</sup>] K. Nakamura, *Bull. Chem. Soc. Jpn.*, **1982**, 55, 2697–2705.